UNIVERSIDADE DE LISBOA

FACULDADE DE CIÊNCIAS

Impact of Fine Particle Pollution on the Natural Ventilation Potential of Commercial Buildings

Doutoramento em Sistemas Sustentáveis de Energia

Nuno Miguel Rocha Martins

Tese orientada por:
Professor Doutor Guilherme Carvalho Canhoto Carrilho da Graça

Documento especialmente elaborado para a obtenção do grau de doutor

2017

UNIVERSIDADE DE LISBOA

FACULDADE DE CIÊNCIAS

Impact of Fine Particle Pollution on the Natural Ventilation Potential of Commercial Buildings

Doutoramento em Sistemas Sustentáveis de Energia

Nuno Miguel Rocha Martins

Tese orientada por:
Professor Doutor Guilherme Carvalho Canhoto Carrilho da Graça

Júri:
Presidente:
- Doutor João Manuel de Almeida Serra, Professor Catedrático
  Faculdade de Ciências da Universidade de Lisboa

Vogais:
- Doutor Manuel Carlos Gameiro da Silva, Professor Catedrático
  Faculdade de Ciências e Tecnologia da Universidade de Coimbra
- Doutor João Carlos Godinho Viegas, Investigador Principal com Habilitação
  Laboratório Nacional de Engenharia Civil
- Doutora Cristina Maria Branquinho Fernandes, Professora Associada com Agregação
  Faculdade de Ciências da Universidade de Lisboa
- Doutor Guilherme Carvalho Canhoto Carrilho da Graça, Professor Auxiliar
  Faculdade de Ciências da Universidade de Lisboa
- Doutora Carla Alexandra Monteiro da Silva, Professora Auxiliar
  Faculdade de Ciências da Universidade de Lisboa

Documento especialmente elaborado para a obtenção do grau de doutor

2017

ACKNOWLEDGEMENTS

First, I appreciate the financial support provided by the Fundação para a Ciência e a Tecnologia (MIT-Portugal Program, SFRH/BD/52084/2013) and Instituto Dom Luiz (UID/GEO/50019/2013).

I would like thank my advisor, Professor Guilherme Carrilho da Graça, for his guidance and for continuously challenging and supporting me throughout these years.

Thank you all in the Buildings Group office, for the friendly work environment, for your inputs, help, support and cake.

Last, although never least, to Ana, Mãe, Pai, André, Melanie and all my friends and family, for all the much needed support, friendship and love. Thank you to all whose path has in some past moment crossed into mine and, in some way, helped me in this work.

ABSTRACT

The majority of office and other non-domestic buildings use mechanical cooling and ventilation, even when an optimized natural ventilation (NV) system could meet cooling and fresh air requirements. However, in most large cities, the outdoor environment is contaminated with a combination of noise, fine particles, heat and toxic gases. This contaminated environment has a detrimental impact on naturally ventilated buildings due to their lack of filtration and outdoor noise attenuation systems. This thesis presents a numerical analysis of the effect of fine particle pollution (PM2.5) on the NV potential of office buildings in California, Europe and Asia. Several years of measured weather and PM2.5 concentration data were used to perform statistical and dynamic thermal and airflow simulation analysis.

In California and Europe, the outdoor temperature is suitable for NV during between 40 and 95 % of the annual working hours. In Asia, that fraction is lower, but can be increased by the availability of personal comfort systems (PCS). Nonetheless, in most cities, PM2.5 levels are high during a majority of those working hours. Detailed simulation results show that a hybrid NV system can reduce the air-conditioning and ventilation electricity consumption of a well-designed office building by up to 83 % (93 % if combined with PCS), in comparison to an office using, during all working hours, a mechanical cooling and ventilation system equipped with a high-efficiency particle filter. Unfortunately, in this hybrid approach, high levels of outdoor PM2.5 penetrate the indoor environment, increasing occupant cumulative exposure by up to six times. To overcome this problem, two exposure control approaches were tested. Using NV only during moments of low outdoor PM2.5 concentrations limits the exposure increase to up to three times but at the cost of reducing energy savings. Equipping NV openings with an electrostatic filter would result in a similar exposure reduction, but at a very low energy cost, taking full advantage of NV's saving potential.

Keywords: Indoor air quality modeling; Natural ventilation; Particle exposure; PM2.5; Thermal simulation

RESUMO

A maioria de edifícios não-domésticos, tais como os de escritórios, utiliza arrefecimento e ventilação mecânicos, mesmo quando um sistema de ventilação natural otimizado poderia satisfazer as necessidades de arrefecimento e de ar novo. Nas cidades mais populosas, o ambiente exterior está contaminado com uma combinação de ruído, partículas finas, calor e gases tóxicos. Este ambiente contaminado tem um efeito negativo nos edifícios com ventilação natural devido à falta de sistemas de filtragem de partículas e de atenuação de ruído exteriores. No caso de edifícios com ventilação mecânica, a utilização de filtros de partículas com elevada eficiência permite limitar a entrada de partículas no ambiente interior, embora aumente a pressão exigida ao ventilador, o que resulta num crescimento do consumo energético. Esta tese apresenta uma análise numérica do efeito de poluição, nomeadamente de partículas finas (PM2.5), no potencial de ventilação natural de edifícios de escritórios em algumas das cidades mais populosas e poluídas da Califórnia, da Europa e da Ásia. Estas três regiões têm climas e níveis de PM2.5 bastante distintos, do que resultam diferentes níveis de dificuldade de aproveitamento do potencial de ventilação natural. Foram utilizados dados meteorológicos e de concentração de PM2.5, medidos ao longo de vários anos, para que fosse possível realizar as análises estatística e de simulação dinâmica térmica e de fluxo de ar.

A análise estatística do potencial de ventilação natural mostrou que as cidades com temperatura exterior mais favorável ao uso de ventilação natural (entre 10 e 26 °C) são San Diego (96 % das horas de trabalho anuais), Burbank (80 %) e Lisboa (81 %). Nas restantes cidades californianas e europeias, este potencial de ventilação natural varia entre 40 e 70 %, enquanto nas cidades asiáticas varia entre 23 e 53 %. A disponibilidade de sistemas de conforto térmico pessoal (PCS) aumenta o intervalo de temperatura favorável ao uso de ventilação natural para 10 a 30 °C, com humidade relativa abaixo de 80 % quando a temperatura é superior a 26 °C. Este intervalo expandido beneficia em particular cidades em que uma fração significativa das horas de trabalho do ano (10 a 14 %) tem temperaturas demasiado altas para o uso de ventilação natural: Sacramento, Fresno, Lisboa, Madrid, Skopje, Pequim, Xangai e Nova Deli.

Se a ventilação natural for utilizada apenas em momentos com baixa concentração exterior de PM2.5 (definido como abaixo de 12 $\mu g/m^3$ na Califórnia e de 10 $\mu g/m^3$ na Europa; na Ásia, foram considerados dois limiares: 10 e 35 $\mu g/m^3$), o seu potencial é reduzido para menos de metade em toda a Europa e Ásia e ainda em Fresno e Burbank, na Califórnia. Nas três cidades asiáticas e em Skopje, o limiar de 10 $\mu g/m^3$ praticamente elimina a possibilidade de uso de ventilação natural. Nas restantes cidades da Califórnia, o efeito limitativo de PM2.5 é menor: 19 a 40 %.

A análise estatística identificou ainda a existência de correlações entre variáveis climáticas e níveis de PM2.5. Em San Diego e Burbank, temperaturas mais altas coincidem com concentrações mais elevadas de PM2.5, nomeadamente devido à formação secundária de sulfato de amónio que é depois aprisionado pela frequente ocorrência de camadas de inversão térmica de baixa altitude. Em Cracóvia e Skopje, a concentração de PM2.5 é mais elevada aquando de temperaturas mais baixas, o que se deve a uma maior produção energética para fazer face às necessidades dos meses mais frios, sendo que na Polónia e ARJ da Macedónia essa produção é maioritariamente baseada em centrais térmicas a carvão. Em Xangai, a concentração de PM2.5 diminui com temperaturas mais altas, embora nesta cidade isto se deva à maior intensidade de precipitação na estação mais quente. Em todas as cidades, a concentração de PM2.5 diminui com o aumento da velocidade de vento. Ventos com velocidades mais altas substituem, geralmente, o ar poluído localmente com PM2.5 por ar mais limpo de regiões vizinhas. No entanto, o vento pode transportar PM2.5 com origem noutros locais, como acontece em Burbank: é frequente o transporte de PM2.5 da cidade vizinha de Los Angeles.

Quanto à variação de PM2.5 durante o dia, a concentração de PM2.5 é mais alta durante a manhã em todas as cidades, uma consequência da maior intensidade de tráfego de veículos durante esse período. Na última hora do período de trabalho, verifica-se o início de um novo período de crescimento de concentração de PM2.5, novamente devido ao tráfego. Em Sacramento, Fresno, Cracóvia, Skopje e Xangai há também um padrão anual: os meses de inverno são mais poluídos do que os meses de verão, embora por razões distintas. Em Sacramento e Fresno, há um aumento de emissão de PM2.5 na estação fria, que é aprisionada pelas cadeias montanhosas envolventes e pelas camadas de inversão térmica de baixa altitude que ocorrem frequentemente durante essa estação. Em Cracóvia, Skopje e Xangai, o padrão anual segue a correlação entre temperatura e PM2.5.

A análise de simulação demonstrou que o uso de ventilação natural permite uma poupança no consumo energético do sistema de aquecimento, ventilação e ar condicionado (HVAC) mecânico em comparação com um cenário em que esse sistema funciona a tempo inteiro: 26 a 83 % na Califórnia, 20 a 58 % na Europa e 7 a 21 % na Ásia. A disponibilidade de PCS permitiu um maior uso de ventilação natural e, portanto, aumentou o seu potencial de poupança de energia: 46 to 93 % na Califórnia, 44 to 77 % na Europa e 16 to 41 % na Asia.

Contudo, o uso de ventilação natural nestas condições resultou num aumento da exposição dos ocupantes do edifício a PM2.5, em comparação com o cenário de utilização a tempo inteiro do sistema de HVAC equipado com um filtro de partículas finas de elevada eficiência: 3.7 a 5.0 vezes na Califórnia, 1.9 a 4.2 vezes na Europa e 2.3 a 3.0 vezes na Ásia. A utilização expandida de ventilação natural devido ao uso de PCS amplifica essa exposição: 4.4 a 5.7 vezes na Califórnia, 2.2 a 5.4 vezes na Europa e 3.3 a 3.9 vezes na Ásia.

Foram propostas duas abordagens para conter este aumento de exposição. A primeira consiste em restringir o uso de ventilação natural a momentos com baixa concentração exterior de PM2.5, do que resulta um menor potencial de poupança de energia: 17 a 63 % na Califórnia, 5 a 40 % na Europa, e 1 a 5 % (com um limite de 10 $\mu g/m^3$) ou 1 a 12 % (com um limite de 35 $\mu g/m^3$) na Ásia. Ainda que possa resultar num acréscimo das necessidades energéticas em comparação com a utilização de ventilação natural sempre que possível, esta abordagem cumpre o seu objetivo: o aumento de exposição é limitado a 2.0 a 3.2 vezes na Califórnia, 1.4 a 2.8 vezes na Europa e 1.2 a 1.8 vezes na Ásia. Novamente, a disponibilidade de PCS permite um maior uso de ventilação natural e uma poupança energética mais assertiva, o que inevitavelmente eleva a exposição a PM2.5. Todavia, com esta abordagem, o ganho que se consegue para a diminuição de exposição a partículas compensa o inevitável aumento do consumo energético, com exceção das cidades de Skopje, Xangai e Nova Deli.

A segunda abordagem consiste em equipar as aberturas na envolvente do edifício, que são utilizadas para ventilação natural, com um filtro eletrostático. Este filtro tem um consumo energético muito reduzido, permitindo aproveitar quase na totalidade o potencial de poupança de energia da ventilação natural. Os níveis de exposição interior a PM2.5 que resultam desta abordagem são semelhantes ou inferiores aos níveis que resultam das condições descritas na abordagem anterior, i.e. o uso de ventilação natural é limitado a momentos de baixa concentração exterior de PM2.5. Deste modo, o rácio poupança de energia/aumento de exposição é máximo para esta abordagem, indicando que o uso de filtros eletrostáticos é potencialmente benéfico ao uso de ventilação natural. Porém, ao contrário da abordagem anterior que poderia facilmente ser implementada atualmente, a utilização de filtros eletrostáticos em combinação com ventilação natural apenas foi testada em ambiente simulado e ainda necessita de desenvolvimento técnico e testes em ambiente laboratorial e em edifícios reais.

Palavras-chave: Exposição a partículas; Modelação de qualidade de ar interior; PM2.5; Simulação térmica; Ventilação natural

CONTENTS

NOMENCLATURE

Abbreviations

AFN	Airflow network
AHU	Air handling unit
AQG	Air quality guideline
CFD	Computational fluid dynamics
DOE	United States Department of Energy
EC	Extended comfort
ESF	Electrostatic filter
FO	Fully open windows
GCA	Generic contaminant algorithm
HVAC	Heating, ventilation and air conditioning
I/O	Indoor/outdoor
IB	Window opens inwards, bottom opening axis
IT	Window opens inwards, top opening axis
IT-*n*	*n*th interim limit
LES	Large eddy simulation
MV	Mechanical ventilation
NoNV	NV is not used
NREL	National Renewable Energy Laboratory
NV	Natural ventilation
NV*n*	NV is used/available only when outdoor PM2.5 level is below *n* $\mu g/m^3$
NVP	NV is used whenever possible
NVS	NV is used/available only when outdoor PM2.5 level is below a safe threshold
NVF	NV is used with openings equipped with an ESF instead of windows
OB	Window opens outwards, bottom opening axis
OT	Window opens outwards, top opening axis
PCS	Personal comfort systems

PM	Particulate matter
PM10	Particulate matter with an aerodynamic diameter below 10 μm
PM2.5	Particulate matter with an aerodynamic diameter below 2.5 μm
P*n*	Measuring point number *n*
RANS	Reynolds-averaged Navier-Stokes
RNG	Re-normalization group
SC	Standard comfort
SNA	Sulfur, nitrate and ammonium compounds
TMY3	Typical meteorological year, version 3
UFP	Ultrafine particles
WHO	World Health Organization
W*n*	Window/opening number *n*
WT	Wind tunnel

Symbols, Variables and Units

$\boldsymbol{A}$	Area [m^2]
$\boldsymbol{C}$	Coefficient
$\boldsymbol{CFL}$	Courant-Friedrichs-Lewy parameter
$\boldsymbol{COP}$	Coefficient of performance
$\boldsymbol{E}$	Electric power [W]
$\boldsymbol{F}$	Particle penetration rate
$\boldsymbol{G}$	Indoor PM2.5 generation rate [10^{-6} μg/s]
$\boldsymbol{H}$	Height [m]
$\boldsymbol{K}$	PM2.5 concentration [μg/m^3]
$\boldsymbol{N}$	Number of summation iterations
$\dot{\boldsymbol{Q}}$	Heat generation [W]
$\boldsymbol{P}$	Cumulative exposure [mg h m^{-3} $year^{-1}$]
$\boldsymbol{PPD}$	Predicted percentage of dissatisfied occupants
$\boldsymbol{PMV}$	Predicted mean comfort vote
$\boldsymbol{R}$	Indoor PM2.5 removal rate
$\boldsymbol{R^2}$	Coefficient of determination
$\boldsymbol{T}$	Temperature [°C]
$\boldsymbol{V}$	Volume [m^3]
$\dot{\boldsymbol{V}}$	Airflow rate [m^3/s]
$\boldsymbol{c}$	Specific heat of air [J kg^{-1} K^{-1}]
d	Differential operator
$\boldsymbol{e}$	Annual energy consumption [kW h m^{-2} $year^{-1}$]
exp	Exponential function
$\boldsymbol{g}$	Acceleration due to gravity [m/s^2]
$\boldsymbol{h}$	Convective heat transfer coefficient [W m^{-2} K^{-1}]
$\boldsymbol{i}$	Summation iteration counter
$\boldsymbol{j}$	Working hours of the year

$\boldsymbol{k}$	Pollutant concentration [ppm]
ln	Natural (base e) logarithm function
$\boldsymbol{\dot{m}}$	Mass flow [kg/s]
$\boldsymbol{p}$	Pressure [Pa]
$\boldsymbol{t}$	Time [s]
$\boldsymbol{u}$	Speed [m/s]
$\boldsymbol{y}$	Measured value
$\boldsymbol{\overline{y}}$	Averaged measured value
$\boldsymbol{\hat{y}}$	Predicted value
$\boldsymbol{x}$	Spatial grid step [m]

Greek Symbols, Variables and Units

Δ	Variation
Σ	Summation
$\boldsymbol{\Phi}$	Annual potential
$\boldsymbol{\eta}$	Efficiency
$\boldsymbol{\rho}$	Air density [kg/m^3]
$\boldsymbol{\varphi}$	Fraction of occurrences of criteria fulfillment for a given individual working hour
$\boldsymbol{\psi}$	Ratio between actual *COP* and that of an ideal Carnot engine

Subscripts

0	Starting value
D	Discharge
HR	Heat recovery
$HVACfilter$	Fine particle cloth filter
NPL	Neutral pressure level
$NVfilter$	Electrostatic filter
T	Increased heat capacitance in the air loop
b	Building
$cond$	Heat pump condenser
$cool$	Heat pump used for cooling
$dist$	Heating or cooling fluid distribution
$evap$	Heat pump evaporator
$heat$	Heat pump used for heating
inf	Infiltration
$inload$	Internal heat sources
$local$	Near NV opening
max	Maximum
$meas$	Measurement
min	Minimum
nat	Natural ventilation
$open$	Opening
out	Outdoors
p	Pressure
$sink$	PM2.5 sink
$source$	PM2.5 source
$stack$	Buoyancy stack effect
sup	Air supply duct

$surface$	Zone surfaces
sys	Mechanical ventilation system
$vent$	Ventilator
w	Opening effectiveness
$wind$	Wind
z	Simulation Zone
$zone$	Other zones

LIST OF FIGURES

LIST OF TABLES

1. INTRODUCTION

Over the last two centuries, human populations have continuously left rural backgrounds and moved into urban areas. This shift, which started with the industrial revolution, has gained momentum especially after the Second World War and has resulted in the worldwide urban population to exceed the rural population for the first time in 2007. By 2050, this continuously growing urban population is expected to double the rural population, which has stagnated since the beginning of the twenty-first century [1]. This urbanization movement has increased the number of large cities and, in the more populated countries, the number of megacities, which are urban locations where tens of millions of people live and work [2].

Within the urban environment, people spend most of their time indoors, whether at home, at work, at school or when taking part in other activities [3, 4], which has increased the use of building air conditioning (also known as mechanical heating, cooling and ventilation, or HVAC) and other electric equipment, which in turn has created a large energy demand. Recent concerns over the cost of this substantial energy consumption and over its environmental consequences, such as air pollution and climate change, have set forth the pursuit of increased energy efficiency and, in the particular case of the building sector, low-energy thermal comfort solutions that limit the use of HVAC systems [5, 6].

One of these solutions is natural ventilation (NV), which occurs when pressure differences generated by wind or buoyancy forces act on one or more openings on the building envelope. Throughout history, NV has always remained the preferred choice for residential buildings [7, 8], while in commercial buildings, NV went from being the single option to somewhat of a lost art as mechanical ventilation (MV) systems became the standard during the second half of the twentieth century.

The hiatus in NV use in commercial buildings resulted in the loss of existing design know-how in a period were comfort and ventilation system performance standards have continuously risen. As a result, currently available simple NV design rules tend to be both overly simplistic and conservative, such as those found in California's Title 24 recommendation of a 5 % minimum ratio between floor and façade opening area and a 20 feet maximum natural flow penetration rule, which limits the use of NV to office areas that are less than 20 feet (about 6 meters) away from a façade with operable windows [9]. Nonetheless, single-sided NV may provide adequate fresh air beyond 6 meters with a window opening area that is less than 5 % [10]. Thus, most office and other non-domestic buildings increasingly use mechanical cooling even when an optimized NV system could meet cooling and fresh air requirements by replacing warm indoor air with cooler outdoor air [11, 12] in the milder months of the year [13, 14].

Interest in the research and use of NV and research in commercial buildings has been rising, especially during the last decades [15, 16, 17, 18]. In the milder months of the year, NV can be an alternative to mechanical systems due to its potential to reduce ventilation and cooling related energy demand as well as sick building syndrome [19, 20, 21]. Nonetheless, another hurdle has recently gained notoriety in limiting the use of NV, especially in urban areas: air pollution [22].

In the last decades of the twentieth century, the health impacts of air pollution became well established in the realm of common knowledge [23, 24]. The term air pollution refers to a group of airborne pollutants that are known to contribute to decreased life expectancy [2]. These include pollutants that consist of one or two substances, such as carbon monoxide (CO), sulfur and nitrogen oxides (SO_x and NO_x) and ozone (O_3), as well as airborne particulate matter (PM), which includes several substances in a wide spectrum of particle sizes.

The health impacts of PM have been under increasing scrutiny in the last two decades, since manmade pollution has resulted in the annual mean levels of airborne fine particles in most large cities exceeding the World Health Organization's (WHO) guidelines for yearly and short-tem human exposure [25]. Although gravity forces the deposition of particles with diameters above 30 μm [26], smaller particles, in particular PM2.5, which are liquid or solid matter with an aerodynamic diameter below 2.5 μm that are suspended in the air, remain suspended for long times and can travel far from their sources.

The effects of human exposure to PM2.5 are especially felt in urban environments, where the higher population density gives rise to a higher pollutant generation combined with a higher density of human targets [2, 27]. For instance, dense city centers have a containment effect on black carbon emissions from fossil fuel-powered transportation, domestic stoves and space heating [28, 29].

The high pollution levels that are found in the environment of most large cities are transported into the indoor environment by the ventilation air. The most widespread approach to limit indoor PM2.5 levels in commercial buildings is the use of cloth filters integrated in MV systems. These filters can reach PM2.5 removal efficiencies above 90 %, albeit at the cost of placing a large pressure load on the ventilation system and increasing the energy consumption of the ventilation fans to levels which are comparable to indoor lighting, with power densities in the range of 5 to 15 W/m^2 [30, 31]. Further, the average energy consumption of a mechanical cooling system has a similar magnitude (or up to twice as much in hot and humid climates), compounding an HVAC-related energy consumption of 50 to 60 % of the total building energy consumption [32, 33]. In locations where electricity generation is based on fossil fuels, this higher power consumption further increases PM2.5 emissions into the environment. In contrast, NV with open windows does not increase PM2.5 emissions. However, NV airflow is driven by low pressure differences, which does not allow the use of cloth filters, enabling the unobstructed inflow of outdoor fine particles.

One approach to break this vicious cycle with limited occupant exposure consists in combining NV with a mechanical HVAC, in a hybrid system that can automatically alternate between the two indoor climate control approaches. When weather conditions are favorable, the use of NV leads to lower energy consumption. Unfortunately, in many cities, there are a significant number of hours when weather conditions are favorable to the use of NV but outdoor PM2.5 levels are high. To avoid contamination during these moments, an automated window control system would only allow for NV use when outdoor PM2.5 levels are below a safe threshold for long-term exposure. During moments with outdoor PM2.5 levels exceeding that threshold, the HVAC system would be in operation, conditioning the indoor environment and indoor PM2.5 levels. The energy savings that result from this hybrid cooling and ventilation system depend on local weather and outdoor PM2.5 levels as well as window-opening requirements. In the case of well-designed buildings with low internal gains, windows that are user-controlled were found to be opened for temperatures as low as 10 °C [34], while the typical maximum outdoor temperature for the use of NV in offices is approximately 26 °C [35]. When needed, both user-controlled and automated openings can be expected to be open within this outdoor temperature range. Thus, a potential for NV use can be quantified by the fraction of working hours when weather conditions are favorable for its use, that is, when the outdoor temperature is between 10 and 26 °C. A given building may use this full potential if there is a need for NV during all these hours, as long as the outdoor PM2.5 levels are not excessive. In warmer climates, an increasingly used approach to supplement natural cooling and ventilation systems consists of low-power consuming individual or localized heating and cooling devices, known as personal comfort systems (PCS) [36]. Localized cooling PCS can allow users to tolerate higher indoor temperatures (up to 30 °C, if humidity does not exceed 80 % [37]), thereby increasing the maximum outdoor temperature that allows for NV use. These systems are usually based on air movement that increases the occupants' heat loss. PCS operating with this principle include chairs with fans [38], ceiling fans [37] or small fans that direct air flow to specific body parts, such as the face or torso [39]. Heating PCS, such as electrically heated chairs [40], typically consist of an electric resistance or radiative element [36],

allowing occupants to tolerate a lower indoor temperature. In addition to increasing the NV potential, due to allowing its use with higher outdoor temperatures, PCS devices can also be used alongside conventional HVAC systems. In these cases, the benefit of these systems is to allow for higher cooling and lower heating set points.

1.1. Research Questions

Overall, the knowledge gap that was addressed in this thesis was the effect of the inter-relation between PM2.5 concentrations, weather and NV use on commercial building energy consumption and occupant exposure. Answering this question requires a simultaneous energy and PM2.5 assessment of the trade-off between NV-induced energy savings and the resultant increase in indoor exposure to PM2.5 that arise from the use of NV.

In this order, the following research questions were the focus of this thesis:

- What fraction of annual working hours is within the outdoor temperature range which allows for the use of NV? How much of those hours have high outdoor PM2.5 levels?
- Which weather events or time periods directly affect outdoor PM2.5 levels?
- What is the energy saving potential of NV in commercial buildings?
- What is the effect of the use of NV on occupant exposure?
- What is the effect of exposure control strategies on energy savings and occupant exposure?

1.2. Thesis Structure

This thesis is structured into six chapters, beginning with this introductory chapter (Chapter 1). Chapter 2 is a review of existing research on the impact of PM2.5 in the built environment. Specifically, this review identifies the main sources and sinks of PM2.5 in outdoor and indoor urban environments, discusses the PM2.5 exposure limits are currently applicable in different parts of the world, summarizes the main socio-economic impacts of the exposure to PM2.5 and identifies the most promising solutions to minimize building occupant exposure. Chapter 3 presents the simulation tools that were used during the development of this research: a validation of nodal and computational fluid dynamics (CFD) models that are used to predict the NV airflow, EnergyPlus, a thermal simulation code, and the Generic Contaminant Algorithm (GCA), a nodal pollutant transport model, available within EnergyPlus. Chapter 4 describes the two complementary analysis approaches used in this research: a simple statistical analysis of the potential for NV use and a detailed simulation analysis of the impact of PM2.5 on the use of NV in an office building. Chapter 5 presents the results and their respective analysis of both approaches, while Chapter 6 delivers the overall conclusions of the research developed in this thesis.

This research has resulted in the publication of a refereed conference paper and four peer-reviewed journal papers. Also, one journal paper has been submitted for publication:

- Paper 1: *A Climate Performance Indicator for Analysis of Low Energy Buildings*, by Nuno R. Martins and Guilherme Carrilho da Graça, published and presented at the *Building Simulation Conference*, in Chambéry (France), in 2013 [41].

- Paper 2: *Validation of numerical simulation tools for wind-driven natural ventilation design*, by Nuno R. Martins and Guilherme Carrilho da Graça, published in *Building Simulation*, in 2016 [42].

- Paper 3: *Impact of outdoor PM2.5 on natural ventilation usability in California's nondomestic buildings*, by Nuno R. Martins and Guilherme Carrilho da Graça, published in *Applied Energy*, in 2017 [43].

- Paper 4: *Simulation of the effect of fine particle pollution on the potential for natural ventilation of non-domestic buildings in European cities*, by Nuno R. Martins and Guilherme Carrilho da Graça, published in *Building and Environment*, in 2017 [44].

- Paper 5: *Effects of airborne fine particle pollution on the usability of natural ventilation in office buildings in three megacities in Asia*, by Nuno R. Martins and Guilherme Carrilho da Graça, published in *Renewable Energy*, in 2018 [45].

- Paper 6: *Impact of PM2.5 in the built environment: a review*, by Nuno R. Martins and Guilherme Carrilho da Graça, submitted to *Renewable and Sustainable Energy Reviews*, in 2017 [46].

Table 1 shows the correspondence between each thesis chapter and these already published and submitted papers.

Table 1 – Correspondence between published and submitted papers and thesis chapters

Chapter Number	Article Numbers
1	2, 3, 4, 5, 6
2	6
3	2
4	3, 4, 5
5	3, 4, 5

2. REVIEW OF EXISTING WORK

To simplify the assessment of PM levels and facilitate the implementation of PM pollution control policies, it is common to categorize airborne PM pollution levels by the total particle mass per cubic meter of air in several particle size ranges defined by the aerodynamic diameter of the largest particles considered in each case (Figure 1 [47, 48, 49]):

- TSP: total suspended particles include any solid or liquid matter in suspension in the air;
- PM10: particles with an aerodynamic diameter below 10 μm;
- PM2.5: particles with a diameter below 2.5 μm, also known as fine particles;
- CP: coarse particles are the fraction of PM10 that does not include PM2.5;
- UFP: ultrafine particles are particles with a diameter below 100 nm, also referred to as PM0.1.

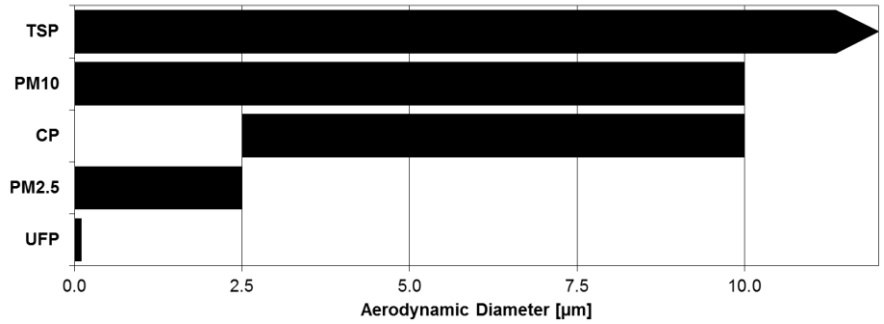

Figure 1 – Particulate matter size categories

Early research on the effects of human exposure to airborne PM used PM10 as the preferred indicator [47, 50]. The larger particles in the PM10 range can enter into the respiratory system but cannot penetrate the pulmonary alveoli. Due to their smaller diameter, particles in the PM2.5 range can damage airway cells, triggering an inflammatory response that diminishes pulmonary immunity and facilitates infectious pathogen attacks [51, 52]. The deeper penetration into the lungs allows PM2.5 to enter the bloodstream, leading to hypertension and damaging blood vessels. Once in the bloodstream, PM2.5 can spread to other organs, such as the heart, damaging its cell structure and function. Continuous exposure to high levels of PM2.5 has also been linked to several diseases, such as diabetes and pre-natal disorders, which in turn can lead to preterm births and several post-birth health issues which can ultimately result in an untimely death. Further, recent estimates of the effects of PM2.5 exposure in European cities indicate that increased exposure can lead to a reduction in statistical life expectancy of six months or more [53]. Many other potential health impacts have been linked to PM2.5, including its mutagenic properties and connection to immunity disorders, creating the need for further research [54]. Because of these significant health impacts, PM2.5 has replaced PM10 as the preferred indicator in most contemporary studies.

Research on the effects of particle size ranges below PM2.5, known as UFP, is still ongoing. Early results indicate that UFP may be more hazardous than PM2.5 due to their smaller size and large surface-to-volume ratio, which in turn increases their reactivity and allows these particles to easily adsorb other pollutants, and promote their transport into the human body [55, 56]. Further, UFP can enter the body not only through the respiratory tract (from where it can travel to other organs, such as the brain, directly, without going first through the lungs), but also through the skin and eyes. As a result, UFP can cause increased respiratory system diseases in lung disease patients, increased cardiac symptoms in cardiovascular disease patients and leukemia in children, among other impacts. Still, more research is needed to fully understand the effect of UFP on human health. Thus, despite the apparent substantial negative effect on human health [55], UFP will not be considered in this review, which will focus on the impact of PM2.5 on both the outdoor and indoor built environment.

Decreasing occupant exposure to PM2.5 while simultaneously providing a comfortable indoor environment at a low energy cost requires innovative solutions, which in turn can only originate from a thorough understanding of the interaction of buildings with their local environment. This review of existing studies of the impact of PM2.5 in the urban built environment aims to answer some of the many questions that face the building design research community when dealing with this problem:

- Section 2.1: What are the main sources and sinks of PM2.5 in urban environments?
- Section 2.2: What exposure limits are currently applicable in different parts of the world? What is the expected evolution of these limits?
- Section 2.3: What are the main sources and sinks of PM2.5 in the indoor environment? What is the average ratio between indoor and outdoor PM2.5 in different types of buildings?
- Section 2.4: What are the most common approaches used to predict indoor PM2.5 levels?
- Section 2.5: What are the main health and socio-economic impacts of the exposure to PM2.5?
- Section 2.6: What solutions have been proposed to minimize indoor exposure and its resulting impacts?

The following sections of this review answer each of these questions. The origin of fine particle pollution in the urban environment is described in Section 2.1, as well as the effect of local climate and topography on PM2.5 levels. Section 2.2 outlines the regulations and guidelines set by national regulators and international organizations to limit the exposure to PM2.5. Section 2.3 discusses the main sources and sinks of PM2.5 in the indoor environment, along with a survey of measured indoor/outdoor PM2.5 concentration ratios. Section 2.4 discusses the simulation models most commonly used to predict indoor PM2.5 levels. Health impacts, as well as the social and economic consequences that arise from the continued exposure to fine particle pollution are enumerated in Section 2.5. Finally, Section 2.6 presents several solutions that have been projected and applied to reduce PM2.5 levels both in the outdoor and indoor environments.

2.1. PM2.5 in the Outdoor Environment

Particles in the PM2.5 range can be directly emitted into the atmosphere, a process known as primary PM2.5, or result from chemical reactions involving precursor gases (secondary formation of PM2.5 [57]). PM2.5 is composed of water-soluble ions, including sulfate, nitrate and ammonium compounds (collectively known as SNA), carbon-based compounds, including elemental and organic carbon, trace elements, organic compounds such as oxygenated volatile organic compounds and polycyclic aromatic hydrocarbons (OVOC and PAH), reactive oxygen species (ROS), water, and inhalable microorganisms [58]. Of these components, SNA, elemental and organic carbon and water form most of the PM2.5 mass that is commonly found in urban outdoor environments.

Motor vehicle traffic is one of the most significant primary PM2.5 sources, contributing with exhaust fume particles (mainly diesel soot), particles that originate from brake and tire wear, and re-suspension of particles that have previously settled on the road surface [59, 60]. Globally, traffic is responsible for approximately one quarter of the urban PM2.5 concentrations, although in South and Southeast Asia, South America and Southwest Europe, traffic's share of PM2.5 concentration reaches 30 to 37 %. In most developed countries, industry and power generation are no longer located within major cities and thus contribute to only 15 % of the PM2.5 levels found in these urban environments. In contrast, industry and power generation are still significant sources (27 to 34 %) of PM2.5 pollution in South Asia, Southern China, Japan and the Middle East.

PM2.5 emission due to domestic fuel burning has also decreased in most developed countries and currently accounts for 20 % of global urban PM2.5. Still, it is the most significant source in Central and Eastern Europe and in Africa (32 to 34 %). Anthropogenic secondary particle formation, such as the oxidation of sulfur and nitrogen oxides into ammonium sulfate and nitrate, respectively [57], accounts for 22 % of urban PM2.5 worldwide. However, in most developed nations, including the Republic of Korea, Canada, the United States and Western Europe, this fraction increases to between 44 and 62 %.

PM2.5 can also originate from natural sources, which include dust from non-urban and non-agricultural soils, sea salt, combustion emissions from wildfires and particles that result from the oxidation of volatile organic compounds from vegetation [57, 61]. These natural sources account for 18 % of the total global PM2.5 levels. Japan and the Middle East are the only regions where natural sources are the most significant source of urban PM2.5 pollution (42 to 52 %) [62].

Although urban PM2.5 has a mostly local and anthropogenic origin [63, 64, 65, 66], local topography and climate affect urban PM2.5 levels, namely by facilitating or barring the dispersion of the locally generated particles. Local mountain ranges limit the dispersion of PM2.5, as shown by the decrease of the concentration of PM2.5 with altitude [67]. Locations surrounded by both mountains and water bodies experience an alternation of sea-land breezes and mountain flows which prevents particles from being swept away, an effect seen in places such as Los Angeles (United States) [68], Seoul (Republic of Korea) [69] and Santa Cruz de Tenerife (Spain) [70]. Local vegetation has also been found to decrease PM2.5 levels, by both intercepting and accumulating particles [71, 72]. In the absence of natural obstacles, high wind speeds typically result in cleaner air, therefore reducing PM2.5 levels [64, 71, 73, 74, 75, 76, 77]. Nonetheless, a combination of no natural obstacles, high wind speeds and other dispersion-favorable conditions can allow the transport of PM2.5 over hundreds of kilometers. Noticeable examples include the transport of PM2.5 from the Ukraine, Belarus and Russia to Finland [78], from China to Japan and the Republic of Korea [79, 80], from Northern China to the East China Sea region [81], from Eastern Siberia (Russia) to Japan [82], from Asia to North America [83] and from Northern Quebec (Canada) to the Northeastern states of the US [84].

Precipitation lowers PM2.5 levels, by both depositing particles that are suspended in the atmosphere and removing those that have settled on surfaces, avoiding their future re-suspension [71, 74, 75, 76, 85, 86, 87, 88]. On the other hand, low atmosphere inversion layers, which are stable atmospheric layers characterized by an increase in temperature with altitude and low wind speeds, do not allow pollutants to be swept away, therefore effectively trapping the locally generated PM. These inversion layers occur frequently in several cities during part [3, 75, 87, 89] or throughout the year [68, 74, 76, 90], driving the increase of urban PM2.5 levels.

No consistent pattern has been found between outdoor air temperature and PM2.5 levels. The increase in temperature can enhance secondary photochemical reactions, which increases the concentration of PM2.5 [76, 80, 91]. However, lower temperatures are correlated with an increase in fossil fuel and biomass combustion and with stagnant atmospheric conditions, therefore also increasing the concentration of PM2.5 [57, 87, 89]. Humidity also has no consistent correlation with PM2.5. Some components of PM2.5, such as nitrates and sulfates, see their concentration increase with relative humidity, while the concentration of other components, such as organic and elemental carbon, decreases with higher humidity levels [80, 85, 92]. Additionally, higher humidity levels can lead to precipitation, which, as already mentioned, decreases overall PM2.5 levels [71].

Periodic variations in PM2.5 levels can be seen in most urban locations, a direct consequence of the also periodic nature of local climate and of PM2.5 sources. At the annual scale, the aforementioned increased use of fossil fuel and biomass for heating and electricity production increases particle levels during the colder months of the year in several places, including parts of California [67], Chile [87], India and China [74, 75, 91, 93, 94, 95]. Other seasonal increases in PM2.5 levels include the spring dust storms in North and West China [75, 76] and summer agriculture biomass burning in Southeast Asia [96]. Areas affected by monsoons or heavy storms, such as South and East Asia [75, 76, 86] see a decrease in particle levels due to the high precipitation and wind speeds. Periodic variations at a daily time-scale also occur in many urban areas, with PM2.5 levels peaking during traffic rush hours, namely during the morning and evening [76, 87, 97].

Overall, the main source of PM2.5 in the urban environment is local man-made combustion, due to direct emission of particles and indirect secondary photochemical reactions of precursor gases that result from traffic and domestic fuel burning. Precipitation and wind are the main PM2.5 sinks in the urban environment. Unfortunately, the low wind velocities that are common in most urban areas do not facilitate the removal of the locally generated particles.

2.2. Outdoor PM2.5 Exposure Limits

No PM2.5 exposure threshold has ever been unequivocally described as safe and capable of providing a complete level of protection against all PM2.5-related adverse health effects [98]. Nonetheless, in order to limit the health impacts of fine particle pollution, the WHO has proposed guideline annual and short-term (24-hour) thresholds. In addition to these global standards, the WHO encourages governments to define and enforce national standards [99]. In addition to the guideline levels, the WHO has defined three interim exposure levels with the goal of progressively lowering PM2.5 concentrations. The WHO suggests the annual average to take precedence over the 24-hour average, since sporadic high PM2.5 events are generally less harmful than annual exposure to high PM2.5 levels.

The current WHO's average annual air quality guideline (AQG) is 10 $\mu g/m^3$. Figure 2 and Table 2 show a summary of the annual PM2.5 exposure limits used worldwide. Australia [100] and the Canadian province of British Columbia [101] were the only national and sub-national jurisdictions to be found to enforce a lower standard: 8 $\mu g/m^3$. Canada (at the federal level) [75, 102], Bolivia [103] and Guatemala [103] match the WHO's guideline. Mexico [75, 103], Singapore [75] and the United States (at the federal level [75, 103, 104], in addition to the state of California's own regulation [105]) set their annual standard at 12 $\mu g/m^3$. The WHO's third interim level (IT-3) of 15 $\mu g/m^3$ is equaled by several Central (the Dominican Republic [103, 106], El Salvador [103, 106], Honduras [107], Jamaica [103], Trinidad and Tobago [103] and the American territory of Puerto Rico [106]) and South American (Ecuador [103, 108], Paraguay [103], Peru [109] and the Argentinian federal capital of Buenos Aires [106, 110]) countries, in addition to Albania [111], Bangladesh [75, 112], Japan [75, 113], Jordan [114], Saudi Arabia [115] and Taiwan [116]. In Brazil [75], Bulgaria [117], Chile [75, 103, 118] and South Africa [119] the annual standard is 20 $\mu g/m^3$. The WHO's second interim level (IT-2) is set to 25 $\mu g/m^3$, which is also the standard in most of Europe (the European Union [75, 120], Montenegro [121], Norway [122], the Republic of Kosovo [123] and Russia [75, 124]), in addition to Colombia [75, 103, 125], Mongolia [126], the Philippines [127], the Republic of Korea [128] and Thailand [129]. The WHO's first interim level (IT-1) of 35 $\mu g/m^3$ is also the standard in China (with the exception of areas that warrant special protection, such as nature reserves, where the standard matches IT-1) [75, 130], the Chinese Special Administrative Region of Hong Kong [75, 131] and Malaysia [132]. Rwanda has also defined a national standard at this level, however it is only applicable to industrial areas [133]. Only India [75, 134] and Egypt [75] were found to set national standards above the WHO's interim limits, at 40 and 50 $\mu g/m^3$, respectively.

The WHO's short-term (24 hour) AQG aims to protect against episodic pollution peaks. This limit is currently set to 25 $\mu g/m^3$, and no current national standard is stricter than this guideline. The 25 $\mu g/m^3$ limit is used by Australia, Bolivia, Guatemala and British Columbia (Canada). Canada (28 $\mu g/m^3$), Paraguay (30 $\mu g/m^3$) and Japan, Russia, Saudi Arabia, Taiwan, the United States and Puerto Rico (United States) (35 $\mu g/m^3$) enforce standards between the WHO's AQG and IT-3. Singapore is the only nation to set a standard at the WHO's IT-1: 37.5 $\mu g/m^3$. Bulgaria and South Africa (40 $\mu g/m^3$) and Mexico (45 $\mu g/m^3$) follow, while Chile, Colombia, Ecuador, Mongolia, the Philippines, the Republic of Korea and Thailand match the WHO's IT-2: 50 $\mu g/m^3$. Brazil and India set their 24-hour standard to 60 $\mu g/m^3$. In Bangladesh, the Dominican Republic, El Salvador, Honduras, Jamaica, Jordan, Peru, Trinidad and Tobago and Buenos Aires (Argentina) the 24-hour standard is 65 $\mu g/m^3$, while in Albania it is 66 $\mu g/m^3$. China, Malaysia and Hong Kong (China) repeat their IT-1-grade standards (75 $\mu g/m^3$), while Egypt defined a standard above those recommended by the WHO (80 $\mu g/m^3$). The European Union, Montenegro, Norway, the Republic of Kosovo and California (United States) have not defined a 24-hour standard. Figure 3 and Table 3 summarize these national 24-hour standards.

Table 2 – Annual mean PM2.5 standards (applicable to urban areas) and comparison with WHO guideline and interim limits; supra and subnational jurisdictions are in italic

Annual Mean [µg/m^3]	**Countries or Jurisdictions**
8	Australia, *British Columbia (Canada)*
10 (WHO AQG)	Bolivia, Canada, Guatemala
12	*California (United States)*, Mexico, Singapore, United States
15 (WHO IT-3)	Albania, Bangladesh, *Ciudad Autónoma de Buenos Aires (Argentina)*, Dominican Republic, Ecuador, El Salvador, Honduras, Jamaica, Japan, Jordan, Paraguay, Peru, *Puerto Rico (United States)*, Saudi Arabia, Taiwan, Trinidad and Tobago
20	Brazil, Bulgaria, Chile, South Africa
25 (WHO IT-2)	Colombia, *European Union*, Mongolia, Montenegro, Norway, Philippines, Republic of Korea, Republic of Kosovo, Russia, Thailand
35 (WHO IT-1)	China, *Hong Kong (China)*, Malaysia
40	India
50	Egypt

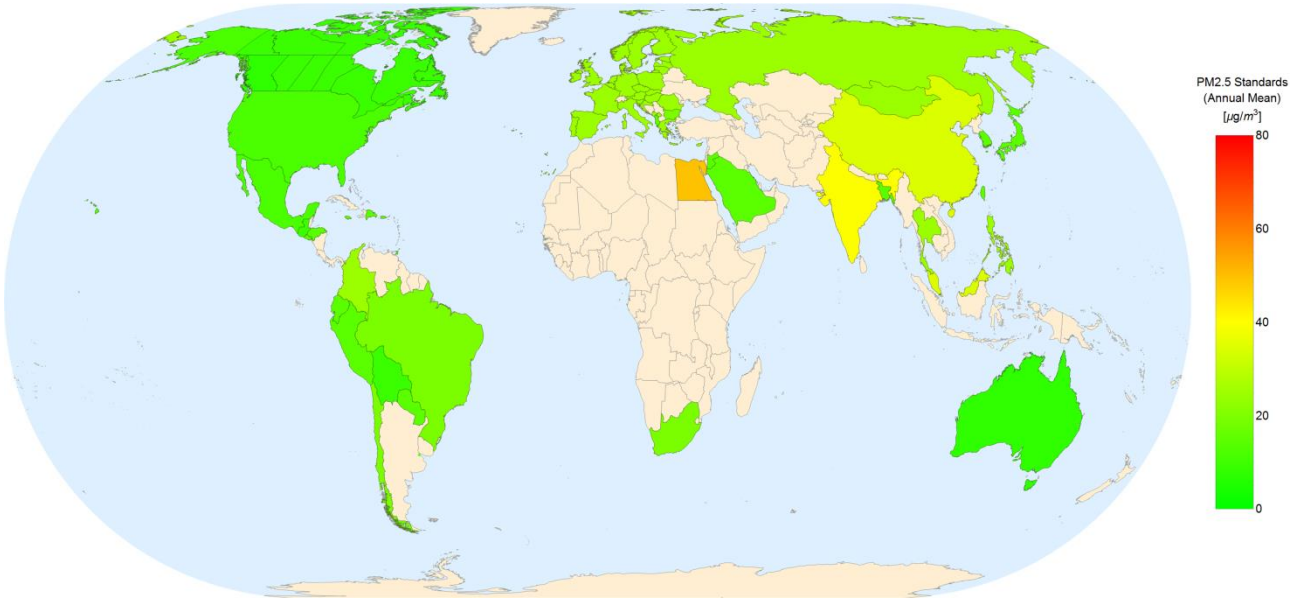

Figure 2 – Annual mean PM2.5 standards (applicable to urban areas)

Table 3 – 24-hour mean PM2.5 standards (applicable to urban areas) and comparison with WHO guideline and interim limits; supra and subnational jurisdictions are in italic

24-Hour Mean [µg/m^3]	**Countries or Jurisdictions**
25 (WHO AQG)	Australia, Bolivia, *British Columbia (Canada)*, Guatemala
28	Canada
30	Paraguay
35	Japan, *Puerto Rico (United States)*, Russia, Saudi Arabia, Taiwan, United States
37.5 (WHO IT-3)	Singapore
40	Bulgaria, South Africa
45	Mexico
50 (WHO IT-2)	Chile, Colombia, Ecuador, Mongolia, Philippines, Republic of Korea, Thailand
60	Brazil, India
65	Bangladesh, *Ciudad Autónoma de Buenos Aires (Argentina)*, Dominican Republic, El Salvador, Honduras, Jamaica, Jordan, Peru, Trinidad and Tobago
66	Albania
75 (WHO IT-1)	China, *Hong Kong (China)*, Malaysia
80	Egypt

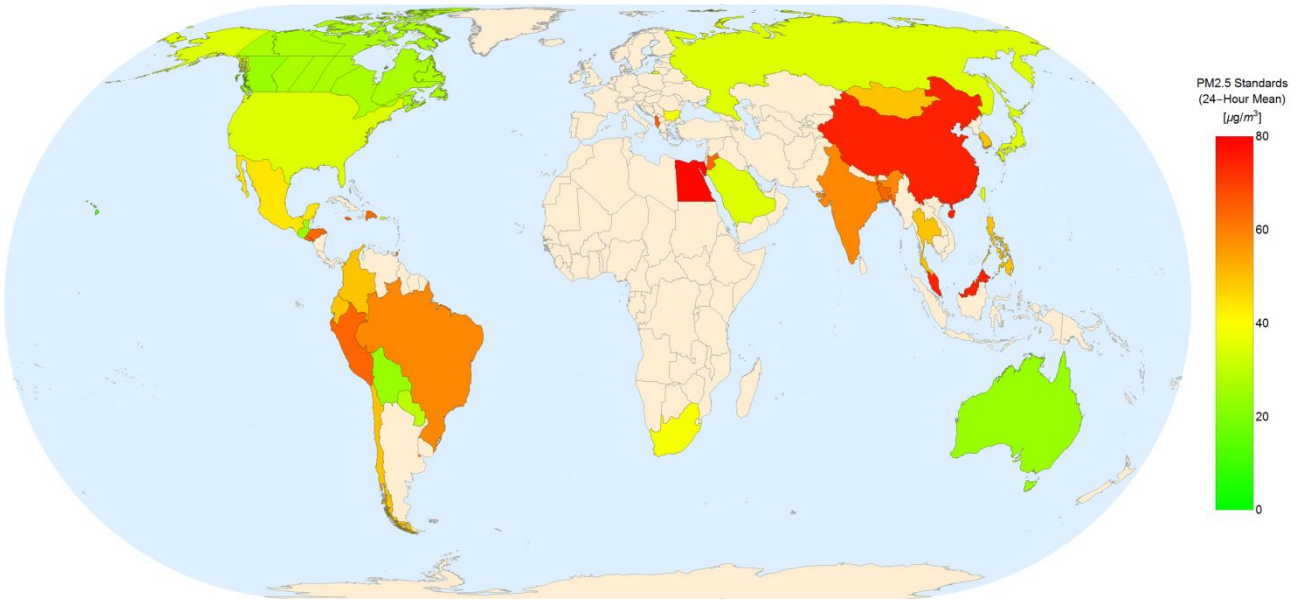

Figure 3 – 24-hour mean PM2.5 standards (applicable to urban areas)

Most countries only update their national standards whenever deemed necessary by their governments and respective advisors and have no prediction on future limits. However, a select number of countries already include a projected decrease in their national PM2.5 standards (Figure 4). Australia will decrease their Ambient Air Quality Measure annual limit from 8 to 7 μg/m^3 and their 24-hour limit from 25 to 20 μg/m^3, by the year of 2025. In 2020, the annual threshold of the Canadian Ambient Air Quality Standards will fall from 10 to 8.8 μg/m^3 and the 24-hour threshold will decrease from 28 to 27 μg/m^3. The European Union, Montenegro, Norway and the Republic of Kosovo will all decrease their annual PM2.5 limit from 25 to 20 μg/m^3, in 2020. Both Malaysia and South Africa predict a two-step decrease. The African nation already decreased their Air Quality Act's annual limit from 25 to 20 μg/m^3 and their 24-hour limit from 65 to 40 μg/m^3, in 2016. In 2030, these will again decrease to 15 and 25 μg/m^3, respectively. In Malaysia, the Ambient Air Quality Standard will be decreased from the current annual threshold of 35 μg/m^3 to 25 μg/m^3, in 2018, and to 15 μg/m^3, in 2020. In the same time periods, the 24-hour threshold will also decrease from the current 75 μg/m^3 to 50 μg/m^3 and then to 35 μg/m^3, respectively.

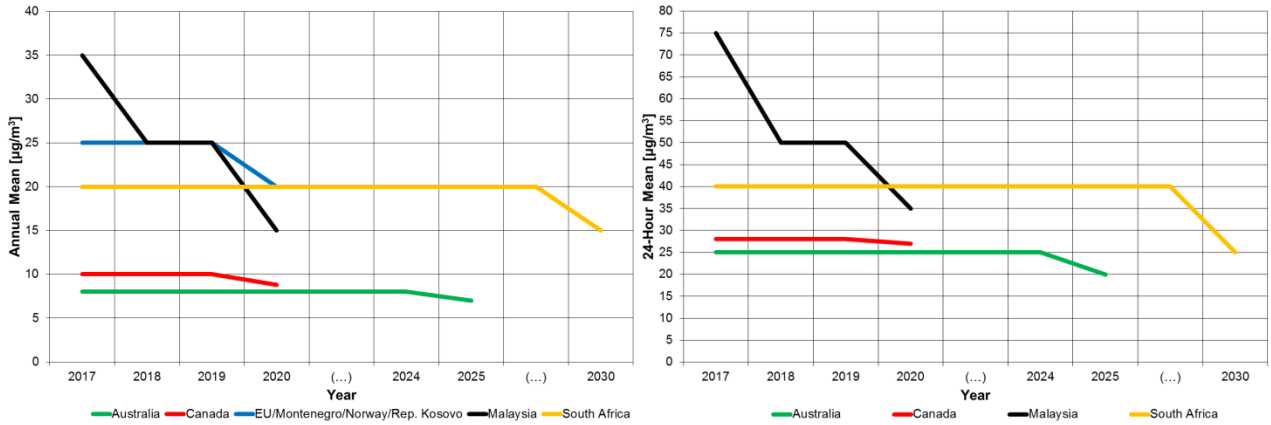

Figure 4 – Evolution of annual and 24-hour mean PM2.5 standards

As can be seen in Figure 2 and Table 2, the strictest annual PM2.5 standards can be found in Australia and in both North and Central America. On the opposite side are the standards found in China, Malaysia, India and Egypt. Further, the standards that are enforced in most of Europe are less demanding than those in less economically developed countries, notably Bangladesh, South Africa and most of Central and South America. This has led to criticism in previous studies [135]. No standards were found for most of Africa and Asia. Although several countries have predicted a reduction in their acceptable outdoor PM2.5 levels, only Australia and Canada will enforce PM2.5 levels below the WHO guideline. Moreover, the Malaysian standard predicts a significant decline, as both the annual and 24-hour PM2.5 levels will be decreased to less than half of the current values by 2020.

2.3. Indoor Environment

In the modern urban environment, people spend most of their time indoors, whether at home, at work, at school or even when engaging in leisure activities [3, 4]. Thus, understanding the relation between the indoor and outdoor PM2.5 levels is the key to characterize exposure. The building envelope is an interface and a filter between indoor and outdoor environments and, in the absence of significant internal sources, indoor levels are expected to be lower than outdoors.

Particles in the outdoor environment are brought indoors by airflow, namely through a combination of infiltration, natural and mechanical ventilation. A small fraction of particles transported by the infiltration airflow through cracks and other unintended small openings do not fully transverse those openings, however nearly all sub-micrometer particles and above 70 % of those between 1 and 2.5 μm in diameter do penetrate into the indoor environment [136]. In the case of MV, cloth filters can be used to limit the penetration of PM2.5. These filters can reach high PM2.5 retention rates, albeit at the cost of a very high pressure load, which increases the power-consumption from the ventilation fans. As for NV, airflow is driven by a low pressure difference, which does not allow for the use of cloth-based air filtration. As a result, in NV systems, outdoor PM2.5 is free to enter the indoor environment without obstruction.

PM2.5 can also be generated in the indoor environment. The combustion of coal [137, 138, 139], wood [140, 141] and other biomass fuel [142, 143, 144, 145] for heating and cooking is an important source in residential buildings. Smoke can be emitted both directly into the home and indirectly, since smoke emitted to the outside can re-enter the building through the infiltration airflow [99]. Cooking also contributes to indoor PM2.5 emissions in homes, restaurants and cooking areas in other building typologies (offices, schools, etc.), since food preparation at high heat leads to the emission of water vapor and other solid and liquid particles [146, 147, 148]. Other combustion instances, such as the use of incense [149, 150], candles [146] and cigarettes [151], also emit PM2.5 into the indoor environment. Printers (and similar devices, such as fax machines or photocopiers) [146, 152] and chalkboards [141, 153] increase PM2.5 levels in schools and office spaces. Other indoor PM2.5 sources include anti-insect [154] and electric air freshener devices [151], as well as cleaning agents and cosmetics [151, 155], such as perfumes and hair sprays [146]. In addition to these sources, one of the most common contributors to high indoor PM2.5 levels in all buildings is the re-suspension of particles that have previously settled onto surfaces [156, 157]. This re-suspension is promoted by occupant movement and, therefore, is most relevant in indoor environments where movement is frequent, such as residential buildings and schools [146, 158, 159, 160]. Surprisingly, cleaning activities, such as sweeping, dusting or vacuum cleaning, can also contribute to re-suspend settled particles [146, 158].

The ratio between indoor and outdoor PM2.5 concentrations, known as I/O, is a simple indicator that provides a preliminary evaluation of the building's indoor PM2.5 pollution [3]. Figure 5 shows the range of measured I/O ratios according to building typology, ventilation strategy and strength of internal PM2.5 sources.

In naturally ventilated buildings with low internal particle sources, the average I/O ratio is close to one, that is, indoor and outdoor PM2.5 concentrations are identical [56, 74, 152, 161, 162, 163, 164, 165, 166, 167, 168, 169, 170]. Also, as expected, without the influence of internal sources, the indoor concentration is dominated by the outdoor concentration, as indicated by the high correlations between both concentrations [56, 163, 164, 165, 171]. However, when significant indoor sources are present, the correlation is lower and the I/O ratio is nearly double, on average, than that ratio in buildings with no indoor sources [51, 147, 158, 172, 173, 174]. The difference in I/O ratio was especially evident in studies that measured buildings with both low and high internal particle sources [146, 153, 172, 175].

Similarly, in mechanically ventilated buildings, the existence of internal sources [146, 152, 155] also increases the average I/O ratio relative to buildings without those sources [146, 147, 152, 159, 168, 175, 176, 177], albeit to a lesser extent: 25 % on average. In these cases, the ventilation system's filter efficiency plays a very significant role in limiting the penetration of outdoor particles: the I/O ratio in buildings that are equipped with high-efficiency filters were on the lower end of the spectrum, while buildings without any filter or with a low-efficiency or damaged one presented I/O ratios closer to those found in buildings that used natural ventilation [167, 177, 178].

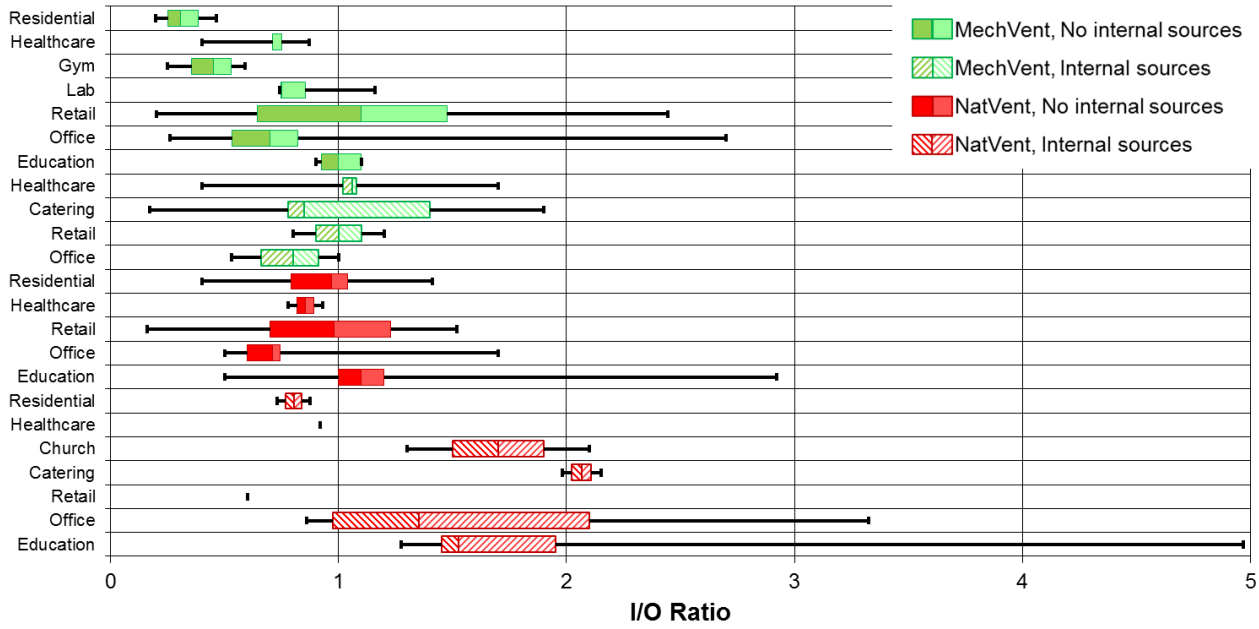

Figure 5 – Selection of studies with PM2.5 I/O ratios by building typology, ventilation type and existence of internal sources; the box plot represents minimum, 25th percentile, median, 75th percentile and maximum

Table 4 – Average PM2.5 I/O ratios by ventilation type and existence of internal sources

Ventilation	Indoor Sources	Average I/O		Standard Deviation
Mechanical	No	0.77	100 %	0.36
	Yes	0.98	127 %	0.38
Natural	No	0.95	123 %	0.35
	Yes	1.81	234 %	0.95

In summary, the PM2.5 particles that are found in the indoor environment can be brought in by the ventilation airflow or can be internally generated by combustion for both heating and cooking. Table 4 presents the average ratios for naturally and mechanically ventilated buildings. As expected, the ratios for mechanically ventilated buildings are lower, although the difference is only substantial in the cases with significant internal particle sources.

2.4. Simulation of Indoor PM2.5 Levels

Increased awareness on the negative effects of PM2.5 in the built environment resulted in the development of several simulation approaches to predict indoor pollutant levels.

The simplest statistical approaches combine typical I/O ratios with a probabilistic window-use model [20, 179] and are the simplest method to assess indoor PM2.5 levels. In more sophisticated cases, these approaches may integrate land-use [180] and building-use models [181, 182, 183, 184]. This approach does not consider several important factors that affect indoor PM2.5, such as changes in the ventilation airflow rate or the effect of different filtration efficiencies but allow for simple overall estimations of the average indoor PM2.5 levels of a sample of buildings [20].

In order to achieve higher precision in the prediction of PM2.5 levels in a specific building, detailed numerical models, such as CFD or nodal models, are the most common approach. These models take into account particle sources (including re-suspension), particle sinks (which includes the settling of particles onto surfaces), and the transport of particles by air movement between the outdoor and indoor environments and between indoor zones.

CFD models predict whole-field data (air velocity, pressure and PM2.5 concentration) for every simulation cell in the simulation domain, considering sources, sinks and the PM2.5 transport between cells. This allows for a detailed calculation of particle levels within the building, but at a very high computational cost. Consequently, CFD is typically used only when a detailed understanding of particle movement is necessary [185, 186, 187, 188, 189, 190].

In the case of nodal models, a single node is attributed to each indoor zone or room, with additional nodes representing the outdoor environment in each ventilation opening or crack in the building's external surfaces. In each time step, these models can compute the current PM2.5 concentration of each node, by calculating the net sum of all sources, sinks and inter-node transport, which is then added to the PM2.5 concentration of the previous time step. This requires a more detailed input than the simplified approaches, resulting in a more thorough characterization of PM2.5 levels within the building. Nonetheless, this approach's computation cost is lower than CFD, due to the simplification of each zone into a single node.

Available nodal model approaches include both ad-hoc models that are developed for particular simulation cases [152, 191, 192, 193, 194, 195, 196, 197, 198], and software packages, which can be used in different cases. Commonly used packages include CONTAM [199, 200, 201, 202], MATLAB Simulink [203, 204] and the GCA, included within the EnergyPlus thermal simulation software package [205]. All of these software packages combine airflow and pollutant transport models.

Overall, nodal models, which include both ad-hoc models and software packages, are the most commonly used approach to simulate indoor PM2.5 levels, as they allow a thorough characterization of PM2.5 levels in the building with a low computational cost. Nonetheless, further model validation is essential to ensure meaningful results.

2.5. Impacts of the Exposure to PM2.5

Fine particle pollution can enter the body through the inhalation airflow, transverse the respiratory tract and reach the pulmonary alveoli, triggering an inflammatory response from the body along this path and decreasing the immunity system's response capability. Further, once in the lungs, PM2.5 can enter the bloodstream and spread to other organs.

PM2.5 has been associated with several negative health impacts in studies performed throughout the world. Studies in Detroit, Michigan (United States) [206] and Shanghai (China) [207] showed that high PM2.5 levels worsened the symptoms of children affected by asthma. In Tokyo (Japan), PM2.5 contributed to the development of allergic conjunctivitis during the non-pollen season [208], while in Italy, a link to obesity is suggested in a preliminary study [209].

In China, one of the countries with the highest PM2.5 levels [75], studies indicate that PM2.5 was the cause of nearly 1.4 million deaths in 2015 [210] due to stroke (PM2.5 is responsible for 40 % of all stroke deaths in China), acute pulmonary infection (33 %). ischemic heart disease (27 %) and lung cancer (24 %) [211]. As for tuberculosis, a PM2.5 concentration increase of 10 $\mu g/m^3$ during the winter was associated with a 3 % increase in cases during the following spring and summer, in Beijing and Hong Kong [212, 213]. In total, 15.5 % of all deaths in China in 2015 [211] and 32 % of the deaths in its major cities in 2013 [214] have been attributed to PM2.5. The increased mortality and the reduction in working hours due to hospital admissions and visiting time resulted in an estimated economic cost of nearly 350 billion Chinese yuan (about 1 % of the national GDP) in 2007. PM2.5 deaths and morbidity mostly affect manufacturing jobs (38 to 51 % of the affected workers), with the remainder of affected people working in service, natural resources, mining and construction [215]. During the month of January of 2013, 690 deaths, 45 thousand acute bronchitis and 24 thousand asthma cases were attributed to a haze event in Beijing, with a total cost of over 250 million US dollars [216]. Additionally, a 1 $\mu g/m^3$ increase in the concentration of PM2.5 is expected to cause a per capita increment of 1.3 US dollars in economic losses [217]. As for the Yangtze River Delta region, over 13 thousand people died in 2010 due to short-term exposure to PM2.5, resulting in an economic cost of 22 billion Chinese yuan [218].

In Europe, despite the lower levels, PM2.5 is still the cause of illnesses, deaths and a financial burden. In the Netherlands, a concentration increase of 10 $\mu g/m^3$ relative to the previous day was correlated with a 0.8 % risk increase in all-cause mortality [219]. The death of 3500 people between 2000 and 2009 in Madrid (Spain) was attributed to PM2.5 [220], as was an increase in emergency hospital admissions in result of aggravated Alzheimer's disease symptoms [221]. The increase in PM2.5 emissions due to biomass burning during the 2012-2013 winter in Thessaloniki (Greece) resulted in new cases of chronic bronchitis and cardiovascular and respiratory diseases, ultimately leading to 200 excess deaths and an economic cost between 200 and 250 million euros [222]. A 23 % growth in the incidence of total anterior circulation infarcts is the result of an interquartile range increase in PM2.5 in South London (United Kingdom) [223]. In Jeddah (Saudi Arabia), PM2.5 has been found responsible for an annual death rate of 1100 people [224].

In the Santiago Metropolitan Area (Chile), a 10 $\mu g/m^3$ increase in PM2.5 concentrations was associated with a 1.3 % increase in hospital admissions due to stroke [225], while in Canada, the same increase over two years results in an increased risk of diabetes (5.3 %), asthma (2.2 %) and high blood pressure (8.3 %) [226]. A proposed retrofit of 10 % of California's (USA) current office building stock to use natural ventilation was shown to result in a 99 to 155 million US dollar-increase in healthcare and mortality costs, due to total mortality, chronic bronchitis, asthma attacks, restricted activity days, strokes, respiratory costs and hospital admissions [20].

Additionally, these negative health effects and financial costs do not affect the population equally, due to the different exposure levels, immunity response, vulnerability to disease and access to healthcare. Young children are especially susceptible to respiratory illnesses [206, 207, 227, 228], while the elderly are mostly affected by cardiovascular disease [227, 229]. Further, people with a lower socioeconomic status, especially those that live in slums, are at a higher risk of exposure to PM2.5. This occurs due to the combined higher indoor use of biomass fuels and substandard housing, which in turn allows a higher infiltration rate of outdoor particles into the indoor environment [230]. Further, this increased exposure mostly affects women and children, especially in the poorer communities, as they are frequently in proximity of indoor PM2.5 sources, namely biomass or coal for cooking and heating [99, 231].

Thus, exposure to PM2.5 leads to significant health impacts, mainly causing cardiovascular and pulmonary diseases. These impacts, in turn, place a significant financial burden, not only on those that are directly affected, but also on the community, namely due to health costs, work absence and increased mortality. Further, this burden has a more negative affect on the communities with a lower socioeconomic status, which are also those that are typically more exposed to PM2.5, which only furthers the negative effects of the exposure to PM2.5.

2.6. Minimizing Indoor Exposure to PM2.5

There are several solutions to limit the exposure to PM2.5 that have been proposed and implemented throughout the world. These solutions can be categorized in accordance to the method used to limit exposure: reducing outdoor PM2.5 sources, reducing indoor PM2.5 sources and reducing the penetration of outdoor PM2.5 into the indoor environment.

Traffic is one of the most significant sources of outdoor PM2.5 and, therefore, has been the focus of several efforts to decrease urban fine particle levels. Progressively stringent emission regulations have forced vehicle manufacturers to decrease the exhaust fume emission of PM2.5. This is achieved by the installation of particle filters, which reduces the direct emission into the atmosphere, and the increase in engine combustion efficiency, which decreases the emission of the gases that are precursors to the formation of secondary particles [71]. The use of cleaner fuels, such as biodiesel, low-sulfur gasoline or natural gas, also decreases precursor gas emissions [58, 71, 80, 232, 233], while vehicles without internal combustion engines do not emit either precursor gases or exhaust particles. Nonetheless, exhaust fumes are not the only source of PM2.5, and hence other measures have also been adopted. Paving unpaved roads, playgrounds, parking lots and other areas, in addition to street cleaning avoids the re-suspension of particles [58, 160, 234]. An increase in urban vegetation can decrease PM2.5 levels [58, 235], although failure to carefully plan the effect of that vegetation can compromise the effectiveness of this approach [236, 237]. Further, limiting vehicle circulation is becoming a common approach to decrease traffic-related PM2.5 emissions. In some locations, vehicles can only circulate every other day, depending on the license plate number [71, 234, 238]. More pollutant-emitting vehicles, such as older (and hence subject to less strict emission regulations) or heavy-duty diesel-powered vehicles, are only allowed to circulate during moments of low traffic intensity, such as at night or during the weekend, or not allowed at all [76, 239, 240]. The time-limited ban, however, might not decrease overall PM2.5 levels, especially if the PM2.5 that is emitted during the allowed periods remains in the atmosphere. In the future, it may happen that traffic will be banned altogether, with few exceptions, such as residents or emergency services. This leads to a shift to soft modes of transport, such as walking or bicycle-riding [241, 242, 243], or to public transport, which itself can be based on low PM2.5-emitting vehicles, such as electric trains or buses. In addition to the decrease in PM2.5 levels, this also brings forth several other additional benefits, such as the increase in physical activity and its consequential health benefits, and the decrease in traffic intensity, which itself reduces noise and traffic-related stress and incidents [62, 241].

Especially in places where industry and power generation are significant PM2.5 sources, several steps can be taken to decrease their negative impacts. In the case of industry, a shift to cleaner fuels and the use of particle filters decrease the emission of PM2.5 into the atmosphere [62, 238, 244]. Particle filters are also an option in fossil-fuel based power generation, but a shift to cleaner and renewable energy sources should be the main focus [71]. Additionally, limiting outdoor biomass combustion, such as straw burning, and wildfire prevention are fundamental steps to decrease overall urban PM2.5 emissions [71].

Controlling indoor PM2.5 sources is an essential step to reduce building occupant exposure to PM2.5. Firewood combustion for cooking and heating can be replaced with cleaner fuels, such as natural or liquefied petroleum gases (LPG), or with electric equipment [139, 142, 143, 144]. Alternatively, high-efficiency biomass-based heating systems with good extraction ventilation can also decrease PM2.5 emissions into the building [245, 246]. Different cooking methods and ingredients, such as preferring safflower oil over olive oil [247] or adding salt and pepper in the early stages of cooking [248], can also reduce the emission of PM2.5. Additionally, some ingredients might increase individual self-protection against the negative effects of PM2.5 [249]. Good extraction ventilation is also fundamental in the case of indoor sources that cannot be easily replaced or forgone, such as cooking or printers and similar devices [250]. Nonetheless, the use of the latter can be decreased by replacing paper with low power-consuming electronic devices [251]. Dust re-suspension

can be prevented through cleaning, although, if done carelessly, it can lead to an increase in unwanted airborne PM2.5 levels due to re-suspension. Finally, portable air cleaners, which are devices that consist of a fan and a filter (either a high-efficiency cloth filter or an electrostatic filter [252, 253, 254, 255, 256, 257, 258, 259, 260, 261] or even botanical elements [262]), actively decrease PM2.5 levels, by circulating indoor air through that filter. Portable air cleaner units equipped with High Efficiency Particulate Arrestance (HEPA) filters typically achieved the highest clean air delivery rates, while those with electrostatic filters usually had lower power consumptions, although they can increase indoor ozone and ultrafine particle levels [255, 258]. Additionally, the portable air cleaners' efficacy is sensible to its location within the building and to the interaction between its own airflow and that of other sources [263, 264, 265].

Finally, the building skin, as an interface between the indoor and outdoor environments, can also play a significant role in reducing indoor PM2.5 levels, by limiting the penetration of outdoor particles. First of all, careful urban planning can avoid buildings with sensitive occupants, such as schools or hospitals, to be located nearby main PM2.5 sources, such as high traffic-intensity highways [60, 160, 231, 266]. Additionally, moving people from slums to proper housing [231] and improving existing buildings' air tightness [267, 268] decreases the penetration of outdoor particles, including the re-entering of indoor-generated PM2.5 that has been extracted to the outdoor environment.

As for the building itself, one of the most commonly used methods is the use of a cloth filter in the MV system. A wide range of PM2.5 retention efficiencies can be found, with very high-efficiency (above 90 %) filters being used in buildings with sensitive occupants, such as hospitals, or that, for some particular reason, require very low indoor PM2.5 levels [268, 269]. Nonetheless, higher filtration efficiencies imply a higher pressure drop through the filter, requiring a more power-consuming fan [270, 271, 272]. In the case of fossil-fuel based electric grids, this leads to an increase in PM2.5 emissions. Further, these filters' high pressure drop bars its use in natural ventilation systems. Ribbed air ducts can also decrease the transport of outdoor fine particles, although the effect on the airflow itself is yet to be addressed [273, 274]. Localized outdoor PM2.5 removal can also reduce the penetration of outdoor particles, although its application outside of semi-enclosed locations has not yet been considered [275]. Other filter technology, with high-efficiency particle removal and low pressure drops, has been proposed, although their widespread real-case use is yet to be developed [276, 277, 278].

Few approaches have been developed to allow the use of natural ventilation while simultaneously controlling for the penetration of outdoor PM2.5. One novel approach would be the use of electrostatic filters in natural ventilation openings. This type of filter is already used in several other applications and can achieve average PM2.5 filtration efficiencies of up to 63 % [279, 280, 281, 282] at a very low energy cost [283, 284, 285]. These filters consist of a channel with wire-electrodes that generate an electric field, which charges the airborne particles, and charged plates to separate those charged particles from the airflow. The pressure drop through this filter is less than 10 Pa, which could allow its use in natural ventilation. However, this approach has only been considered in simulated environments and lacks field testing as well.

Overall, limiting man-made combustion, namely by decreasing traffic or shifting to cleaner energy sources is the most efficient path for decreasing outdoor PM2.5. The use of cleaner energy sources indoors also decreases PM2.5 levels within the built environment, as does the use of effective extraction ventilation for indoor sources. To limit the penetration of outdoor PM2.5 through the incoming airflow, several innovative solutions are needed. Ultimately, one of the most important steps is to increase public awareness of PM2.5, encouraging people and national governments, on their behalf, to engage in these solutions as well as developing other solutions.

3. SIMULATION TOOLS AND VALIDATION

During the design phase, simulation tools are fundamental to predict the performance of any equipment or passive approaches in order to verify that the building's thermal behavior ensures a comfortable environment for its occupants. In this order, the following sections describe the simulation tools that were used throughout this research. Section 3.1 is a validation of airflow network or nodal models (AFN) and CFD simulations for a naturally ventilated office building using wind tunnel (WT) measurements as the reference for external pressure coefficients and effective airflow rate prediction. This validation focuses specifically on wind-driven cross ventilation with no buoyancy effects. In addition to the validation, this study compares the average window open area required to meet a given target flow rate that is predicted by the two numerical models for a typical weather year. Finally, the CFD simulation model is used to study the effect of partially open windows on the effective flow rate (an effect that typical WT studies fail to capture).

The following Section, 3.2, describes EnergyPlus, which is the software package that was used to simulate indoor thermal environments and the effect of the use of NV on those environments. Finally, Section 3.3 presents the Generic Contaminant Algorithm, the nodal model that is included within the EnergyPlus software package and was used to predict indoor fine particle levels.

3.1. Natural Ventilation Simulation

In contrast with the steady energy source used in mechanical ventilation, the variable pressure differences that drive NV systems make the sizing of ventilation openings a difficult task [286]. The hiatus in NV use in commercial buildings, a consequence of the preferred use of MV systems which resulted in the loss of existing design know-how, has led to currently available simple NV design rules being overly simplistic and conservative. California's Title 24 [9], which limits the use of natural ventilation to office areas that are less than 20 feet (6 meters) away from a façade with operable windows, is an example of these limitations. Yet, it is possible that, in tall rooms, single-sided natural displacement ventilation may provide adequate fresh air beyond 6 m with a window opening area that is less than 5 % [10]. To overcome these restrictions and test new design possibilities engineers need improved airflow simulation tools or, when available, reliable measurements. These tools must incorporate a wide range of factors that affect the variations in pressure distribution around and inside the building, such as building and surrounding geometry, incoming wind and differences between internal and external temperature [287].

Measurements can be performed in scaled wind tunnel models or, in rare instances, in full-scale. Both methods have known limitations. When possible, full-scale measurements would be the ideal choice. However, controlling boundary conditions is very difficult [288, 289, 290]. In contrast, scaled building model boundary layer WT experiments can have clearly defined boundary conditions. Still, this approach can be time-consuming and expensive [291]. Further, downscaling the building apertures is difficult: scaled model walls tend to be disproportionally thick and apertures are usually modeled as fully open holes with variable area. These crude approximations affect the aperture pressure loss [292] and fail to capture the inflow deflection produced by partially open windows [293]. In spite of these limitations, scaled WT measurements are the reference method for building natural ventilation modeling [294], particularly for determining pressure coefficients and effective flow rates in buildings with fully open windows.

Numerical simulation approaches for NV design range from simple AFN to complex three-dimensional CFD simulations (see Table 5). AFN models are based on the orifice flow equation and have low computation time and high numerical stability [295]. As a result, these models are commonly used to predict bulk NV airflow in hourly thermal simulation software tools [15, 296]. In AFN models, wind pressure effects in each external opening are modeled using pressure coefficients (C_p) that can be obtained from WT measurements or CFD simulations. In contrast with AFN, CFD is able to produce whole flow field data in full-scale. For this reason, CFD simulations tend to have high computation time and variable numerical stability. Further, CFD simulation results are sensitive to a large number of user-defined computational parameters. Although there have been continuous improvements in CFD tools, the typical accuracy of this methodology, when applied to NV, remains an open issue [297, 298, 299, 300]. In spite of this, CFD has reached a development stage that makes it a candidate for use as an accessible and flexible virtual wind tunnel, either producing the pressure coefficients that are required for AFN models or the whole flow field for particular wind directions and window configurations.

Table 5 – Natural ventilation modeling methods analyzed in this paper

Method	**Predicted Variables**	**Requirements**	**Effort/Time**
Wind tunnel (WT)	External pressures, Effective airflow rates	Wind tunnel Scaled model	High
Computational fluid dynamics (CFD)	Whole field data (Pressures, velocities, etc.)	CFD model	Medium
Airflow network (AFN)	Bulk airflow rates	Pressure coefficients (C_p from WT or CFD)	Low (when C_p is available)

3.1.1. Numerical Simulation Tools

The standard CFD approach for building natural ventilation design is RANS (Reynolds-averaged Navier-Stokes) combined with different variants of the *k-ε* turbulence model [299]. This approach is the preferred choice due to its robustness [301] and tested precision for different building ventilation applications [302]. In addition to the standard *k-ε* model, variants such as the RNG (Re-normalization Group) *k-ε* model [303], the realizable *k-ε* model [304], and the *k-ω* model [305] are also being increasingly used in NV applications. These models address several known limitations in the standard *k-ε* model, namely, overestimation of turbulence energy [306] and difficulty in describing flows close to surfaces [307]. In the future, RANS may be replaced by large eddy simulation (LES), a more detailed approach that is based on space filtering of turbulent structures and explicit dynamic modeling of the large eddies. For the time being, RANS is preferred over LES due to its significantly lower computational cost [308, 309].

AFN models use a network of nodes connected by nonlinear pressure dependent flow resistances [295, 310]. A typical AFN model will have one node for each building zone plus a variable number of outside nodes. The bulk airflow rate for a given aperture is calculated from the pressure difference between the zones that the aperture connects. For wind-driven airflow, the incoming flow rate can be calculated using the following variant of the aperture Equation (1) [311]:

$$\dot{V} = A_{open} \times C_D \times u_{wind} \times \sqrt{\Delta C_p} \quad (1)$$

A discharge coefficient (C_D) of 0.6 was used [311]. The non-linear system of *n* equations that results from applying mass conservation to the building zones and *n* building apertures is then solved numerically. An average pressure coefficient was calculated for each side of the building and used within a single equation. These pressure coefficients (C_p), are defined as the ratio of local wind-driven static pressure and the incoming wind pressure, as shown in Equations (2) and (3) [312]:

$$C_p = \frac{p_{local}}{p_{wind}} \quad (2)$$

$$p_{wind} = \frac{\rho \times u_{wind}^2}{2} \quad (3)$$

The upcoming subsections present existing comparisons between CFD, AFN and WT, for three relevant flow parameters:

- Pressure coefficients: comparison between CFD and WT.
- Effective airflow rates: comparison between CFD and WT.
- Bulk airflow rates: comparison between CFD and AFN.

The accuracy of the numerical simulation methods will be assessed using the coefficient of determination, R^2, (Equation (4)) and an average normalized error (Equation (5)), defined as follows:

$$R^2 = 1 - \frac{\sum_{i=1}^{N_{meas}} (y_i - \hat{y}_i)^2}{\sum_{i=1}^{N_{meas}} (y_i - \bar{y})^2} \tag{4}$$

$$Average\ Error = \frac{\sum_{i=1}^{N} \frac{|y_i - \hat{y}_i|}{N_{meas}}}{\sum_{i=1}^{N} \frac{|y_i|}{N_{meas}}} \tag{5}$$

3.1.1.1. Pressure Coefficients

Eight previous studies that compare pressure coefficients obtained from CFD with WT measurements were identified (Table 6). The average errors found in these studies vary between 7 and 47 % and the R^2 values between 0.420 and 0.995. A more detailed analysis reveals a higher agreement for cases with normal or near-normal incoming wind (the first six studies in the table [313, 314, 315, 287, 316, 317]. Cases with more complex building geometry or a wider range of incoming wind angles display a lower accuracy [303], with the largest error found in a case with several near buildings and multiple incoming wind angles [318].

Table 6 – R^2 and average error between WT and CFD pressure coefficients for previous studies

Ref.	Case Study/Turbulence Model	Wind Angle (normal = 0°)	R^2	Average Error [%]
[313]	Isolated wind tower Standard *k-ε* model	0°	0.995	7
[314]	Isolated real-shaped building Reynolds Stress model	0°	0.995	9
[316]	Cube-shaped isolated building RNG *k-ε* model/Standard *k-ε* model	0°	0.972 (RNG) 0.847 (Standard)	13 (RNG) 33 (Standard)
[287]	Isolated real-shaped building Realizable *k-ε* model	0° and 45° to surface	0.985	14
[317]	Venturi-shaped roof RNG *k-ε* model	0° to 45° to surface, 15° interval	0.974	11
[315]	Isolated real-shaped building RNG *k-ε* model/Standard *k-ε* model	0° and 45° to surface	0.960 (RNG) 0.912 (Standard)	21 (RNG) 25 (Standard)
AVERAGE ERROR (incoming wind angles between 0 and 45° to surface)				**17**
[303]	L and U-shaped isolated building RNG *k-ε* model	0°, 45° and 180° to surface (Three)	0.932	23
[318]	Building with near interference RNG *k-ε* model	0° to 345° to surface, 22.5° interval (Sixteen)	0.420	47
AVERAGE ERROR (studies including all incoming wind angles)				**35**

3.1.1.2. Effective Airflow Rates

Due to non-homogeneous mixing between the airflow entering the room and existing room air, effective flow rates are lower than the bulk airflow through the building's openings. In NV design, CFD simulations are often used to calculate the effective airflow rate in specific room locations. The most commonly used methodology to calculate the effective flow rate is the concentration decay method. Starting with an evenly distributed non-buoyant pollutant concentration, this method determines the effective flow rate by finding the best fit between the pollutant decay curve and the solution of the concentration decay (Equation (6)) [312]:

$$k(t) = k_0 \times exp\left(-\frac{\dot{V}}{V} \times t\right) \quad (6)$$

The results of two existing studies that compare CFD and WT effective airflow rate are shown in Table 7. Due to the higher complexity that results from the inclusion of internal partitions, the second case has a much lower correlation. Further, a more detailed analysis of the results revealed that, as in the case of pressure coefficients, smaller incoming wind angles (0-30°) lead to lower discrepancies: as the incoming wind angle approaches 90°, the airflow deviates from cross-ventilation and begins to resemble shear-driven ventilation. Due to the difficulty of CFD to model this type of ventilation, the disparity between CFD and WT effective flow rates increases for these cases.

Table 7 – R^2 and average error between wind tunnel and CFD effective flow rates for previous studies

Ref.	**Case Study/Turbulence Model**	**Wind Angle (normal = 0°)**	R^2	**Average Error [%]**
[311]	Isolated building Standard k-ε model/RNG k-ε model	0° to 90° to surface, 10° interval (Ten)	0.613 (Standard) 0.541 (RNG)	32 (Standard) 33 (RNG)
[305]	Cube-shaped isolated building with inner divisions Standard k-ω model	0° to 90° to surface, 30° interval (Four)	–0.296	29
			AVERAGE ERROR	**31**

3.1.1.3. Bulk Airflow Rates

Bulk flow rates are usually not measured in WT studies because it is impossible to insert a velocity sensor in the small openings that are used without affecting the flow. Further, a set of measurements in known locations in the window plane would be required for an accurate flow measurement.

This review identified two studies comparing flow rates predicted by CFD with AFN predictions (using WT pressure coefficients), which are presented in Table 8. As in the previous cases, configurations with incoming wind angles that are closer to normal incidence [310] have significantly better results: 6 % average error, versus 28-34 %.

Table 8 – R^2 and average error between AFN and CFD bulk flow rates for previous studies

Ref.	**Case Study/Turbulence Model**	**Wind Angle (normal = 0°)**	R^2	**Average Error [%]**
[310]	Cuboid-shaped isolated buildings WT C_p Standard k-ε model	0° and 45° to surface (Two)	0.944	6
[311]	Isolated building WT C_p Standard k-ε model/RNG k-ε model	0° to 90° to surface, 10° interval (Ten)	0.679 (Standard) 0.688 (RNG)	28 (Standard) 34 (RNG)
			AVERAGE ERROR	**23**

3.1.2. Case Study and Methodology

This section presents the present case study: a two-story 940-square meter office building located in Alameda, California (15 km from San Francisco). The focus of this validation study is the open-plan, 109-square meter office room on the second floor of the building shown on the right-hand side of Figure 6. The following subsections describe the models used to simulate this room and the methodology employed in this study.

Figure 6 – Aerial view (left), wind tunnel model of the main building and surrounding buildings (right)

3.1.2.1. Wind Tunnel Measurements

The wind tunnel model used in this study was built and measured by CPP Wind [319]. The model is a 1:70-scale replica of the building and its immediate surroundings, within a 100-meter ratio. The modeled room has four openings, labeled W1 to W4, as can be seen in Figure 7. Each window has an opening area of 1.66 cm^2, leading to wall porosity of 0.54 %. To simulate the variable incoming wind direction (0° to 345°, in 15° intervals) the model is placed on a rotary table. A logarithmic incoming wind profile was used [320], with a wind velocity of 8.148 m/s at 0.202 m and a surface roughness of 4.36 mm (Table 9). Similarity requirements were ensured to be in accordance with existing modeling guidelines [321, 322, 323, 324].

Table 9 – Wind tunnel velocity and turbulence intensity profiles

Height [m]	Velocity [m/s]	Turbulence Intensity [%]
0.076	6.464	23.4
0.103	6.892	22.2
0.126	7.469	22.5
0.154	7.770	21.9
0.202	8.148	19.1
0.253	8.570	18.8
0.305	8.892	18.2
0.405	9.520	18.0
0.510	10.009	16.3
0.610	10.337	16.4
0.814	11.347	15.9
1.066	12.046	13.5
1.218	12.442	12.2

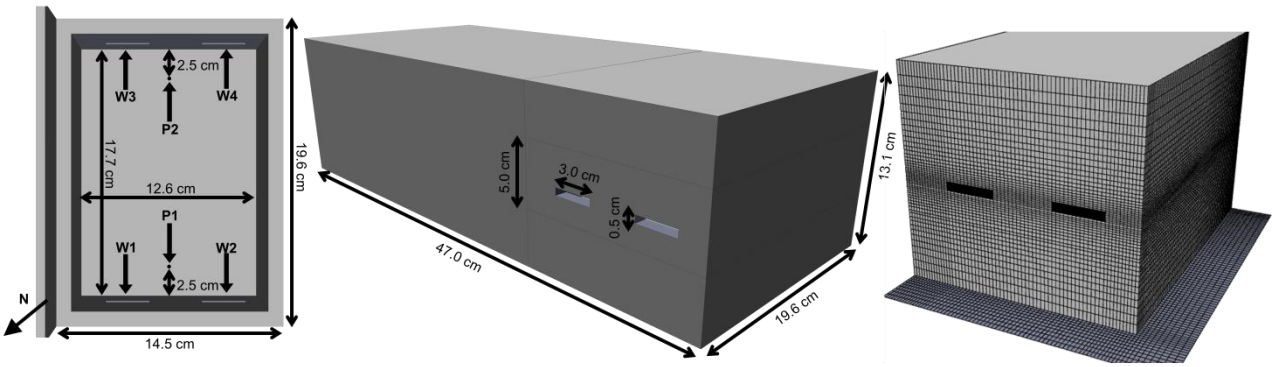

Figure 7 – Building openings layout and concentration measuring points (left), main building model dimensions (center), computational grid surrounding the main building openings (right)

Wind pressure coefficients were measured using an array of six flush surface pressure taps along the edge of each opening. Effective airflow rates were calculated for each wind direction using the concentration decay methodology. Pollution concentration was monitored at 200 Hz with two fast flame ionization detectors (FFID), located at two points, P1 and P2, positioned at mid-height, mid-width and 2.5 cm away from walls.

As can be seen in Figure 8, pollutant concentration between both measurement points differs during the filling phase (when the non-buoyant pollutant source is active). However, once the source is removed, incoming air increases the homogeneity of the pollutant concentration within the building model, leading to a difference of less than 10 % between both points for most incoming wind directions.

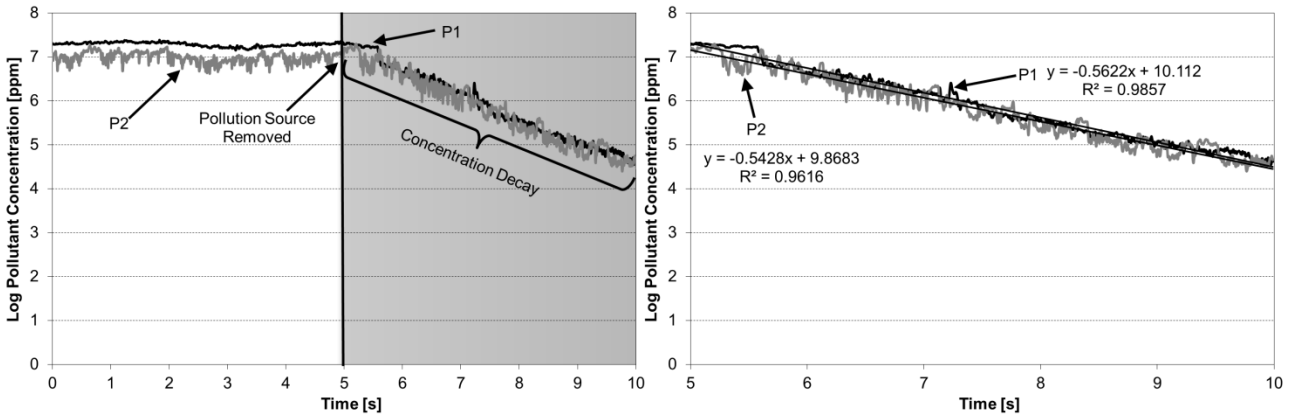

Figure 8 – Pollution concentration within the WT building model over time (left, 15° incoming wind) and focus on concentration decay (right)

3.1.2.2. CFD Simulations

The CFD model (Figure 7 and Figure 9) used in this validation study is a virtual full-scale replica of the wind tunnel model (Figure 6). The simulations were performed using the commercial CFD package PHOENICS 3.6 [325]. The simulation models were set up in accordance with the recommendations of Tominaga et al. [326] and Franke et al. [327].

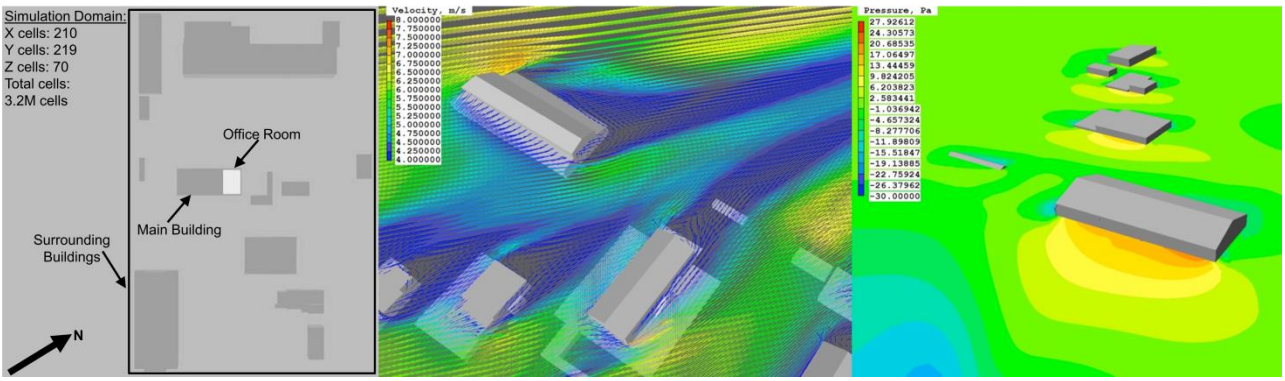

Figure 9 – CFD simulation domain (left), flow field (center, 75° incoming wind) and pressure field (right, 300° incoming wind)

In the case of the computation domain, the recommended minimum 15 H_b distance (H_b being the height of the building) between the model and the outlets is kept around the built area, easily allowing the rotation of the incoming wind. The use of a 15 H_b distance, combined with a domain height of 6 H_b (higher than the recommended minimum of 5 H_b) led to a blockage ratio of less than 0.5 %, lower than the recommended maximum of 3 %.

The simulation's spatial grid must be sufficiently detailed to accurately describe the airflow. However, an excessively detailed grid requires a longer simulation time, without providing any increase in accuracy. Thus, further exploratory runs were performed to achieve an optimal spatial discretization. Three simulation grids, with 2.8, 3.2 and 3.9 million cells (named low, medium and high resolution, respectively) were tested to calculate the bulk airflow rate for four incoming wind directions. The results of these test runs are presented in Table 10.

Table 10 – Bulk airflow rates regarding grid resolution exploratory runs

Wind Direction [degrees]	**Low Resolution [dm^3/s]**	**Medium Resolution [dm^3/s]**	**High Resolution [dm^3/s]**
15	1.31	1.33	1.33
105	1.24	1.26	1.26
195	0.82	0.80	0.80
285	1.04	1.06	1.06

As can be seen, a lower spatial resolution carries differences (up to 3 %) regarding the airflow rate, while the higher resolution brings no significant changes (less than 1 %) and requires a lengthier simulation time. Thus, the medium resolution grid was chosen for the subsequently described simulations.

In addition to an adequate spatial grid, transient simulations require a time step that avoids excessive simulation time while still providing realistic results. A conservative approach to define this time step is given by Equation (7):

$$\Delta t = CFL \times \frac{\Delta x_{min}}{u_{max}} \tag{7}$$

The Courant-Friedrichs-Lewy parameter (*CFL*) should have a maximum value of one, as indicated by Anderson Jr. [328]. This limit ensures that the simulation fluid can only move a maximum of one grid step per time step. Failure to meet this requirement might lead to an inaccurate fluid movement, as intermediate fluid positions are not simulated. Regarding the present simulations, the value of this parameter was set to one.

Analysis of Table 6 to Table 8 indicates that the most popular turbulence closure models used in NV simulation are the standard *k-ε* and the RNG *k-ε* models. For conciseness, this study used only the standard *k-ε* turbulence model. A set of exploratory runs showed that the results did not change significantly when using the RNG *k-ε* model.

The hybrid-differencing numerical scheme (HDS) was used for all variables. This numerical scheme employs both the first-order upwind-differencing scheme (UDS), in high-convection regions, and the second-order central-differencing scheme (CDS), in low-convection regions.

The simulated wind directions are not always perpendicular to the domain's boundaries. Thus, two wind inlets are used to replicate the logarithmic wind profile used within the WT tests, in combination with two zero static pressure outlets on the opposite sides and top of the domain [329].

The lower boundary is modeled as fully-rough to match the wind profile's surface roughness of 4.36 mm. All other solid objects that were used for the building models are defined as smooth.

The flow field and equation residuals were monitored for each simulation and, in the case of transient runs, for each time step. Each simulation, or time step, was considered converged and was therefore concluded when a stationary flow field was obtained and when the residuals for all variables was lower than 10^{-4}.

Finally, wind-driven pressures were obtained for 24 incoming wind directions in the same measurement positions used in the WT model. Regarding the effective flow rates, a comparison was performed for a scenario with all four windows opened (W1-W4 in Figure 7). The CFD simulations used non-buoyant heat as the tracing pollutant. At the beginning of each simulation, this pollutant's concentration was constant and uniformly distributed. The evolution of this concentration throughout the simulation was registered at two points, located at equivalent positions of the points named P1 and P2 in the WT measurements. Transient simulations were required, due to the time-dependent nature of this method, as shown in Equation (6). The equivalent pollutant decay equation when using non-buoyant heat is shown in Equation (8), which can be simplified, leading to Equation (9):

$$\rho \times c \times [T(t) - T_{out}] = \rho \times c \times [T_0 - T_{out}] \times exp\left(-\frac{\dot{V}}{V} \times t\right) \quad (8)$$

$$\Delta T(t) = \Delta T_0 \times exp\left(-\frac{\dot{V}}{V} \times t\right) \quad (9)$$

Applying logarithms to Equation (9) leads to a linear regression (Equation (10)), which can be applied to the evolution of temperature difference through time. The product of the slope of this function and the room's volume results in the effective airflow rate for that given location:

$$ln[\Delta T]\,(t) = -\frac{\dot{V}}{V} \times t + ln(\Delta T_0) \quad (10)$$

3.1.2.3. AFN Simulations

The AFN approach was used to calculate wind-driven bulk airflow rates that were compared with CFD predictions. Using Equation (1) the incoming airflow into the room was calculated for 24 incoming wind directions, using pressure coefficients from WT and CFD. As discussed above, bulk flow rates were not measured in the WT.

3.1.2.4. Relative Average Window Opening Area

The goal of this analysis was to calculate the average window opening area predicted by the three airflow modeling methods that were tested. The analysis compares the relative opening areas predicted for a given target wind-driven flow rate. For this reason, the results obtained do not depend on the target flow rate. The calculations were performed for a whole year considering a 9-to-5 office occupation schedule and using two different wind scenarios:

- Isotropic constant wind speed.
- TMY3 (Typical Meteorological Year, version 3) hourly wind data for San Francisco, based on the NREL (National Renewable Energy Laboratory) dataset, recorded from 1973 to 2005 [330].

3.1.2.5. Effects of Window Geometry

Due to the downscaling difficulties discussed above, the WT model used in this study has an unrealistically thick wall and modeled all windows as fully open holes. To make the analysis of the effects of window geometry more realistic, the CFD model used to assess the effect of window geometry on internal flow has a thinner wall (the scaled equivalent to a 0.17 m thickness). In cross-ventilated buildings with square apertures the air flows into the room as an approximately axis-symmetric jet [10]. In contrast, most window geometries affect the flow field by deflecting incoming air towards a given location in the room [292, 293]. To assess the impact of different window geometries on the effective flow, CFD simulations were performed for eight wind directions (0°-315°, in 45° intervals) using the same two sensor locations shown in Figure 7. This analysis considered five different geometries:

- IB: Window opens **inwards**, **bottom** opening axis
- IT: Window opens **inwards**, **top** opening axis
- OB: Window opens **outwards**, **bottom** opening axis
- OT: Window opens **outwards**, **top** opening axis
- FO: Fully open windows (**reference case**).

As can be seen in Figure 10, a 25.1-degree tilted opening, which alters the direction of the airflow within the building, was added to each window of the first four geometries. Furthermore, this change in window geometry results in a 76 % reduction in the effective opening area.

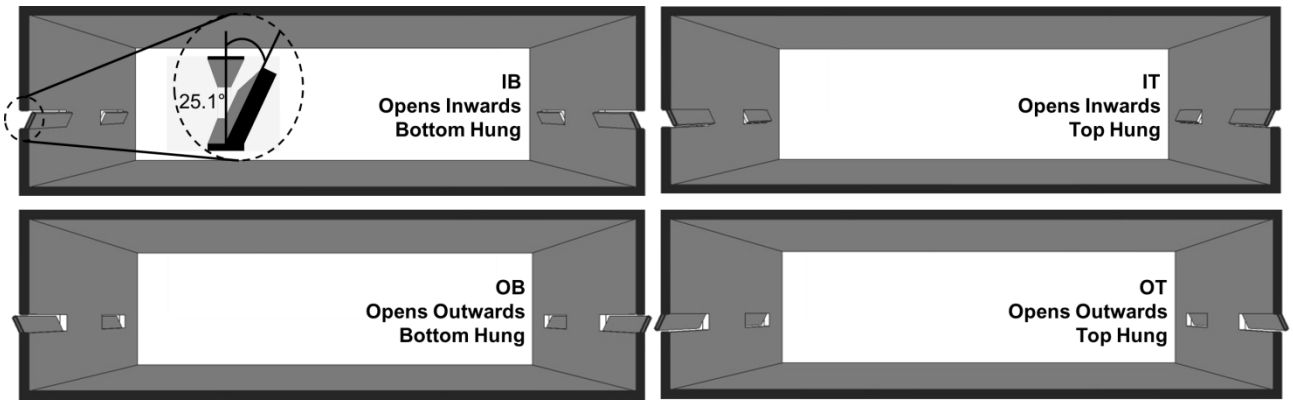

Figure 10 – Window opening geometry scenarios

3.1.3. Validation Results

This section presents the results of the validation, divided in four subsections focusing on: pressure coefficients, effective airflow rates, bulk airflow rates and discussion of results. In all subsections, the error indicators introduced in Section 3.1.1 are used to quantify the differences between the methods.

3.1.3.1. Pressure Coefficients

Figure 11 shows a comparison between CFD and WT pressure coefficients for the 24 wind directions used in this study. The coefficient of correlation and the average error obtained in this comparison are shown in Table 11. Analysis of the results shows better agreement in the predictions for W1 and W4 (compared to W2 and W3). As can be seen in Figure 7, W2 and W3 are closer to the edge of the building, a region where local recirculation and instability make CFD modeling more difficult. Still, the agreement obtained is better than a similar case analyzed by Zhang & Gu [318] (a multi-incoming wind angle assessment of a building with surrounding buildings: R^2 of 0.420 and an average error of 47 %). Overall, the error indicators are close to previous studies based on isolated buildings (R^2 between 0.847 and 0.995 and average error between 7 and 33 %).

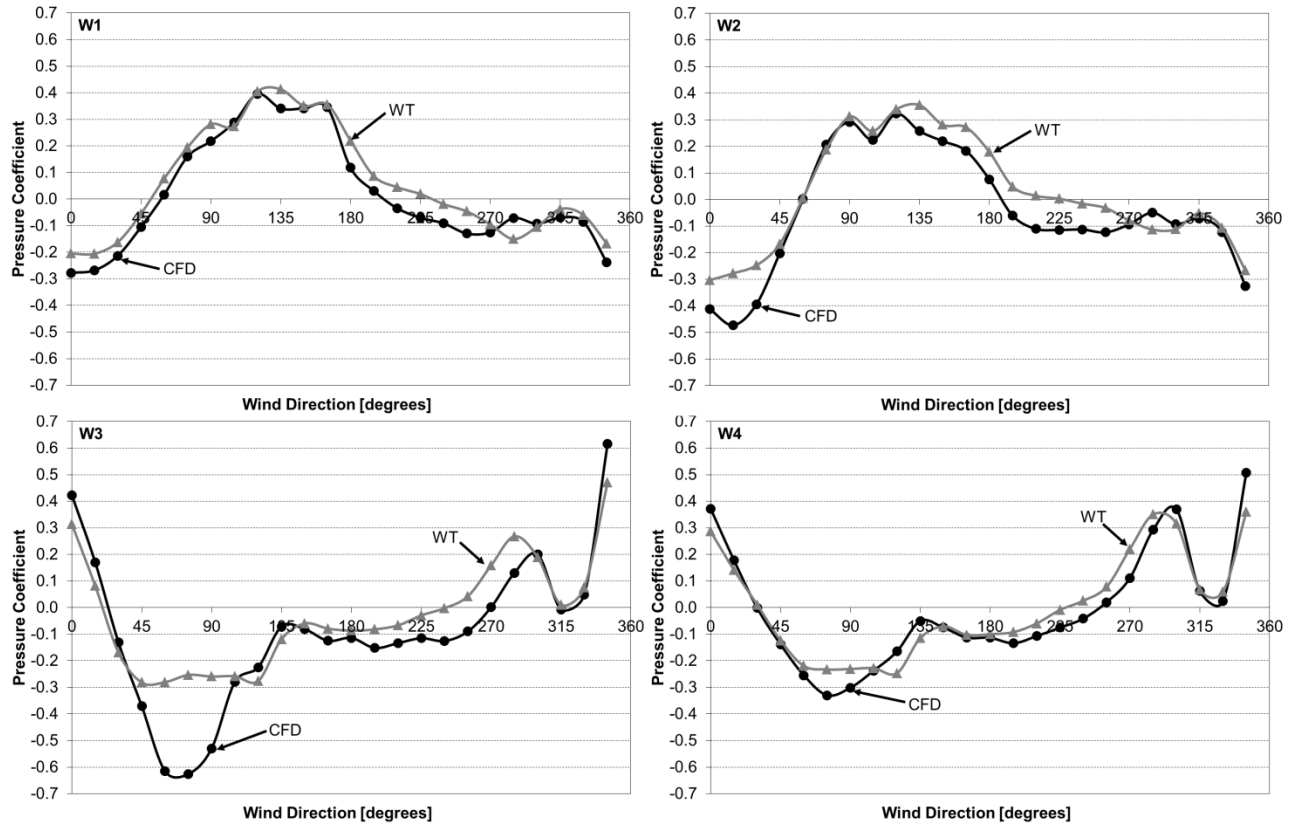

Figure 11 – Pressure coefficients for Windows W1 to W4

Table 11 – R^2 and average error between wind tunnel and CFD pressure coefficients

Opening	***R*²**	**Average Error [%]**
W1	0.920	30
W2	0.854	37
W3	0.776	48
W4	0.922	30
All Windows	**0.836**	**37**
	Review Average Error	**35**

3.1.3.2. Effective Airflow Rates

Figure 12 presents a comparison between CFD and WT predictions of effective flow rates for 24 wind directions. The coefficient of correlation and the average error for this comparison are shown in Table 12. Analysis of the results reveals two levels of agreement, depending on the incoming wind direction:

- Wind directions between 195° and 30° lead to lower errors.
- Wind directions between 45° and 180° lead to larger errors.

For incoming wind between 195° to 30°, there is a good agreement: R^2 of 0.749, a result in the upper range of previously performed studies (see Table 7, R^2 between –0.296 and 0.963). The second group (45° to 180°) has a negative coefficient of determination, a result that also occurred in the study of Nikolopoulos et al. [305]. The average error for this group of wind directions is 37 %, slightly above the review average (31 %). The larger error might be the result of local flow instability near the openings (the wake of the larger surrounding buildings and the main building). Further, for these directions, the effective flow rate is overestimated, a problem that also occurred in a recent full-scale CFD validation for a large building with lateral incoming wind in site with interfering surrounding buildings [288]. For all wind directions, the coefficient of determination is 0.628 and the average error is 32 % (similar to the review average of 31 %).

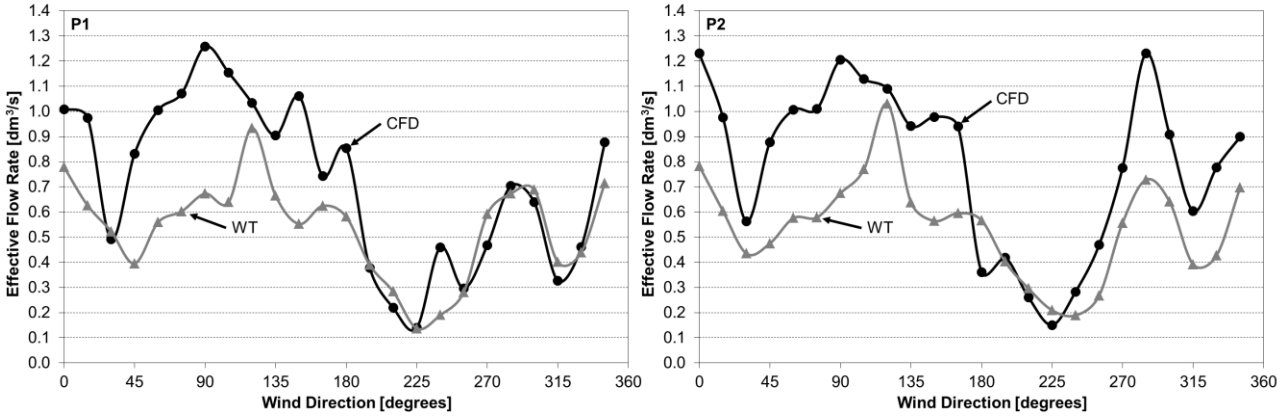

Figure 12 – Effective flow rates for measuring Points 1 and 2

Table 12 – R^2 and average error between wind tunnel and CFD effective flow rates

Wind Directions	**Point**	***R²***	**Average Error [%]**
195° to 30°	P1	0.736	19
	P2	0.886	33
	Average P1/P2	**0.749**	**27**
45° to 180°	P1	–0.957	37
	P2	–0.157	36
	Average P1/P2	**–0.436**	**37**
All Directions	P1	**0.564**	30
	P2	**0.703**	35
	Average P1/P2	**0.628**	**32**
		Review Average Error	**31**

3.1.3.3. Bulk Airflow Rates

Bulk airflow rates were calculated with AFN and CFD models. AFN calculations used two alternative sources of pressure coefficients: WT and CFD. The bulk flow rates obtained with the AFN model, shown in Figure 13, display a systematic under-prediction. This effect was previously studied by Karava et al. [331], Kato et al. [332] and later quantified by Carrilho da Graça [333]. According to these studies, AFN models cannot consider momentum conservation between inflow and outflow. This conservation effect leads to an increased bulk flow rate that cannot be predicted using the aperture equation-based approach: for these cases CFD is the best option.

In spite of this systematic difference, bulk flow rate predictions display the lowest average errors obtained in this study (shown in Table 13). Clearly, the square root dependence (Equation (1)) of the bulk airflow rate on the wind generated pressure difference reduces the impact of existing errors of the pressure coefficients. Further, these calculations simultaneously use the pressure coefficients for all four windows, thereby averaging the impact from individual errors. Both the average error (20 %) and the R^2 obtained are comparable to the review average (23 %, and 0.679-0.944).

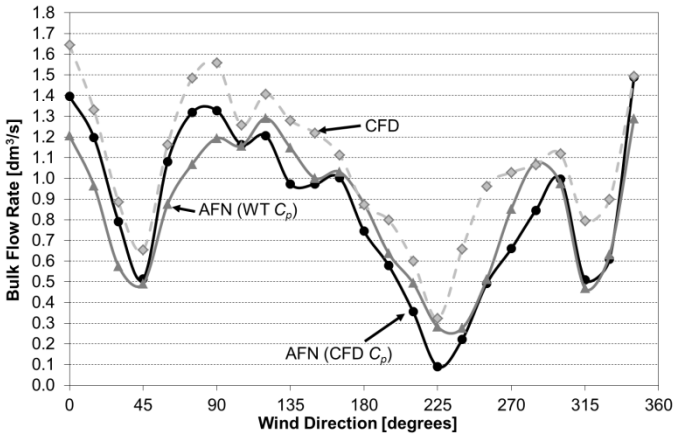

Figure 13 – Bulk flow rates

Table 13 – R^2 and average error between AFN and CFD bulk flow rates

Methods	***R²***	**Average Error [%]**
AFN (CFD C_p)/AFN (WT C_p)	0.851	14
AFN (CFD C_p)/CFD	0.729	20
AFN (WT C_p)/CFD	0.734	21
	Review Average Error	**23**

3.1.3.4. Discussion

Table 14 shows a comparison between the results obtained in this and previous studies. In all cases, the errors obtained are similar to the average of existing studies. In the case of predicting pressure coefficients, RANS CFD displayed good agreement with WT measurements, with a coefficient of determination of 0.84 and average normalized error of 37 %. The highest discrepancies occur in surfaces that are exposed to flow recirculation generated in the wake of large surrounding buildings. The results obtained for effective flow rates display low accuracy for incoming wind directions between 45° to 180°, with a 37 % average error and a negative coefficient of determination. This wind quadrant has surrounding buildings that are closer to the naturally ventilated office. Further, the use of only two sensor locations in the room may contribute to these differences, as any imprecision in the prediction of the inflow jet angle will have a relevant impact in the results. Bulk airflow rates produced the lowest average errors: 21 % when comparing CFD to AFN with WT C_p. This decrease is a direct consequence of the proportionality between airflow rate and the square root of the pressure difference.

Table 14 – Summary of error indicators obtained for this study and existing studies

Variable	**Tool**	**Average Error This Study [%]**	**Average Error Review [%]**
Pressure coefficients (C_p)	CFD	37	35
Bulk flow rate	CFD & AFN	21	23
Effective flow rate	CFD	32	31

3.1.4. Impacts in Window Design

This section presents an analysis of the impacts of the models in NV design. It begins with an analysis of predicted average window opening area and concludes with an evaluation of effects of detailed window geometry.

3.1.4.1. Average Window Opening Area

The analysis of average window opening area used two different wind profiles: isotropic constant wind and hourly San Francisco wind data (TMY3 file). Figure 14 shows the occurrence distribution of wind by speed and direction for San Francisco, revealing a predominance of winds in the 255° to 315° quadrant. This asymmetric distribution increases the cumulative impact of differences in predicted flow rate for these wind directions. Therefore, the lower flow rate differences that were found for that range of wind directions are expected to decrease the discrepancy between the calculated opening areas. The relative average window opening predicted is shown in Table 15. WT is the reference for effective flow rate predictions, whereas for bulk flow rate, the reference is AFN with WT pressure coefficients.

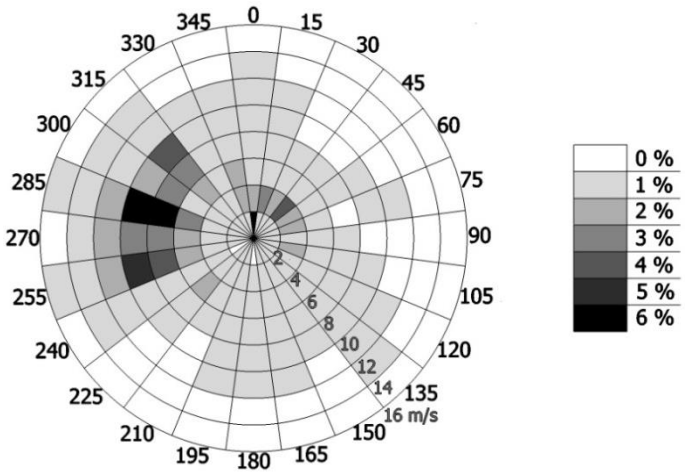

Figure 14 – San Francisco wind distribution

For both scenarios, the WT-based flow rates results in the highest average window opening area, a direct consequence of the lower flow rates predicted for most wind directions (Figure 12). The larger discrepancy is found in the AFN (WT C_p)/CFD comparison: in this case, the larger flows predicted by CFD result in a 30-40 % reduction in predicted window area. The impact of the local distribution of wind by speed and direction on the predictions is not significant (variations of less than 10 %).

Table 15 – Relative average window opening area

Wind Data	**Relative Average Window Opening Area Effective Flow Rate [%]**		**Relative Average Window Opening Area Bulk Flow Rate [%]**		
	WT	**CFD**	**AFN (WT C_p)**	**AFN (CFD C_p)**	**CFD**
Isotropic (constant wind)	100	80	100	82	61
San Francisco	100	74	100	91	67

3.1.4.2. Window Geometry Effect

Figure 15 shows the predicted variations of average effective flow rate obtained in points P1 and P2 for the four different window geometries shown in Figure 10. Table 16 presents the effective flow rate results normalized using the reference fully open (FO) window effective flow result. In all cases studied, inclusion of detailed window geometry leads, on average, to an increase in the effective flow rate due to improved mixing of the room air (in some wind angles up to 30 %). Clearly, a complete NV design analysis should include the effects of flow deflection by partially open windows.

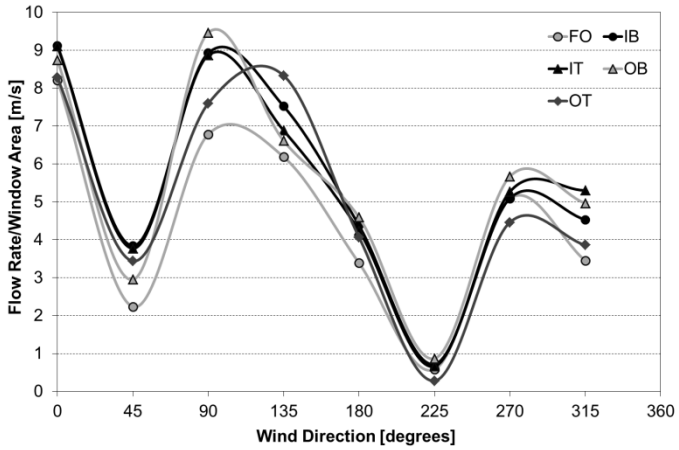

Figure 15 – Average effective (decay method) flow rates per window opening area for different window strategies

Table 16 – Average variation between fully open and each other window opening scenario

Case	Average difference from FO [%]
IB	+19
IT	+19
OB	+18
OT	+16
AVERAGE	+18

3.2. Thermal Simulation

Detailed hourly simulation was performed using EnergyPlus, an open source building thermal simulation software code that has been continuously developed by the United States Department of Energy (DOE) [296] through several of its research laboratories, including the NREL, and the Lawrence Berkeley (LBNL), the Oak Ridge (ORNL) and the Pacific Northwest National Laboratories (PNNL). With the initial goal of replacing the aging and remarkably difficult to maintain and modify existing thermal simulation software developed by the DOE and the United States Department of Defense, DOE-2 and BLAST, respectively, the development of EnergyPlus began in 1996 and its first version was released in 2001 [334]. Since then, EnergyPlus has become one of the most commonly used thermal simulation tools.

By taking the building description and local environmental conditions (such as weather) as inputs, the EnergyPlus simulation manager simultaneously computes building systems and heat and mass balance equations. One example is the heat balance on a given zone's air, which is given by Equation (11) [335]:

$$\begin{aligned} \rho \times c \times C_T \times \frac{dT_z}{dt} &= \sum_{i=1}^{N_{inload}} \dot{Q}_{inload,i} + \sum_{i=1}^{N_{surface}} h_{surface,i} \times A_{surface,i} \times \left(T_{surface,i} - T_z\right) \\ &+ \sum_{i=1}^{N_{zone}} \dot{m}_{zone,i} \times c \times \left(T_{zone,i} - T_z\right) \\ &+ \dot{m}_{inf} \times c \times (T_{out} - T_z) + \dot{m}_{sys} \times c \times \left(T_{sup} - T_z\right) \end{aligned} \quad (11)$$

This equation is based on the conservation of energy and has energy flow units (J/s or W), which at each time step calculates the convective heat flow inflowing and leaving that zone's indoor air:

- $\rho \times c \times C_T \times \frac{\mathrm{d}T_z}{\mathrm{d}t}$: is the change in energy stored in air of the zone z. The coefficient C_T is typically set to unity, although higher values can be used to account for the capacitance in the air loop not within the zone;
- $\sum_{i=1}^{N_{inload}} \dot{Q}_{inload,i}$: accounts for convective internal heat sources;
- $\sum_{i=1}^{N_{surface}} h_{surface,i} \times A_{surface,i} \times \left(T_{surface,i} - T_z\right)$: refers to the heat transfer between the zone air and the zone's surfaces;
- $\sum_{i=1}^{N_{zone}} \dot{m}_{zone,i} \times c \times \left(T_{zone,i} - T_z\right)$: is the heat transferred by air movement between zones;
- $\dot{m}_{inf} \times c \times (T_{out} - T_z)$: accounts for the heat transfer by the infiltration of outdoor air;
- $\dot{m}_{sys} \times c \times \left(T_{sup} - T_z\right)$: is the heat transfer by the heating and cooling air systems;

Similar heat balance equations exist for the heat exchange between surfaces and radiative energy sources, the latent heat exchange between indoor sources, indoor air and air movement throughout the building and the outdoor environment, the conductive heat transfer through building sources and the capacitive heat storage effect of the building's thermal mass. The software package's Integrated Solution Manager numerically resolves these heat balance equations in addition to mass balance equations (regarding the flow of air, carbon dioxide or other pollutants throughout the building and the outdoors), according to the constraints and specifications detailed by the building model and the local environmental conditions, in order to calculate the desired outputs.

The DOE has also developed the Commercial Reference Building Models of the National Building Stock dataset [336]. This database includes building energy simulation models for fifteen commercial building typologies (small, medium and large offices; primary and secondary schools; stand-alone retail, strip mall and supermarket; quick and full-service restaurants; small and large hotels; hospital and outpatient health care; and warehouse) and a single residential one (midrise apartment). Three different building models are available for each typology and represent three different construction eras: pre-1980, post-1980 and new construction. For each of these construction eras, the differences in the building models reflect the different construction standards that were in force during those time periods, resulting in different insulation values, lighting levels and HVAC equipment and efficiencies. These models are not intended to be representative of any specific building but rather to perform studies on building energy performance and occupant comfort.

3.3. Indoor PM2.5 Levels

The Generic Contaminant Algorithm (GCA) is a mass balance equation included within the EnergyPlus software package to model the indoor levels of any given pollutant (apart from carbon dioxide, which has its own mass balance equation), such as PM2.5. The coupling of the pollutant model with a thermal simulation model allows an ongoing update of some of the pollutant transport model's inputs. One of these parameters is the natural ventilation airflow rate, which can change due to occupants opening or closing windows in accordance with their thermal comfort, consequently altering the rate of outdoor particle penetration [205].

The mass balance model equation is shown in Equation (12) [335]:

$$\rho \times V_z \times \frac{dK_z}{dt} = \sum_{i=1}^{N_{source}} \rho \times G_i \times 10^6 - \sum_{i=1}^{N_{sink}} \rho \times R_i \times K_z + \sum_{i=1}^{N_{zone}} \dot{m}_{zone,i} \times \left(K_{zone,i} - K_z\right) + \dot{m}_{inf} \times (K_{out} - K_z) + \dot{m}_{nat} \times (K_{out} - K_z) + \dot{m}_{sys} \times \left(K_{sup} - K_z\right) \quad (12)$$

This equation is based on mass conservation and, in the case of PM2.5 being the modeled pollutant, has concentration-mass flow units (μg kg s^{-1} m^{-3}), modeling the change in indoor pollutant concentration, at each time step:

- $\rho \times V_z \times \frac{\mathrm{d}K_z}{\mathrm{d}t}$: is the change in the indoor pollutant concentration of a given zone;
- $\sum_{i=1}^{N_{source}} \rho \times G_i \times 10^6$: is the sum of indoor pollutant sources;
- $\sum_{i=1}^{N_{sink}} \rho \times R_i \times K_z$: is the sum of indoor pollutant sinks;
- $\sum_{i=1}^{N_{zones}} \dot{m}_{zone,i} \times \left(K_{zone,i} - K_z\right)$: is the transport of pollutant between zones;
- $\dot{m}_{inf} \times (K_{out} - K_z)$: is the transport of pollutant by infiltration;
- $\dot{m}_{nat} \times (K_{out} - K_z)$: is the transport of pollutant by natural ventilation;
- $\dot{m}_{sys} \times \left(K_{sup} - K_z\right)$: is the pollutant transported by the ventilation supply duct into the simulation zone.

This equation, in its default form, does not allow for a correct modeling of PM2.5 as the indoor pollutant. PM2.5 is suspended and not dissolved in the air, as occurs with gaseous pollutants, thus a fraction of the PM2.5 transported by the infiltration airflow settles within the building cracks before entering the building, which is not modeled by default. The default model also does not account for the reduction in the transport of outdoor PM2.5 through the ventilation ducts, i.e. the effect of a cloth particle filter.

Nonetheless, the EnergyPlus source code is open source, allowing the ad-hoc implementation of these features that are not provided in the default model, namely the infiltration particle penetration rate, cloth filters within the mechanical ventilation system or even other types of filtration.

4. METHODOLOGY

The methodology used to study the effects of high levels of PM2.5 on the usability of natural ventilation is shown schematically in Figure 16. Two complementary analysis approaches were used and are shown in the center of the figure:

- A simple statistical analysis of the occurrence of favorable NV weather conditions and whether these favorable moments are affected by high PM2.5 levels, in addition to a multivariable correlation analysis between outdoor PM2.5, weather and time (on a daily and yearly scale).
- A detailed simulation analysis of the impact of NV on the HVAC electricity consumption and indoor PM2.5 exposure of an office building.

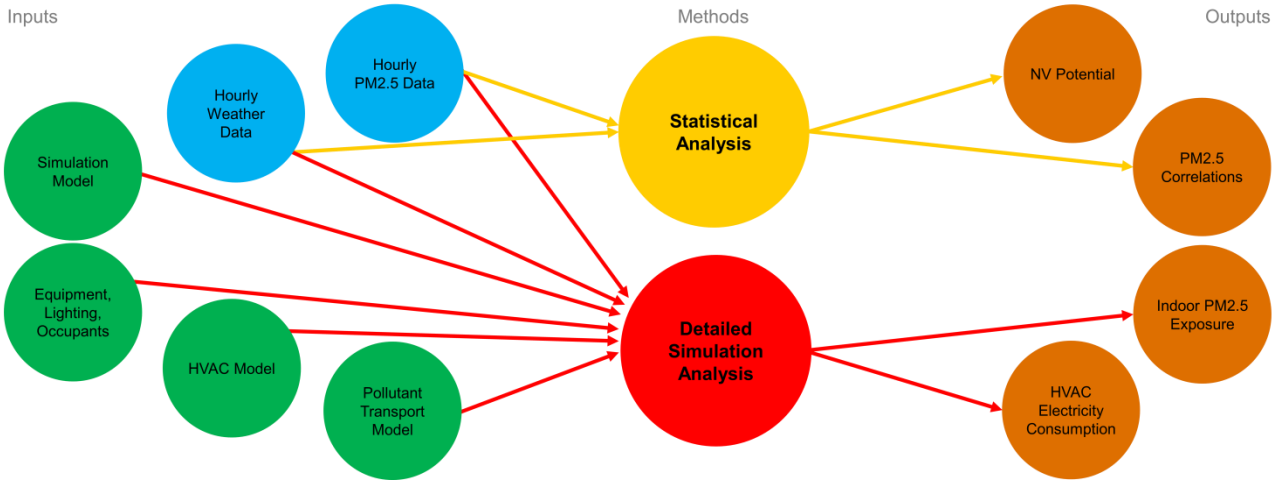

Figure 16 – Methodology diagram

Both approaches use several years of measured hourly weather and PM2.5 data. The statistical analysis provides a simple assessment of the impact of PM2.5 on NV availability. This initial phase also includes a multivariable correlation analysis that seeks to identify weather and time patterns that impact PM2.5 and NV.

The detailed simulation analysis uses the measured hourly weather and PM2.5 data as input to a building thermal and airflow simulation model of a typical medium-size naturally ventilated office building. This methodology predicts the impact of PM2.5 and NV use in terms of occupant exposure and building HVAC electricity consumption. The simulation model that was used has four main components:

- The building geometry and material properties, to assess heat transfer.
- Equipment, lighting and occupant loads and schedules.
- Building HVAC and NV airflow model.
- Pollutant air transport model, to predict the penetration of outdoor PM2.5, deposition of particles onto surfaces, re-suspension from those surfaces and filtering by the HVAC system.

The next subsections describe the two analysis approaches in detail.

4.1. Weather and PM2.5 Data

This research focused on three regions throughout the world, which present contrasting difficulties regarding the usability of NV and the limiting effect of PM2.5 pollution: California (United States), Europe and Asia. California is a state that has long been in the vanguard of renewable energy technologies and NV use in non-domestic buildings [13, 337]. Five cities within the largest metropolitan areas in this State (Figure 17 [338, 339] that account for nearly 90 % of the state's population [340] were chosen: San Diego, Burbank, Fresno, Sacramento and Livermore. Sacramento, Livermore and Burbank have warm temperate climates with dry summers. In all three cities, winters are mild, while summers are warm in Livermore and Burbank (*Csb* in the Köppen-Geigen climate classification [341, 342]) and hot in Sacramento (*Csa*), which can hinder this city's ventilative cooling potential. As for Fresno and San Diego, both cities have arid steppe climates, with mild winters and low precipitation levels. Nonetheless, temperatures are typically higher in Fresno (*BSh*, hot arid steppe), which should decrease the usability of NV in comparison to San Diego (*BSk*, cold arid steppe) and the rest of the state. Overall, local climate is not especially challenging in California, with most of the temperature-related NV limitations occurring due to high temperatures during the summer season. However, the large populations in these urban areas might lead to high PM2.5 levels which could then limit the use of NV. Nonetheless, both the United States [75, 103, 104] and the state of California [105] have the strictest PM2.5 regulations among the regions assessed under this research, which can reduce that limiting effect.

Figure 17 – Location of San Diego, Burbank, Fresno, Sacramento and Livermore, and transport of coarse particles by the Santa Ana winds in Southern California (lower left corner).

In Europe, nine cities were selected (Figure 17 [343]): Antwerp (Belgium), Krakow (Poland), Lisbon (Portugal), London (United Kingdom), Madrid (Spain), Paris (France), Prague (Czech Republic), Skopje (the Former Yugoslav Republic of Macedonia) and Strasbourg (France). These cities are the center of some of the largest urban areas in Europe that house and employ several million people each, leading to high particle levels, as discussed in several previous studies [98, 344]. Most of these cities have warm and fully humid temperate climates, characterized by warm summers and cool winters (*Cfb*). Similarly to California, higher temperatures during part of the summer season might be a limitation to the use of NV. However, this region also faces a distinct challenge: very low temperatures during the winter can also disallow the use of NV in that season as well as possibly resulting in a need for mechanical heating. As for Lisbon (*Csa*) and Madrid (*BSk*), the local climates are similar to those found in California and, thus, so are the predicted weather-related NV usability limitations.

Figure 18 – Location of Antwerp, Krakow, Lisbon, London, Madrid, Paris, Prague, Skopje and Strasbourg

Finally, in Asia, where previous studies have shown that high outdoor pollution can significantly hinder the use of NV [22], three of the five most populous megacities were chosen [2] (Figure 17 [345]): Beijing and Shanghai, in China, and New Delhi, in India. These three cities are located in the most polluted regions of the world, namely East-Central China and the Indo-Gangetic plain, and rank among the twenty most polluted cities in the world (New Delhi tops the list [75]). In addition to high air pollution levels, local climate is also very warm and therefore challenging for passive cooling and ventilation systems. New Delhi's monsoon-influenced humid subtropical climate (*Cwa* [346]) is characterized by high temperatures during most of the year. Beijing has a monsoon-influenced humid continental climate (*Dwa*), with cold winters and hot and humid summers. Hot and humid summers characterize Shanghai's humid subtropical climate (*Cfa*), although winters are not as severe as in Beijing [347]. Clearly, in these three megacities, the use of NV to provide indoor comfortable conditions and acceptable indoor quality is difficult and requires innovative hybrid solutions that combine active and passive systems.

Figure 19 –Location of Beijing, Shanghai and New Delhi

The selection of cities for each of these three regions was also conditioned by the availability of simultaneous hourly weather and PM2.5 data. Weather data was obtained from the Third Version of National Solar Radiation Database [348, 349] for California and New Delhi, the MACC-RAD [350] (solar radiation data) and the NCEI Integrated Surface Data [351] databases for Europe, and the White Box Technologies historical weather database [352] for Beijing and Shanghai. The California Air Resources Board [353] and the EEA AirBase [354] databases provided the PM2.5 data for California and Europe, while data for China [355] and India [356] was obtained via the U.S. Department of State Air Quality Monitoring Programs in those two countries. The weather datasets consisted of an hourly record of dry bulb and dew point temperatures, relative humidity, atmospheric pressure, wind speed and direction, and direct beam, diffuse horizontal and global horizontal solar radiation. The datasets for California and Asia, as well as the solar radiation dataset for Europe were complete. However, data was missing for a limited set of time steps in the European weather database and in all PM2.5 databases. In order to limit the impact of missing PM2.5 data, in cities with at least two PM2.5 measuring stations, all available stations in each city (Table 17) were taken into account and their measurements were averaged, at each timestamp (considering the number of stations available).

Table 17 – Number of measuring stations for cities with more than one station

City	Measuring Points
San Diego	2
Fresno	5
Antwerp	3
Krakow	3
Lisbon	2
London	10
Madrid	9
Paris	2
Prague	8
Skopje	2

The still remaining data gaps were managed differently in the two research approaches. In the case of the statistical analysis, a normalization approach [15] was used to calculate natural ventilation yearly potentials. Each individual working hour (e.g. January 2, 8 a.m.) was assessed for all years: the number of times each set of criteria was fulfilled was divided by the number of times that the data for that working hour was available (Equation (13)). The average yearly potentials are then given by the ratio of the sum of the previous calculation and the average number of yearly working hours (Equation (14)).

$$\varphi_i = \frac{\sum_{j=1}^{N_j} \begin{cases} 1, & if\ criteria\ is\ fulfilled \\ 0, & if\ criteria\ is\ not\ fulfilled\ OR\ data\ is\ not\ available \end{cases}}{\sum_{j=1}^{N_j} \begin{cases} 1, & if\ data\ is\ available \\ 0, & if\ data\ is\ not\ available \end{cases}} \tag{13}$$

$$\Phi = \frac{\sum_{i=1}^{N} \varphi_i}{N_j} \tag{14}$$

In the detailed simulation analysis, in order to minimize the uncertainties that would arise from large data gaps, only city-year datasets with less than 10 % of missing PM2.5 measurements and a maximum consecutive gap of 5 weather measurements (only applicable to Europe) were considered. Further, linear interpolation was used to complete the dataset for gaps of less than 24 hours [357]. In the case of longer gaps, simulation results, i.e. cumulative indoor PM2.5 exposure and HVAC electricity consumption, were ignored for those periods and compensated by extrapolation of the remaining results. The PM2.5 availability for each city and year and the resulting city-year datasets that were used in the detailed simulation analysis are highlighted in bold in Table 18. Table 19 presents the maximum consecutive weather data gap for each city and year in Europe.

Table 18 – PM2.5 data availability [%] for each city and year; years used in the detailed hourly simulation analysis are shown in bold

City	2005	2006	2007	2008	2009	2010	2011	2012	2013	2014
San Diego	–	–	**98**	**98**	**97**	**96**	**92**	–	–	–
Burbank	–	–	–	–	**97**	**99**	**95**	–	–	–
Fresno	**98**	**100**	**98**	**99**	**97**	**100**	**100**	–	–	–
Sacramento	**100**	**98**	**94**	**95**	81	**92**	**93**	–	–	–
Livermore	**99**	**99**	**95**	**98**	**99**	67	**99**	–	–	–
Antwerp	–	90	92	87	95	100	96	**99**	–	–
Krakow	–	–	–	**100**	**99**	**100**	**99**	**99**	–	–
Lisbon	**100**	**100**	100	**100**	**100**	**97**	**100**	**100**	–	–
London	**100**	**100**	100	**96**	**100**	**100**	**100**	**100**	–	–
Madrid	100	**100**	100	**100**	**100**	**100**	100	**100**	–	–
Paris	–	–	–	–	–	–	–	**98**	–	–
Prague	**100**	**100**	100	**100**	**100**	**100**	100	**100**	–	–
Skopje	–	–	–	–	–	–	–	**100**	–	–
Strasbourg	–	–	–	–	–	–	96	**91**	–	–
Beijing	–	–	–	–	–	**92**	**92**	**94**	**99**	**99**
Shanghai	–	–	–	–	–	–	–	**97**	**98**	**98**
New Delhi	–	–	–	–	–	–	–	–	**92**	**91**

Table 19 – Maximum consecutive weather data gap in hours for each city and year in Europe; years used in the detailed hourly simulation analysis are shown in bold

City	2005	2006	2007	2008	2009	2010	2011	2012	2013	2014
Antwerp	–	3	12	13	7	9	24	**3**	–	–
Krakow	–	–	–	**4**	**5**	**3**	**2**	**3**	–	–
Lisbon	**4**	**2**	11	**4**	**4**	**1**	**1**	**1**	–	–
London	**4**	**3**	11	**4**	**5**	**5**	**1**	**1**	–	–
Madrid	11	**2**	11	**4**	**5**	**1**	10	**1**	–	–
Paris	–	–	–	–	–	–	–	**1**	–	–
Prague	**2**	**3**	11	**3**	**5**	**1**	8	**1**	–	–
Skopje	–	–	–	–	–	–	–	**3**	–	–
Strasbourg	–	–	–	–	–	–	12	**4**	–	–

4.2. Statistical Analysis

The statistical analysis calculates, for each city, the yearly average percentage of office working hours when NV can be used. Working hours were defined as those between 8 a.m. and 6 p.m. [358] (corrected for daylight saving time, whenever applicable), excluding weekends and public holidays. There are two versions of the NV potential indicator, depending on the availability of PCS systems in the office space:

- The standard comfort (SC) scenario considers that NV can be used when the outdoor temperature is between 10 and 26 °C [34, 35];
- The extended comfort (EC) scenario expands the range to between 10 and 30 °C [34, 37] due to the availability of PCS. Since there are no PCS systems that can deal with high humidity, the expansion of the temperature range to 26 to 30 °C is limited to relative humidity below 80 % [37].

To assess the impact of high outdoor PM2.5 concentrations on the two cases, the following PM2.5 concentration thresholds are used:

- NV12: applied only in California; at each given moment, NV is only available if the outdoor PM2.5 concentration is below the United States and California PM2.5 regulatory threshold: 12 $\mu g/m^3$ [75, 103, 104, 105];
- NV10: applied in both Europe and Asia; NV is only available if the outdoor PM2.5 concentration is below the WHO's air quality guideline: 10 $\mu g/m^3$ [99].
- NV35: applied only in Asia; NV is only available if the outdoor PM2.5 concentration is below the WHO's first interim target: 35 $\mu g/m^3$ [99].

Additionally, this phase included a correlation analysis between PM2.5 concentrations and weather variables that directly affect the ventilation flow rate and, consequentially, the occupants' exposure to PM2.5 of outdoor origin, namely temperature and wind speed and direction. Further, this correlation analysis was extended to the variance in time of PM2.5 levels through the hours of the day and the months of the year: if NV is used when PM2.5 levels are higher, then occupant exposure increases.

4.3. Detailed Simulation Analysis

The building model used in the detailed simulation analysis was based on the Medium Office Model of the standard United States Department of Energy Commercial Reference Buildings dataset [336]. Only the middle level of the three-story reference building was kept, with the ceiling and floor plates connected to create periodic boundary conditions [359]. This approach simplifies the simulation at the expense of ignoring boundary effects on the first and last levels. Whenever the top floor is well insulated, this approximation is conservative, since the expected cooling thermal demand from the top and bottom floors can be lower than the middle floors due to increased ceiling (top level) and floor (ground level) slab thermal inertia.

The standard version of the Medium Office Model does not allow for optimal use of NV in all the floor plan since part of the occupied area was more than 6.096 meters from an opening (the maximum depth that can be naturally ventilated with windows in a single façade, according to the California Mechanical Code [9]). To facilitate NV use, the original building model was adapted, as shown in Table 20, obtaining a building that, when weather conditions allow, can be fully naturally ventilated and has an improved passive thermal behavior (building construction details are shown in Table 21). The geometry of the modified building model used in this research is shown in Figure 20. Restroom [360, 361], corridor [362] and vertical access (stairs [363] and elevator [361]) zones were added to the new model's core, complying with state and federal minimum size regulations. The original model's windows were replaced by low-emissivity double-glazing windows [296] that comply with the state's Energy Code [364]. Further, a horizontal shading fin was added above each window to avoid excessive solar gains. Lastly, indoor thermal mass was set to an equivalent of two 10 cm wooden layers throughout the office zones [365], while outdoor air infiltration was defined as 0.00136 $m^3 s^{-1}$ per square meter of external area [366].

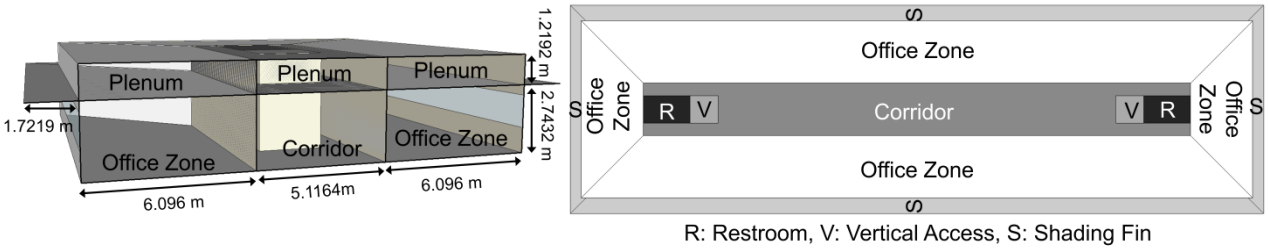

Figure 20 – Building simulation model section cut and zones

Table 20 – Building model parameter sources

Parameter		**Ref.**	**Value**
Base Model	Constructions	[336]	–
Perimeter Zones	Zone Depth	[9]	6.096 m
Internal Mass	Furniture	[365]	2×0.10 cm/m^2
Windows	Construction	[296]	–
	Thermal Properties	[364]	1.333 W m^{-2} K^{-1}, U-value; 0.283, SHGC
Restrooms	Number	[360]	3, per gender
	Dimensions	[361]	–
Vertical Access	Elevator	[361]	–
	Stairs	[363]	–
Corridor	Dimensions	[362]	–
Air Tightness	Infiltration Rate	[366]	0.00136 m^3 s^{-1} m^{-2} (of external area); ×0.25 when HVAC is on

Table 21 – Building construction materials (outmost to inmost layer)

Construction		**Thickness [mm]**	**Conductivity [W m^{-1} K^{-1}]**	**Thermal Resistance [m^2 K/W]**
Floor	Concrete	101.6	1.311	–
	Carpet	–	–	0.2165
Drop Ceiling	Drop Ceiling Tiles	12.7	0.057	–
Interior Wall	Gypsum	12.7	0.160	–
	Gypsum	12.7	0.160	–
Exterior Wall	Wood Siding	10.0	0.110	–
	Steel Frame Wall Insulation	53.9	0.049	–
	Gypsum	12.7	0.160	–
Window	Low-emissivity Coated Glass	6.0	0.900	
	Argon	12.7	0.016	
	Clear glass	6.0	0.900	

4.3.1. Equipment, Lighting and Occupant Loads

Occupant metabolic and latent heat, lighting and office equipment all contribute to the thermal load that must be removed by the cooling system. To accurately define each of these thermal loads (Table 22), the open plan office area was divided into individual workspaces with 11.6 m^2 of floor area, a typical value for an office. In a typical office, not all workspaces are in use during the whole day. The hourly occupation used in the simulations followed the average measured weekday office occupation profile shown in Figure 21 [358].

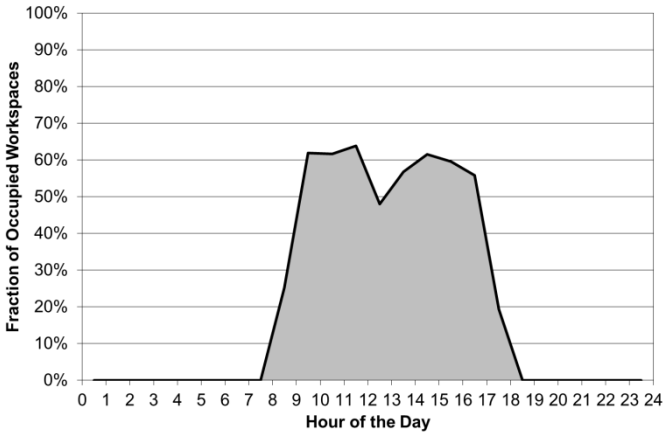

Figure 21 – Workspace occupation throughout the day

Light power density was set to the California Energy Code's maximum requirements [9], at 8.07 W/m^2 in the office zones and at 6.46 W/m^2 in the remaining zones. During the unoccupied hours (nighttime, holidays and weekends), light power density was reduced to 25 % in all zones [251]. Office equipment power density was based on Johnston et al. [251]: each workspace consisted of a desktop computer, an LCD monitor, a VoIP phone and one medium multifunction printer for every ten workspaces, averaging 9.74 W/m^2 [251, 367]. In the unoccupied periods, desktop computer loads were reduced by 64 % and LCD monitors by 80 %, while phones and printers were completely turned off [251]. Table 22 shows the values and sources used for the lighting, equipment and occupant loads.

Table 22 – Equipment, lighting and occupant loads parameter sources

Parameter		**Ref.**	**Value**
Lighting	Load	[9]	8.07 W/m^2, offices; 6.46 W/m^2, remaining zones; ×0.25, unoccupied period
	Schedule	[251]	–
Equipment	Load and Schedule	[251]	9.74 W/m^2; ×0.33, computers, unoccupied period; ×0.20, monitors, unoccupied period
Occupation	Density	[367]	11.6 m^2/workspace
	Schedule	[358]	–

4.3.2. HVAC Model

The model's HVAC system includes a rooftop air handling unit (AHU) with an integrated heat pump (Figure 22), with the specifications shown in Table 23. In order to meet the requirements of the California Mechanical Code's air renewal requirements [9], this system provides outdoor air at the rate of 8.5 m^3 per hour and per person and 1.1 $m^3\ hour^{-1}\ m^{-2}$, with a total inflow and exhaust fan pressure drop of 1438 Pa and an average fan efficiency of 50.1 % [368], as can be seen in Table 24.

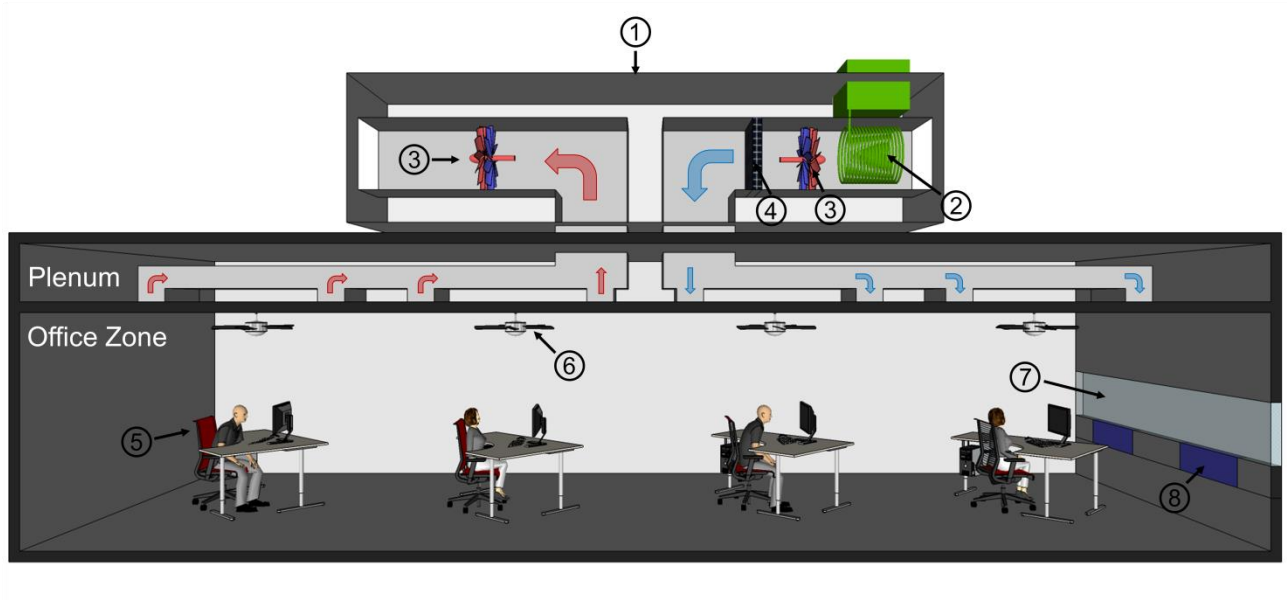

Figure 22 – HVAC layout: (1) Rooftop air handling unit; (2) Heat pump and heat exchanger; (3) Fans; (4) Cloth filter; (5) Heated chair; (6) Ceiling fan; (7) Window; (8) NV electrostatic filter

Table 23 – Air handling unit electricity consumption parameters

Variable	Heating	Cooling	Ventilation
T_{dist} [°C]	45	5	–
T_{cond} [°C]	$T_{dist} + 5$	$T_{out} + 5$	–
T_{evap} [°C]	$T_{out} - 5$	$T_{dist} - 5$	–
ψ [%]	40	40	–
Distribution loss [%]	10	10	–
Distribution pumps [%]	10	10	–
η_{HR} [%]	80	–	–
η_{vent} [%]	–	–	50.1
p_{vent} [Pa]	–	–	1438

Table 24 – HVAC model parameter sources

Parameter		Ref.	Value
Mechanical Ventilation	Ventilation Rate	[9]	8.50 $m^3\ h^{-1}$ $person^{-1}$, office; 1.10 $m^3\ h^{-1}\ m^{-2}$, office and corridor
	Pressure Load	[369]	1438 Pa
	Fan Efficiency	[369]	50.1 %
Air Handling Unit	Heat Pump Efficiency	[368]	40 %
	Heat Recovery Efficiency	[370]	80 %
Heating & Cooling	Set Points	[35]	20 °C, heating; 26 °C, cooling; SC
		[40]	18 °C, heating; EC
		[37]	30 °C, cooling; EC
	Heated Chair Power	[40]	16 W/chair
	Fan	[37]	1.6 m/s; 1 fan/workspace

Two HVAC set point scenarios were used, according to the availability of PCS:

- SC: the HVAC system alone maintains the building indoor temperature between 20 and 26 °C, the recommendations of the ISO 7730:2005 standard for a category B office, which ensures a predicted mean comfort vote (*PMV*) between –0.5 and +0.5, which is equivalent to a predicted percentage of dissatisfied (*PPD*) occupants below 10 % [35].
- EC: the HVAC system maintains the building indoor temperature between 18 and 30 °C. This extended temperature range is due to the existence of PCS, namely heated chairs and ceiling fans, which were chosen in order to allow the same predicted comfort levels, namely $-0.5 \leq PMV \leq +0.5$ and $PPD \leq 10$ %. These PCS are used to supplement the AHU. Heated chairs are in operation when occupied and if the zone temperature drops below 20 °C [40]. Ceiling fans provide an additional cooling effect whenever the zone temperature is above 26 °C [37].

At each simulation time step, a coefficient of performance (*COP*) was calculated to predict the energy consumption of the rooftop AHU, which is a function of the heat pump's evaporator and condenser temperatures (Table 23) and the heat pump's efficiency (ψ) (Equations (15) and (16)).

$$COP_{heat} = \psi_{heat} \times \frac{T_{cond} + 273.15}{T_{cond} - T_{evap}} \tag{15}$$

$$COP_{cool} = \psi_{cool} \times \frac{T_{evap} + 273.15}{T_{cond} - T_{evap}} \tag{16}$$

The heat pump's efficiency is the ratio between its actual *COP* and that of an ideal Carnot engine and was considered to be 40 % [369]. The AHU was equipped with a heat recovery system with an efficiency of 80 % [370], although it was only used in Europe and Asia, where heating needs were higher. Further, 10 % of the produced heat load was considered lost in the distribution system, while the electric consumption was increased by 10 % to account for the consumption of the water circulation pumps [15]. Finally, the electric energy required to power the fan was calculated with Equation (17).

$$E_{vent} = \frac{p_{vent} \times \dot{V}_{vent}}{\eta_{vent}} \tag{17}$$

The heating, cooling and ventilation annual energy consumption of this developed simulation model was compared with the results of the Californian Commercial End-Use Survey [371], a database that presents the energy consumption of several non-domestic building types. The model's energy load was found to be within the range for office buildings (Table 25).

Table 25 – Validation of HVAC electricity consumption

Parameter **[kW h m^{-2} year^{-1}]**	**Simulation Model**	**Database**
Cooling	36	28 to 38
Heating	5	2 to 5
Ventilation	16	14 to 33

Nevertheless, the original simulation model was modified as described above to improve its passive thermal behavior and equipment efficiency, allowing a 60 to 75 % decrease in overall HVAC energy consumption.

4.3.3. Modeling of Single-Sided NV

The use of NV leads to energy savings that can be quantified as the difference in the building's yearly HVAC electricity consumption with NV and without NV. In both HVAC set point scenarios, the following two NV-use scenarios were used to quantify these two cases:

- NoNV: Mechanical ventilation is in operation during all working hours. NV is not used.
- NVP: Hybrid natural/mechanical ventilation is available during all working hours. In each of the four office zones and at each time step, windows are opened (Table 26), as NV replaces the centralized HVAC system if the outdoor temperature is between 10 °C and that zone's air temperature. Further, if the outdoor temperature is above 26 °C, NV is only available if the outdoor relative humidity is below 80 %. During the unoccupied hours, namely at night and during weekends and holidays, NV is available with the same constraints.

Two approaches were proposed to limit the increase in occupant exposure to PM2.5 that results from the use of NV: limiting its use to moments of low outdoor PM2.5 concentrations and using an electrostatic filter (ESF) to limit the transport of PM2.5 by the naturally ventilated airflow:

- NVS: same temperature criteria as NVP. However, windows are only opened if the outdoor PM2.5 concentration is below the following thresholds:
    - California (NV12): 12 μg/m^3 [75, 103, 104, 105];
    - Europe (NV10): 10 μg/m^3 [99].
    - Asia, two thresholds were considered (NV10 and NV35, respectively): 10 and 35 μg/m^3 [99].
- NVF: same NV-use criteria as NVP. When NV is used, openings equipped with an ESF (described in Section 4.3.5) are used instead of windows (Table 26).

Table 26 shows a summary of the systems used in the eight scenarios considered in the detailed simulation analysis.

Table 26 – Indoor climate control systems used in the detailed simulation approach

Indoor Climate Control System	**SC**				**EC**			
	NoNV	**NVP**	**NVS**	**NVF**	**NoNV**	**NVP**	**NVS**	**NVF**
Rooftop air handling unit	●	●	●	●	●	●	●	●
PCS					●	●	●	●
Operable windows		●	●			●	●	
ESF				●				●

The model considers wind and buoyancy-driven single-sided natural ventilation [372] (Equations (18) to (20)). In the case of wind-driven NV, a typical urban wind profile was used to reduce the wind speed profile in the measured weather data [367].

$$\dot{V}_{wind} = C_w \times A_{open} \times u_{local} \tag{18}$$

$$\dot{V}_{stack} = C_D \times A_{open} \times \sqrt{2 \times g \times H_{NPL} \times \frac{|T_z - T_{out}|}{T_z + 273.15}} \tag{19}$$

$$\dot{V}_{nat} = \sqrt{\dot{V}_{stack}^2 + \dot{V}_{wind}^2} \tag{20}$$

In each office zone, the maximum openable window area is 5 % of its gross floor area [9], which is equivalent to a window-to-wall ratio (WWR) of 3.5 % for the two larger office zones and 2.5 % for two smaller office zones). Nonetheless, window opening area has been shown to increase linearly with the outdoor temperature, while never reaching a completely open position [373] (Table 27). Thus, the opening area was considered to range from 1 % of the floor area, for an outdoor temperature of 10 °C, to 3.5 %, for 30 °C, as given by Equation (21):

$$A_{open} = A_{open,max} \times (0.0242 \times T_{out} - 0.037) \tag{21}$$

Table 27 – Natural ventilation parameter sources

Parameter		**Ref.**	**Value**
Natural Ventilation	Opening Area	[9, 373]	1 to 3.5 % of floor area
	Single-Sided Ventilation Modeling	[372]	–

4.3.4. Pollutant Transport Model

The prediction of internal PM2.5 levels was performed with a modified version of the GCA that is available in the building thermal simulation tool that was used for this research (EnergyPlus). The standard version of the GCA cannot model the reduction in the transport of outdoor pollutants into the building that results from both the settling of PM2.5 transported by the infiltration airflow within building cracks and the incorporation of a fine particle filter in the rooftop AHU. To overcome this limitation, the standard GCA model equation was modified and implemented in a custom version of EnergyPlus. The equation used to predict internal PM2.5 is given by Equation (22):

$$\rho \times V_z \times \frac{dK_z}{dt} = \sum_{i=1}^{N_{source}} \rho \times G_i \times 10^6 - \sum_{i=1}^{N_{sink}} \rho \times R_i \times K_z + \sum_{i=1}^{N_{zone}} \dot{m}_{zone,i} \times \left(K_{zone,i} - K_z\right) + \dot{m}_{inf} \times (F \times K_{out} - K_z) + \dot{m}_{nat} \times (K_{out} - K_z) + \dot{m}_{sys} \times \left(\left[1 - \eta_{HVACfilter}\right] \times K_{sup} - K_z\right) \quad (22)$$

Equation (23) is a term of Equation (12) which refers to the transport of outdoor pollutant by the infiltration airflow: if the outdoor particle concentration is higher than within the simulation zone, more polluted air is entering the building; if not, the infiltration airflow is introducing cleaner air. Equation (24) shows the change that was applied: the outdoor particle concentration is corrected by the particle penetration rate, which was considered to be 80 % [205].

$$\dot{m}_{inf} \times (K_{out} - K_z) \quad (23)$$

$$\dot{m}_{inf} \times (F \times K_{out} - K_z) \quad (24)$$

Further, the term that models the transport of outdoor pollutant by the ventilation supply duct into the simulation zone is shown in Equation (25): if the particle concentration is larger in the supply duct than in the simulation zone, the ventilation system is introducing air with a higher pollutant concentration; if not, the system is introducing cleaner air. Equation (26) shows the change that was applied: the particle concentration in the supply duct is corrected by a factor which takes the filter's efficiency into account. This was considered to be a MERV 14-grade filter (equivalent to an F8-grade filter [374]), which has an effective PM2.5 removal efficiency of 71.4 % [31] and which was kept constant throughout the simulation, as high-efficiency filters are usually not affected by particle loading during use [375, 376].

$$\dot{m}_{sys} \times \left(K_{sup} - K_z\right) \tag{25}$$

$$\dot{m}_{sys} \times \left(\left[1 - \eta_{HVACfilter}\right] \times K_{sup} - K_z\right) \tag{26}$$

Additionally, the deposition rate on indoor surfaces was set to 0.19 h^{-1} [205] and the occupant-induced re-suspension obtained in Thatcher & Layton [193] was used (see Table 28). Both parameters are constant throughout the simulation, due to the difficulty in accurately modeling their change through time, an approach followed by other studies [205, 376]. Further, the floor loading, which affects the re-suspension rate, is based on a surface area that is 60 % hard floor and 40 % carpet that are each equally distributed between tracked and untracked surfaces.

Table 28 – Pollutant transport model parameter sources

Parameter		**Ref.**	**Value**
Contaminant Modeling	Deposition Rate	[205]	0.19 h^{-1}
	Infiltration Particle Penetration Rate	[205]	80 %
	Re-suspension	[193]	59.8 μg/cm^2, floor load; 4.4×10^{-7} h^{-1}, rate
Cloth Fine Particle Filter	Efficiency	[31, 375, 376]	71.4 %

4.3.5. Addition of an electrostatic filter to the pollutant transport model

A further modification to the GCA model equation was required to model the effect of the electrostatic filter that was used in the NVF scenario and is shown in Equation (27):

$$\rho \times V_z \times \frac{dK_z}{dt} = \sum_{i=1}^{N_{source}} \rho \times G_i \times 10^6 - \sum_{i=1}^{N_{sink}} \rho \times R_i \times K_z + \sum_{i=1}^{N_{zone}} \dot{m}_{zone,i} \times \left(K_{zone,i} - K_z\right) + \dot{m}_{inf} \times (F \times K_{out} - K_z) + \dot{m}_{nat} \times \left(\left[1 - \eta_{NVfilter}\right] \times K_{out} - K_z\right) + \dot{m}_{sys} \times \left(\left[1 - \eta_{HVACfilter}\right] \times K_{sup} - K_z\right) \quad (27)$$

The term in Equation (28) refers to the pollutant transport into the simulation zone from the outside by the naturally ventilated airflow. The change that was applied is shown in Equation (29): the outdoor particle concentration is corrected by a factor that considers the electrostatic filter's efficiency into account.

$$\dot{m}_{nat} \times (K_{out} - K_z) \quad (28)$$

$$\dot{m}_{nat} \times \left(\left[1 - \eta_{NVfilter}\right] \times K_{out} - K_z\right) \quad (29)$$

This filter has an effective PM2.5 removal efficiency of 63 %, which was kept constant in the simulation, assuming regular cleaning [280]. A voltage of 27.5 kV is required for filter operation, while the electrical current is assumed to be proportional to the PM2.5 mass flow rate through the filter and was calculated as 26.5 µA per unit µg/s, totaling a power consumption of 0.73 W s/µg (Table 29).

Table 29 – Electrostatic filter parameter sources

Parameter		**Ref.**	**Value**
Electrostatic Filter	Efficiency	[280]	63 %
	Power Consumption	[280]	0.73 W s/µg (27.5 kV; 26.5 µA s/µg)

5. RESULTS AND ANALYSIS

The next subsections present the results of the analysis of the impact of high outdoor PM2.5 levels on NV, beginning with the statistical analysis and followed by the detailed simulation analysis.

5.1. Statistical Analysis

The average annual NV potential, calculated using measured hourly data, is shown in Figure 23 (California), Figure 24 (Europe), Figure 25 (Asia) and Table 30. The yearly percentage of working hours during which the outdoor temperature is suitable for NV use, i.e. 10 to 26 °C for standard comfort (SC) and 10 to 30 °C (and relative humidity below 80 % for temperatures above 26 °C) in the case of extended comfort (EC), is given by the sum of the green and red bars. The red bar alone shows the decrease in NV potential due to PM2.5 levels above each region's concentration threshold (12 $\mu g/m^3$ in California, 10 $\mu g/m^3$ in Europe and both 10 and 35 $\mu g/m^3$ in Asia), while the green bar represents the working hours with both adequate temperatures and low PM2.5 levels. The blue bar shows the fraction of hours with an outdoor temperature that is too low for NV use (below 10 °C), while the yellow bar represents those when either the outdoor temperature (above 26 °C (SC) or 30 °C (EC)) or the outdoor relative humidity (above 80 %, when the temperature is between 26 to 30 °C (EC)) is too high.

In California, the simple analysis indicates that there is the potential to use NV during at least half of the working time for all cities. With SC criteria and without particle effects, the NV potential (adding the green and red bars in the figure) is highest in San Diego and Burbank, at about 95 and 80 %, respectively. In the remaining cities, that fraction falls to between 60 and 70 %. In Fresno and Sacramento, unavailable NV occurs mainly in the summer, due to the excessively high temperatures. In Livermore, the opposite situation occurs, i.e. NV is unavailable mostly during the winter. Accordingly, Fresno and Sacramento see the highest increase in NV potential due to the availability of PCS: NV becomes available for an additional 12 and 10 %, respectively, of the annual working hours which previously had excessively high outdoor temperatures. This increase in NV potential is lower in Burbank (8 %) and Livermore (7 %) and minimal in San Diego (2 %), since standard comfort criteria already allowed for the use of NV in nearly all working hours in this city.

When considering the negative effects of airborne particles, Burbank has the highest loss in potential, falling from 80 % NV availability to under 25 % of working hours (SC criteria). This is due to the continuously high particle levels, a consequence of the particle entrapment caused by alternating sea-land breezes and mountain flows. In Fresno, availability also falls to about 25 %, mostly due to higher PM2.5 during the winter and the particle entrapment within the San Joaquin Valley. Livermore presents the lowest impact of PM2.5 concentration, with natural ventilation availability falling from 70 % to just below 60 %. When high outdoor PM2.5 is taken into account, the increased availability of NV due to the use of PCS is diminished, ranging from an additional 1 % of the annual working hours in San Diego to 7 % in Sacramento.

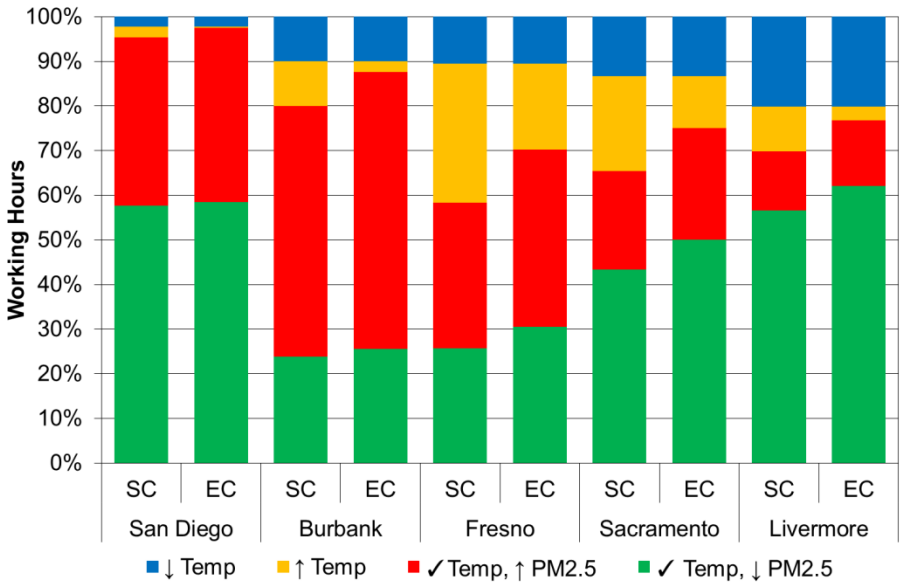

Figure 23 – Distribution of working hours according to temperature in California: ✓ Temp: temperature and humidity are within the NV thresholds; ↑ Temp: temperature or humidity are above the NV threshold; ↓ Temp: temperature is below the NV threshold; ↑ PM2.5: PM2.5 is above threshold; ↓ PM2.5: PM2.5 is equal to or below threshold

In Europe, this analysis shows that Lisbon has the highest NV potential (81 %) with SC criteria, while the lowest potential is found in Skopje (40 %). In all other cities, NV can potentially be used during at least half of the working hours, ranging from 50 to 65 %. In most cities, the availability of NV is limited by the excessively cold temperatures during the winter. Madrid and Skopje are exceptions, with similar occurrences of too hot and too cold temperatures. In Lisbon, excessively warm summer temperatures are the main limitation. Consequently, in these three cities, the availability of PCS results in an increase in NV potential from 10 % (in Lisbon) to 12 % (Skopje). In the remaining European cities, the additional NV potential is marginal: 1 % (in London) to 5 % in (Prague).

In all European cities, high PM2.5 levels reduce the NV potential by at least 50 %. Antwerp and Lisbon are the less affected cities, with a loss in potential only slightly above 50 % (52 and 51 %, respectively). On the other hand, NV potential in London is reduced by 82 %, while high particle levels remove nearly all NV hours in Skopje. Finally, Krakow, Prague and Strasbourg see their NV potentials fall by about 70 %, while in Madrid and Paris the decrease is approximately 60 %.

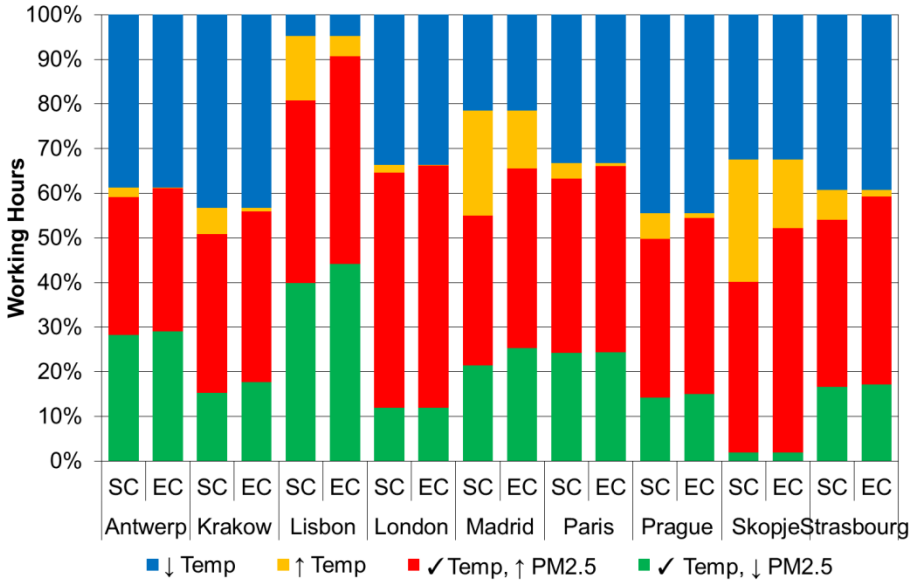

Figure 24 – Distribution of working hours according to temperature in Europe: ✓ Temp: temperature and humidity are within the NV thresholds; ↑ Temp: temperature or humidity are above the NV threshold; ↓ Temp: temperature is below the NV threshold; ↑ PM2.5: PM2.5 is above threshold; ↓ PM2.5: PM2.5 is equal to or below threshold

In Asia, optimal NV conditions with SC criteria only occur in approximately half of the working hours (53 %) in Shanghai, 40 % in Beijing and 23 % in New Delhi, which are lower than most cities in the other analyzed regions. In all Asian cities, availability of PCS devices (EC criteria) increases the NV potential by 12 to 14 % of the annual working hours. The highest relative increase occurs in New Delhi, as NV is now available in nearly 40 % of the working hours. In Beijing, the potential for NV rises to about half of the annual working hours, while in Shanghai, the annual NV potential increases to 65 %.

Two outdoor PM2.5 concentration thresholds were used to limit the availability of NV: NV10 (10 µg/m^3) and NV35 (35 µg/m^3). As expected, NV availability is more impacted by the stricter NV10 threshold, which nearly eliminates the possibility for the use of NV during working hours in all three cities. The NV35 limit also has a significant impact: in Beijing, the availability is reduced to 13 % (SC) and 17 % (EC), a loss of about two-thirds of the non-PM2.5-restricted potential. In Shanghai, more than half of the potential is lost (20 and 26 % availability, for SC and EC criteria, respectively). In New Delhi, even with this higher threshold, NV use is still nearly impossible.

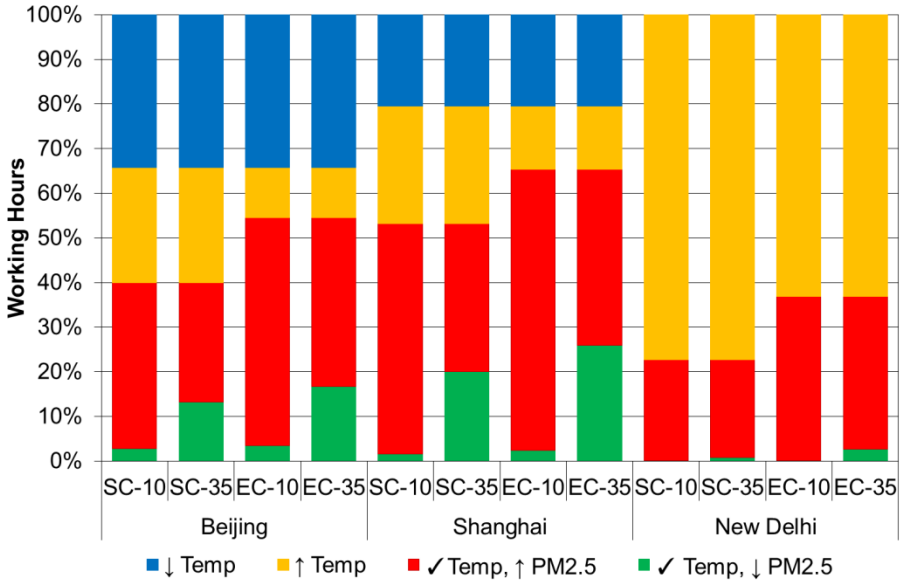

Figure 25 – Distribution of working hours according to temperature in Asia: ✓ Temp: temperature and humidity are within the NV thresholds; ↑ Temp: temperature or humidity are above the NV threshold; ↓ Temp: temperature is below the NV threshold; ↑ PM2.5: PM2.5 is above threshold; ↓ PM2.5: PM2.5 is equal to or below threshold

Table 30 – Distribution of working hours according to temperature [%]: ✓ Temp: temperature and humidity are within the NV thresholds; ↑ Temp: temperature or humidity are above the NV threshold; ↓ Temp: temperature is below the NV threshold; ↑ PM2.5: PM2.5 is above threshold; ↓ PM2.5: PM2.5 is equal to or below threshold

City	SC				EC			
	✓ Temp, ↓ PM2.5	✓ Temp, ↑ PM2.5	↑ Temp	↓ Temp	✓ Temp, ↓ PM2.5	✓ Temp, ↑ PM2.5	↑ Temp	↓ Temp
San Diego	58	38	2	2	58	39	0	2
Burbank	24	56	10	10	26	62	2	10
Fresno	26	33	31	10	31	40	19	10
Sacramento	43	22	21	13	50	25	12	13
Livermore	57	13	10	20	62	15	3	20
Antwerp	28	31	2	39	29	32	0	39
Krakow	15	36	6	43	18	38	1	43
Lisbon	40	41	14	5	44	47	5	05
London	12	53	2	34	12	54	0	34
Madrid	21	34	24	21	25	40	13	21
Paris	24	39	3	33	24	42	1	33
Prague	14	36	6	44	15	39	1	44
Skopje	2	38	28	32	2	50	15	32
Strasbourg	17	37	7	39	17	42	1	39
Beijing (NV10; NV35)	3; 13	37; 27	26	34	3; 17	51; 38	11	34
Shanghai (NV10; NV35)	2; 20	52; 33	26	20	2; 26	63; 39	14	20
New Delhi (NV10; NV35)	0; 1	23; 22	77	0	0; 3	37; 34	63	0

5.1.1. Correlation between PM2.5, Wind Speed and Direction and Outdoor Air Temperature

Correlations were investigated between PM2.5 and three weather variables: temperature, wind speed and wind direction. The correlations focused on daytime working hours with NV potential, considering both SC (air temperature between 10 and 26 °C) and EC criteria (10 to 26 °C for any humidity, or 26 to 30 °C and relative humidity below 80 %). Outdoor air temperature and wind speed were binned to the nearest integer and an average PM2.5 concentration was calculated for each of these bins. The air temperature correlation can identify significant PM2.5 sources and the potential impact on indoor exposure: if PM2.5 levels rise with the increase in temperature, then so will exposure, since window opening area also increases with temperature. The wind speed correlation was restricted to velocities of less than 7 m/s in California, 10 m/s in Europe and 12 m/s in Asia, since the number of hours above these thresholds was very low (less than 4 % of the time). Finally, the wind direction correlation seeks to identify directions that bring air with significantly high or low particle concentrations and considers only wind speeds equal to or above 3 m/s, to only account for winds that transport air from outside each location. Table 31 shows the coefficients of determination (R^2) and linear regression slopes that were obtained.

The correlation between PM2.5 and temperature found a wide range of results. In California (Figure 26), San Diego and Burbank show good correlations and an increase in average particle concentration with temperature. In both cities, warmer weather leads to a rise of the formation of secondary ammonium sulfate, a significant component of PM2.5 [57], although this effect is limited to temperatures below 25 °C in Burbank. These locally generated particles are then trapped by the low inversion layers, which frequently occur throughout the year. Further, this increase in PM2.5 concentration with temperature is a problem in light of typical window opening approaches. Fresno shows no correlation between PM2.5 and temperature. Livermore and Sacramento show good and moderate coefficients of determination, respectively, although the change in average PM2.5 with temperature is low for both cities.

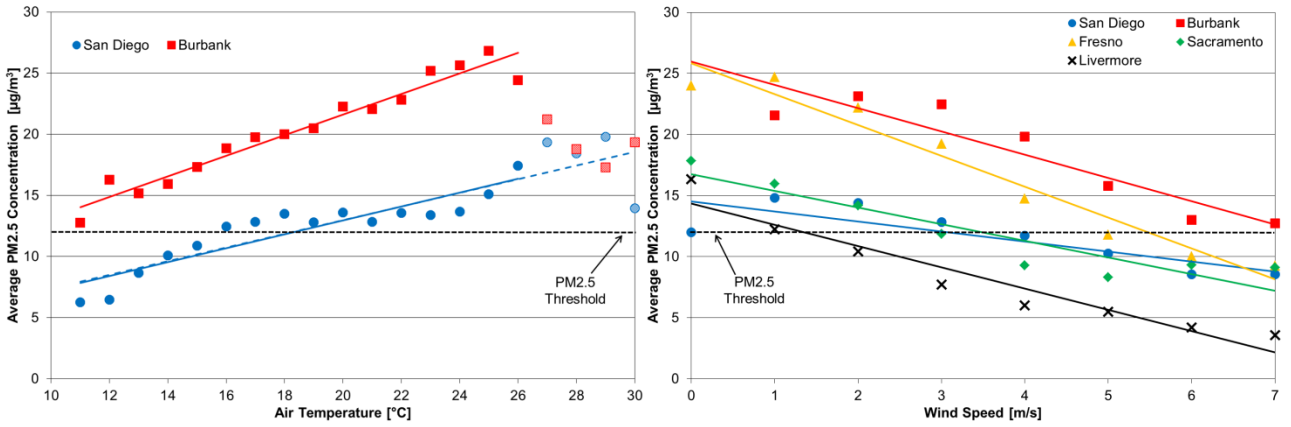

Figure 26 – Variation of average PM2.5 with air temperature for Burbank (SC only) and San Diego (both SC and EC) and variation of average PM2.5 with wind speed for all cities in California (SC only); SC: full points and regression line; EC: full and striped points and dotted regression line

In Europe (Figure 27), only Krakow and Skopje show significant air temperature correlation slopes and coefficients. Specifically, PM2.5 levels increase with the decrease in temperature in both cities, which are located in countries (Poland and FYRO Macedonia, respectively) with a fossil fuel-dependent (mainly coal) energy grid [377, 378]. The higher energy use during colder time periods increases PM2.5 levels. Elsewhere in Europe, outdoor PM2.5 levels do not significantly change with temperature.

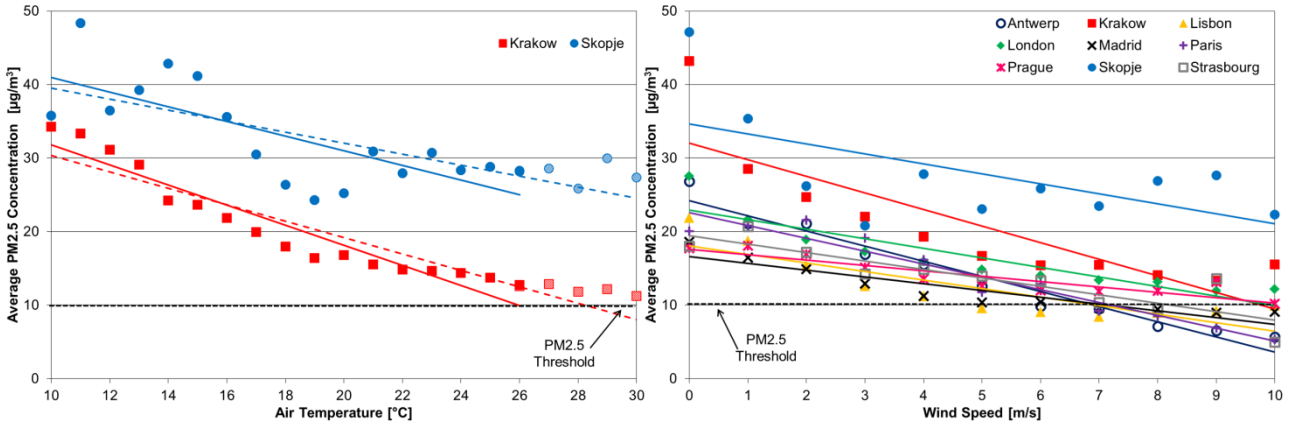

Figure 27 – Variation of average PM2.5 with air temperature (both SC and EC criteria) for Krakow and Skopje and variation of average PM2.5 with wind speed for all cities in Europe (SC only); SC: full points and regression line; EC: full and striped points and dotted regression line

Shanghai is the only Asian city to show both a strong coefficient of determination and a high change of average PM2.5 concentration with temperature (Figure 28). This city's subtropical climate is characterized by high precipitation levels during the warmer season [379], resulting in PM2.5 levels decreasing with the increase in air temperature. In Beijing, PM2.5 levels are unaffected by the variation in air temperature, while no correlation can be established between air temperature and PM2.5 in New Delhi.

In the case of wind speed (Figure 26 for California, Figure 27 for Europe and Figure 28 for Asia), all cities show the expected trend of lower PM2.5 concentrations for higher wind velocities. Low wind speeds do not transport particles that, in most cases, are locally generated.

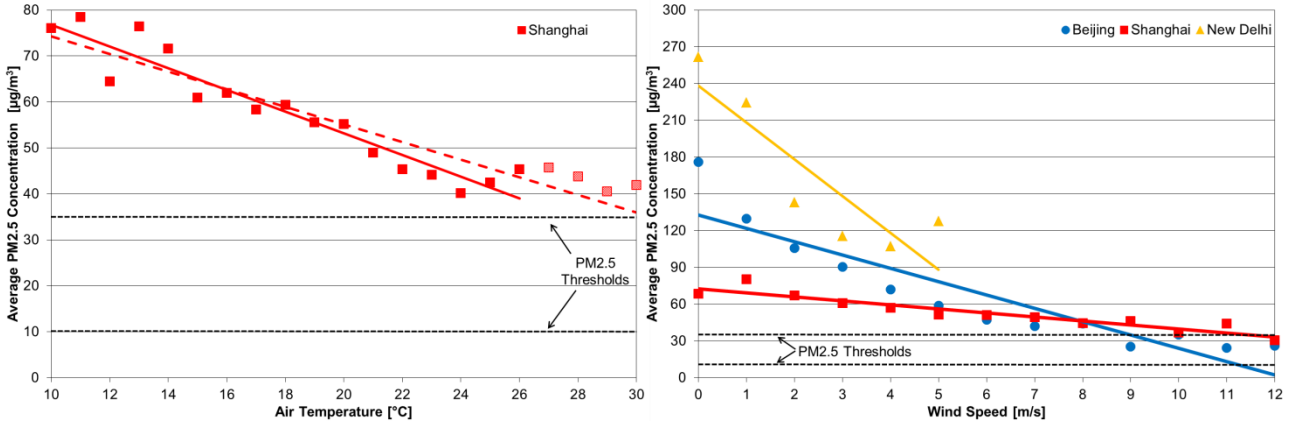

Figure 28 – Variation of average PM2.5 with air temperature (both SC and EC criteria) for Shanghai and variation of average PM2.5 with wind speed for all cities in Asia (SC only); SC: full points and regression line; EC: full and striped points and dotted regression line

Table 31 – Variation of average PM2.5 with air temperature and wind speed; highest temperature correlation slopes (absolute value above 0.5 °C per μg/m^3 increase) are highlighted in bold as are coefficients of determination above 0.8 for both air temperature and wind speed correlations

City	Air Temperature				Wind Speed			
	SC		EC		SC		EC	
	Slope	R^2	Slope	R^2	Slope	R^2	Slope	R^2
San Diego	**0.57**	**0.83**	**0.56**	**0.79**	–0.82	0.70	–0.79	0.68
Burbank	**0.84**	**0.95**	0.37	0.34	–1.91	**0.86**	–1.88	**0.86**
Fresno	–0.03	0.01	–0.12	0.16	–2.53	**0.95**	–2.59	**0.98**
Sacramento	–0.24	0.69	–0.12	0.32	–1.36	**0.86**	–1.26	**0.85**
Livermore	**0.20**	**0.93**	**0.19**	**0.95**	–1.74	**0.93**	–1.52	**0.97**
Antwerp	–0.01	0.00	–0.07	0.04	–2.06	**0.96**	–2.05	**0.95**
Krakow	**–1.37**	**0.91**	**–1.12**	**0.88**	–2.25	0.71	–2.08	0.69
Lisbon	–0.26	0.65	–0.01	0.00	–1.16	0.73	–1.14	0.75
London	0.10	0.18	0.30	0.50	–1.30	**0.82**	–1.28	**0.84**
Madrid	0.08	0.38	0.04	0.16	–0.92	**0.86**	–0.89	**0.88**
Paris	–0.19	0.47	0.05	0.02	–1.74	**0.94**	–1.77	**0.95**
Prague	–0.19	0.73	–0.10	0.40	–0.73	**0.83**	–0.72	**0.85**
Skopje	**–0.99**	**0.54**	**–0.75**	**0.51**	–1.36	0.36	–1.39	0.42
Strasbourg	–0.05	0.05	0.14	0.20	–1.14	0.77	–1.13	0.77
Beijing	0.11	0.00	–0.01	0.00	–10.87	**0.83**	–10.19	**0.86**
Shanghai	**–2.36**	**0.91**	**–2.01**	**0.88**	–3.29	**0.88**	–3.44	**0.90**
New Delhi	0.32	0.00	**–1.97**	**0.09**	–30.01	0.77	–23.03	0.71

Finally, the few consistent patterns that were found between PM2.5 and wind direction (considering only wind speeds above 3 m/s) are shown in Figure 29. In Livermore (California), the most frequent wind directions are Southwest to Northwest, which correspond to some of the lowest average particle concentrations. Wind from these directions originates from the San Francisco Bay area, replacing the local air with less polluted air. A similar effect occurs in Shanghai (Asia), where the most frequent wind directions (Northeast to Southeast) bring in less polluted air from the East China Sea. In Antwerp and Lisbon (Europe), the locally generated particles are also removed by winds that frequently originate in cleaner neighboring areas, namely South to West and Northwest to Northeast, respectively. The opposite occurs in Burbank (California), with the most frequent wind direction (Southwest) coinciding with the highest average PM2.5 concentration: wind brings in polluted air from the nearby city of Los Angeles, which adds to the locally generated particles.

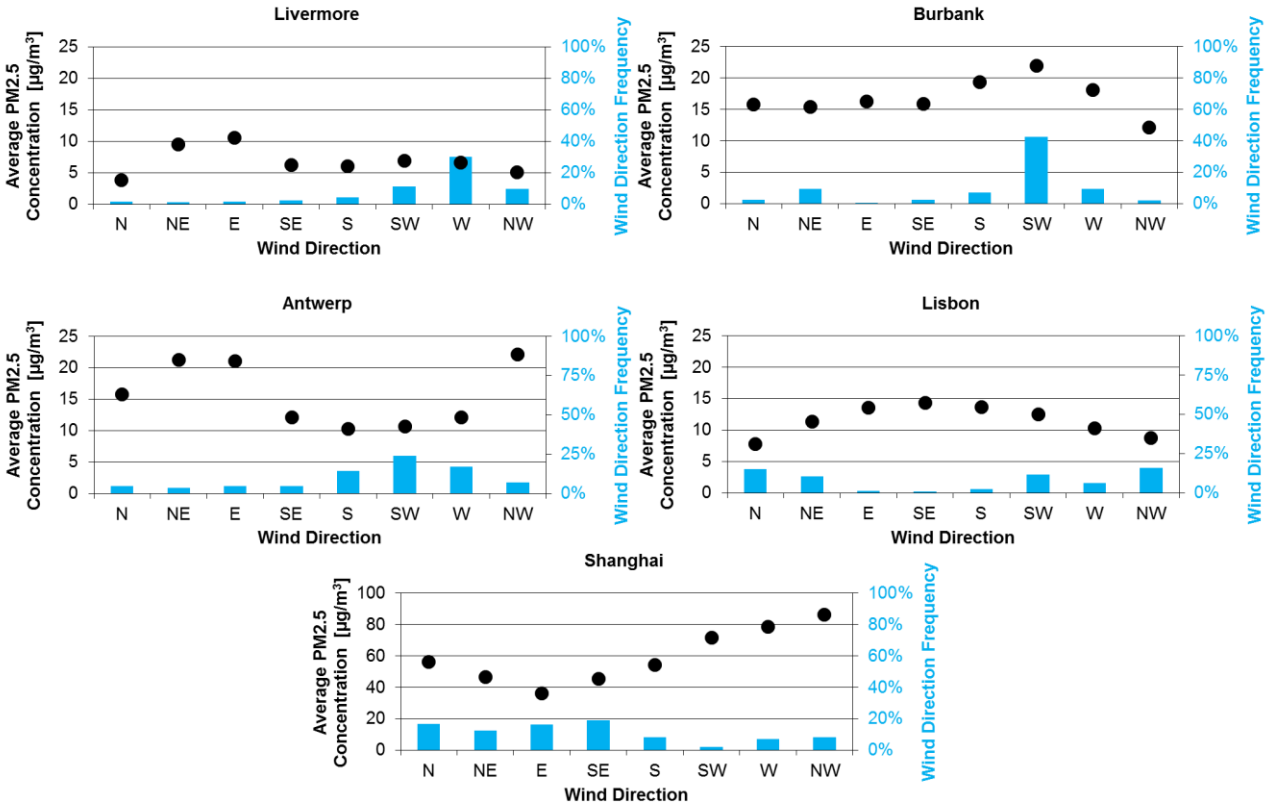

Figure 29 – Variation of average outdoor PM2.5 with wind direction for Burbank, Livermore, Antwerp, Lisbon and Shanghai (SC criteria only)

5.1.2. Hourly and Monthly Variation of PM2.5

An average PM2.5 concentration was calculated for each month of the year and each working hour of the day. This analysis can determine when higher PM2.5 concentrations occur: a coincidence with higher NV availability is a concern, as it will lead to an increase of exposure to PM2.5 of outdoor origin. On the other hand, if higher NV availability coincides with lower PM2.5 concentrations, occupant exposure is lower.

Outdoor PM2.5 concentrations were higher during the morning and, in some cities, in the final hour of the working day, a pattern typically found in urban locations, which is attributed mainly to commuter traffic. This trend is troublesome, since commercial building occupants typically open a larger number and area of windows during the morning [34], which, following these results, leads to an increase in exposure.

In the case of California, no significant monthly variation was found in San Diego, while in Livermore, the variation was low and average PM2.5 was found to be below 12 $\mu g/m^3$ for all months except January (13 $\mu g/m^3$). The monthly PM2.5 concentrations for Sacramento, Fresno and Burbank, the Californian cities with the highest variation throughout the year, are shown in Figure 30 and the fraction of monthly working hours with available NV is shown in Figure 31.

Sacramento and Fresno present a higher concentration of PM2.5 during the winter months due to the increase in particle-emitting activities and the entrapment of those locally generated particles by both the surrounding mountain ranges and the low altitude inversion layers that occur during that season. This will have a greater impact in Fresno, as temperatures are within the natural ventilation range during more of those months' working hours. In both cities, EC criteria increases the availability of NV mostly in the warmer months (as occurs in all cities in California), when PM2.5 levels are lower.

In Burbank, average PM2.5 concentrations are high throughout the year, reaching its peak in August and September. However, during those months NV potential (with SC criteria) is at its lowest, which can mitigate the exposure to PM2.5 of outdoor origin. Nonetheless, the increase in NV availability due to the extension of the NV-adequate temperature range (EC criteria) takes place during those warmer, more polluted months, which can increase the exposure to PM2.5.

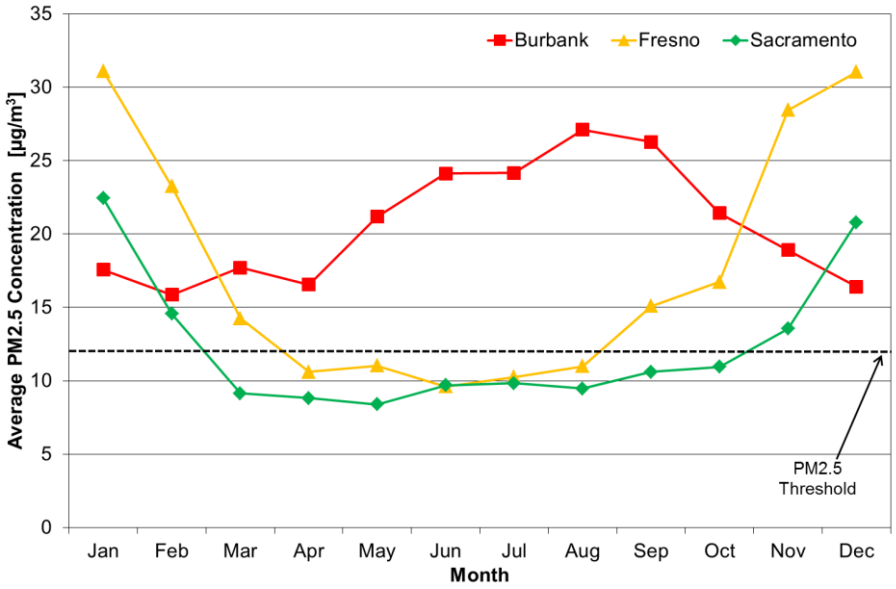

Figure 30 – Monthly variation of average PM2.5 concentrations in Burbank, Fresno and Sacramento (California, SC criteria only)

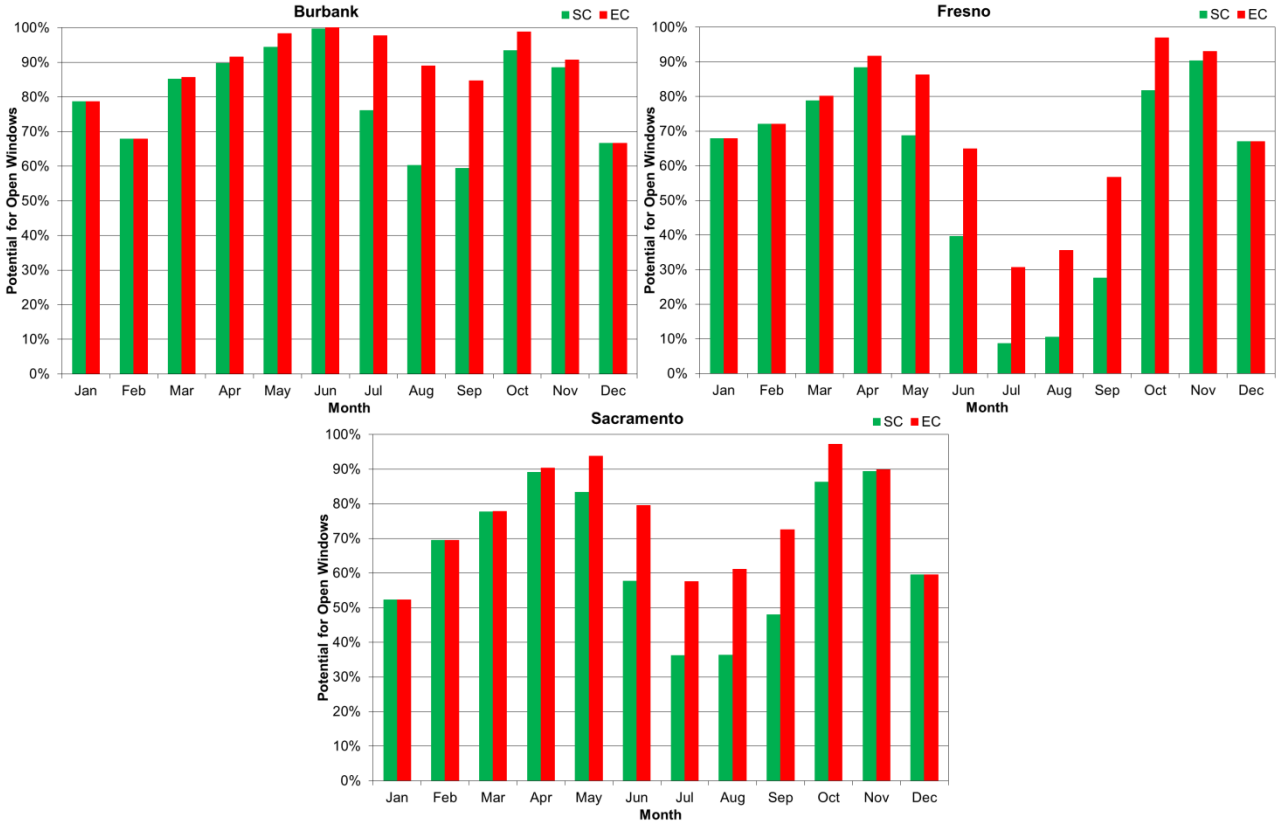

Figure 31 – Monthly variation of the potential for NV use during working hours in Burbank, Fresno and Sacramento (California, both SC and EC criteria)

In Europe, the cities with the highest monthly change in PM2.5 are Krakow and Skopje (Figure 32). Figure 33 shows the availability of NV-adequate temperatures in both cities. In Skopje, outdoor PM2.5 concentrations are higher in the colder mid-season months, which also have a higher NV availability and therefore can increase PM2.5 exposure. Conversely, in Krakow, warmer months have higher NV availability and lower PM2.5 levels. In these two cities, the shift to EC criteria increases the availability of NV during the less-polluted summer months, which can allow an increase in ventilative cooling without an increase in occupant exposure. In all other cities, no significant pattern was found regarding the monthly variation of PM2.5. Similar to California, EC criteria increases the availability of NV during the summer months in all cities, as well as during the warmer mid-season months in Lisbon and Madrid.

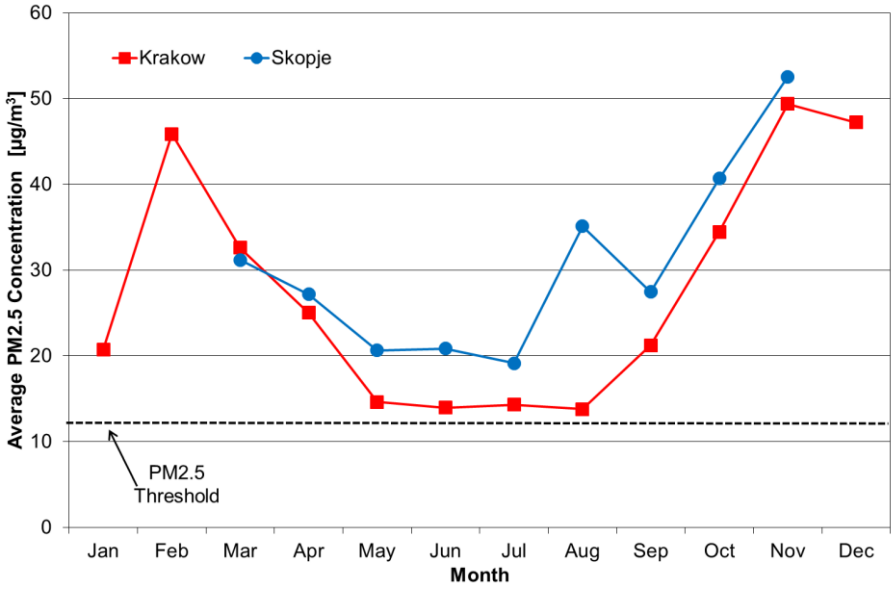

Figure 32 – Monthly variation of average PM2.5 concentrations in Krakow and Skopje (Europe, SC criteria only)

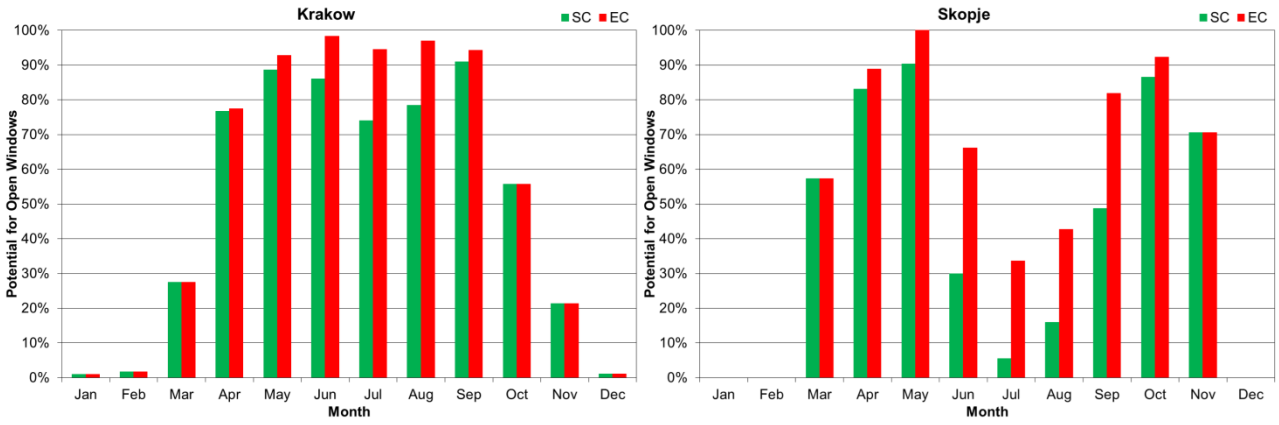

Figure 33 – Monthly variation of the potential for NV use during working hours in Krakow and Skopje (Europe, both SC and EC criteria)

Finally, Figure 34 presents the monthly variation of average PM2.5 concentrations in Asia, while the monthly availability of NV can be seen in Figure 35. In both Chinese cities, conditions for NV occur during the mid-season. Low temperatures during the winter and high temperatures during the summer limit the use of NV in those seasons. In New Delhi, NV is only available during the coldest months of the year. However, PM2.5 levels are highest during these months, resulting in the use of NV furthering the increase in indoor PM2.5 levels. EC criteria increase the availability of NV in New Delhi, although it is still mostly limited to the colder, more polluted season. In Beijing, the potential for NV rises, especially in the summer months. In Shanghai, the increase occurs in the summer and warmer mid-season months, which coincide with the less-polluted months of the year.

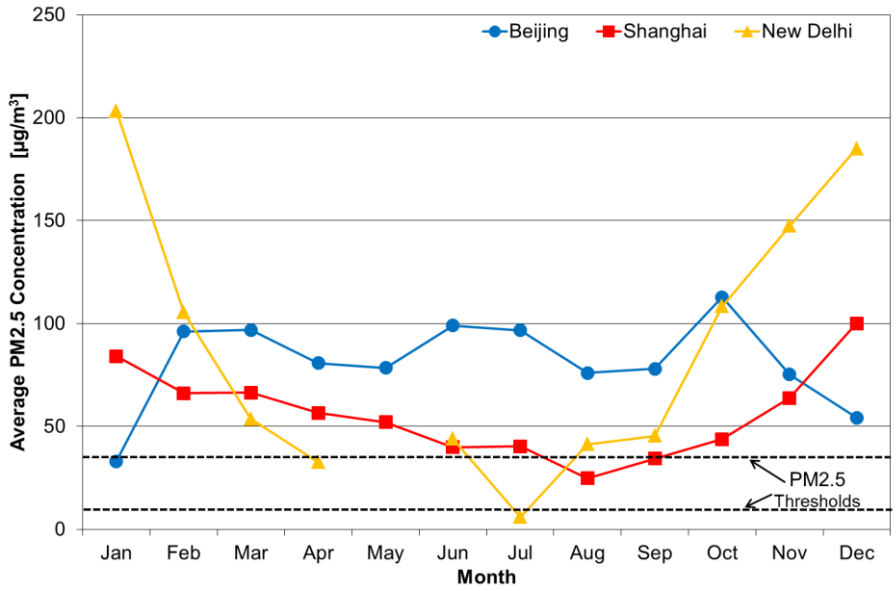

Figure 34 – Monthly variation of average PM2.5 concentrations in Beijing, Shanghai and New Delhi (Asia, EC criteria only)

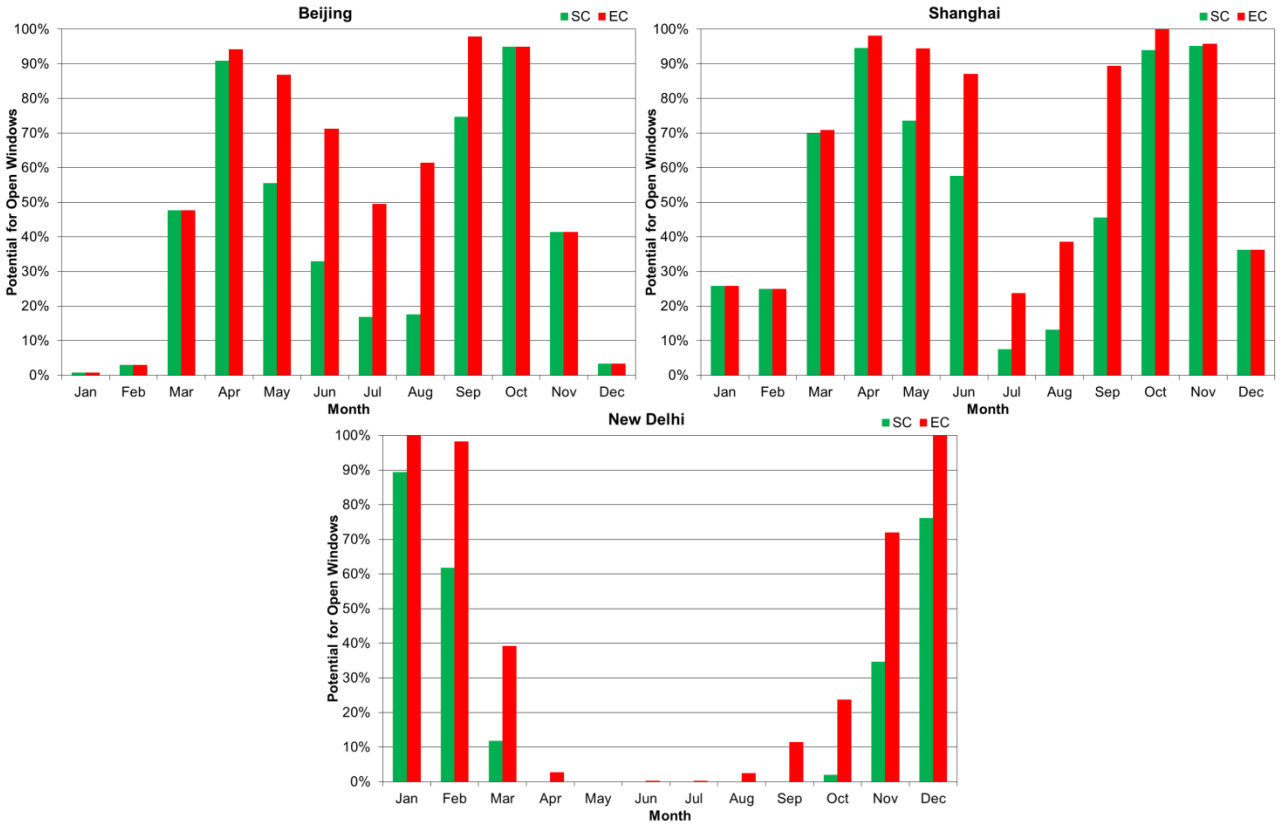

Figure 35 – Monthly variation of the potential for NV use during working hours in Beijing, Shanghai and New Delhi (Asia, both SC and EC criteria)

5.2. Detailed Simulation Analysis

The results of the detailed simulation analysis are summarized over the following subsections: the yearly electricity consumption due to heating, cooling and ventilation; the increase in cumulative indoor exposure to PM2.5 of outdoor origin during working hours; and the ratio between the yearly energy savings (Δe) and the increase in cumulative exposure to PM2.5 of outdoor origin (ΔP), in order to quantify the trade-off between energy savings and increased exposure.

5.2.1. Energy Savings

The annual electricity consumption of the HVAC system for each NV-use scenario is shown in Figure 36 (California), Figure 37 (Europe) and Figure 38 (Asia):

- NoNV: this scenario's electricity consumption is given by the sum of the four bars (red, black, blue and green).
- NVS: the sum of the blue, black and red bars is this scenario's electricity consumption; green is the energy that is saved.
- NVF: the electricity consumption is the sum of the red and black bars; the black bar is the electricity consumption of the electrostatic filters; the sum of green and blue is this scenario's energy savings.
- NVP: the red bar gives the electricity consumption; the sum of all other bars is this scenario's energy savings.

Table 32 presents the yearly HVAC energy savings for each NV-use scenario relative to each NoNV scenario.

As expected, for each HVAC set point scenario, the NoNV scenario results in the highest energy consumption. On the opposite end is the NVP scenario, where HVAC electricity consumption is reduced by the replacement of mechanical ventilation and cooling by natural ventilation that introduces cooler air into the building. In California, using NV whenever it can provide a cooling effect decreases the HVAC consumption by 26 to 83 % with SC criteria. However, if NV is only used when PM2.5 levels are low, savings decrease to between 17 and 63 %. The availability of PCS in the NoNV scenario leads to a 3 to 7 % decrease in HVAC consumption in Sacramento and Fresno and to a 4 to 13 % increase in San Diego and Burbank. In Livermore, the effect is negligible. These low differences are due to the heated chairs' and ceiling fans' (mainly the latter) power load nearly offsetting the decrease in the rooftop AHU's already optimized consumption due to the building's improved passive thermal behavior. Nonetheless, the most significant advantage of these PCS is the higher NV availability, resulting in a higher reduction in HVAC electricity consumption: NVP savings increase to up to 93 % and NVS savings up to 86 %. Using both SC and EC criteria, the energy savings of the NVF scenarios are nearly identical to those of NVP, due to the electrostatic filter's very low energy consumption.

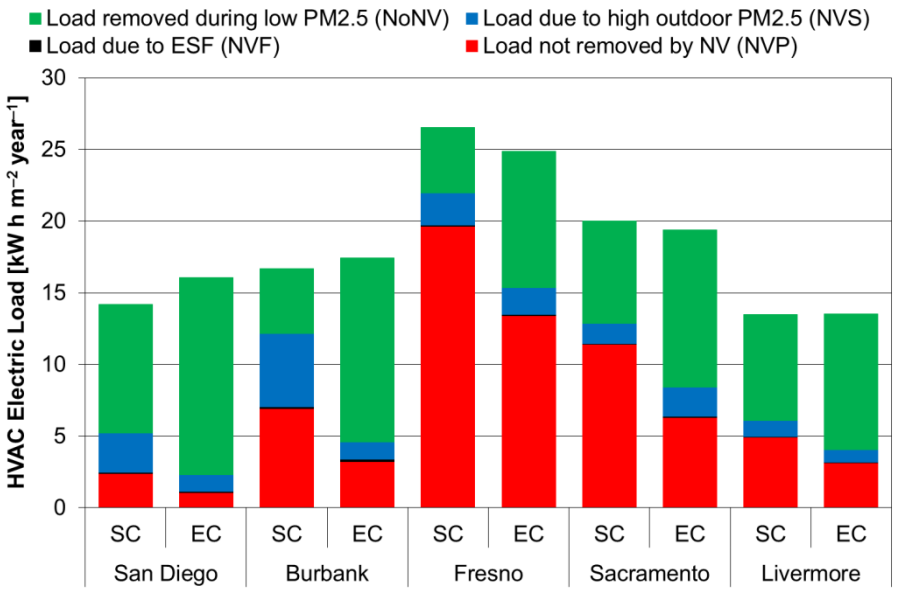

Figure 36 – Yearly HVAC electric load for each NV-use scenario in California

In Europe, the higher need for heating and the lower overall availability of NV result in a lower energy saving potential of the NVP scenario: 20 to 58 % with SC criteria. High outdoor PM2.5 has a more limiting effect in this region than in California, with the NVS scenario leading to energy savings between 5 and 40 %. The effect of PCS on the NoNV scenarios is, similarly to California, low: 1 to 8 % savings in Strasbourg, Prague, Krakow, Madrid and Skopje, and 1 to 3 % energy consumption increases in Paris, Antwerp, London and Lisbon. Again, EC criteria allow a higher NV availability and, consequentially, higher energy savings: up to 83 % for NVP and up to 63 % for NVS. The higher PM2.5 levels result in a slightly higher ESF electricity consumption. However, this consumption is still nearly negligible, thus the energy savings of the NVF scenario are similar to that of NVP.

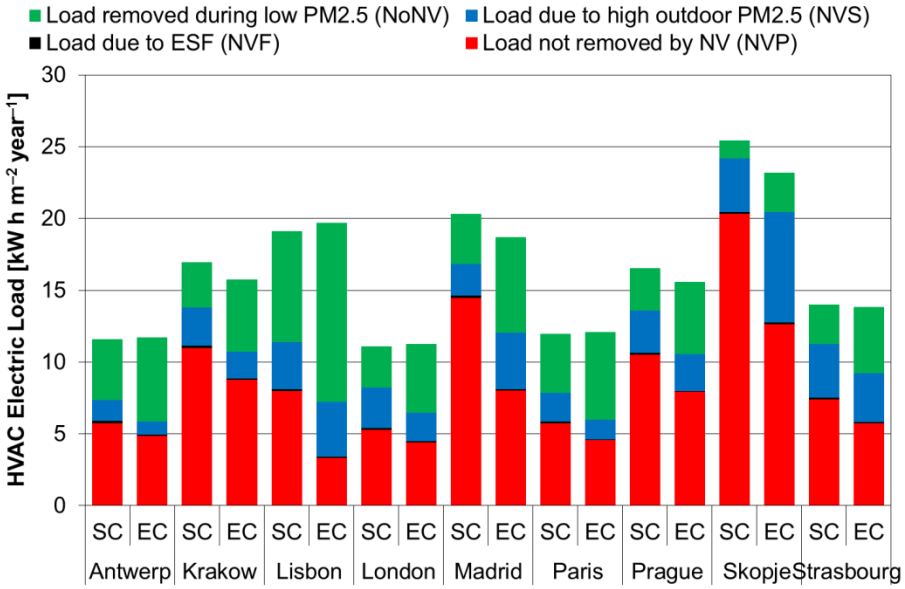

Figure 37 – Yearly HVAC electric load for each NV-use scenario in Europe

PCS without NV lead to a 6 to 11 % decrease of the annual HVAC electricity load in Asia. In the SC scenario, NVP reduces the annual HVAC consumption by 7 % in New Delhi, 16 % in Beijing and 21 % in Shanghai. These low annual savings are mostly due to severe seasonal limitations in the use of NV in all three cities. In New Delhi, where most of the year is excessively warm for NV, its use leads to energy savings above 65 % in the cooler months (December to February). However, between April and October, savings are nearly inexistent, leading to the overall low annual savings. In Shanghai and Beijing, where winters are too cold and summers are too warm, most savings occur during the mid-season. With EC criteria, the increased availability of NV increases the HVAC energy savings: 16 % in New Delhi, 41 % in Beijing and 45 % in Shanghai. In New Delhi, NV allows savings above 50 % between November and March, although during the remaining months, outdoor temperatures are still too high to allow any significant energy savings. In Beijing, most savings still occur during the mid-season, although a higher share of the yearly decrease in electricity consumption now occurs during the summer. In Shanghai, no seasonal change occurred, with most savings due to the use of NV still befalling on the mid-season. Restricting the use of NV to moments with outdoor PM2.5 levels below 10 µg/m^3 (NV10) leads to the lowest energy savings: 1 to 5 % with SC criteria, 4 to 15 % with EC. Since there is very low availability of NV during working hours, most of these savings occur due to the use of NV during the unoccupied period, which preemptively cools the building before its occupation. Despite its less restrictive threshold (35 µg/m^3), the NV35 scenario with SC criteria does not result in a substantial increase in savings: 1 to 12 %. However, with EC criteria, savings are increased to 22 % in Beijing and 35 % in Shanghai. In New Delhi, savings are still remarkably low: 4 %. Finally, the use of an electrostatic filter (NVF) leads to savings similar to those found in the NVP scenario, differing only due to the filter's low electric consumption.

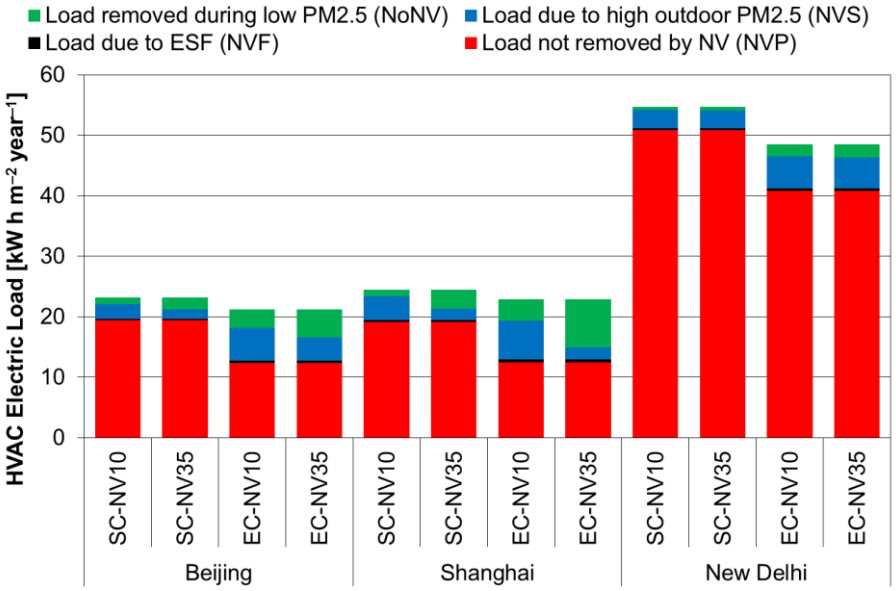

Figure 38 – Yearly HVAC electric load for each NV-use scenario in Asia

Table 32 – Average yearly HVAC energy savings (absolute [kW h m^{-2} $year^{-1}$] and relative [%] decrease) for each NV-use scenario relative to each NoNV scenario

City	SC			EC		
	NVP	NVF	NVS	NVP	NVF	NVS
San Diego	11.8; 83 %	11.7; 83 %	9.0; 63 %	15.0; 93 %	14.9; 93 %	13.8; 86 %
Burbank	9.8; 59 %	9.7; 58 %	4.5; 27 %	14.2; 82 %	14.1; 81 %	12.8; 74 %
Fresno	6.9; 26 %	6.8; 26 %	4.6; 17 %	11.5; 46 %	11.4; 46 %	9.5; 38 %
Sacramento	8.6; 43 %	8.6; 43 %	7.1; 36 %	13.1; 68 %	13.0; 67 %	11.0; 57 %
Livermore	8.5; 63 %	8.5; 63 %	7.4; 55 %	10.4; 77 %	10.3; 76 %	9.5; 70 %
Antwerp	5.8; 50 %	5.7; 49 %	4.2; 36 %	6.8; 58 %	6.7; 57 %	5.8; 50 %
Krakow	5.9; 35 %	5.8; 34 %	3.1; 19 %	6.9; 44 %	6.8; 43 %	5.0; 32 %
Lisbon	11.1; 58 %	11.0; 57 %	7.7; 40 %	16.3; 83 %	16.2; 83 %	12.4; 63 %
London	5.8; 52 %	5.6; 51 %	2.8; 25 %	6.8; 61 %	6.7; 60 %	4.8; 42 %
Madrid	5.8; 29 %	5.6; 28 %	3.4; 17 %	10.7; 57 %	10.6; 57 %	6.6; 35 %
Paris	6.2; 52 %	6.1; 51 %	4.1; 34 %	7.5; 62 %	7.4; 61 %	6.1; 50 %
Prague	6.0; 36 %	5.9; 35 %	2.9; 18 %	7.6; 49 %	7.5; 48 %	5.0; 32 %
Skopje	5.0; 20 %	4.9; 19 %	1.2; 5 %	10.5; 45 %	10.4; 45 %	2.7; 12 %
Strasbourg	6.6; 47 %	6.5; 46 %	2.7; 19 %	8.0; 58 %	8.0; 58 %	4.6; 33 %
Beijing (NV10; NV35)	3.7; 16 %	3.5; 15 %	1.0; 5 %; 1.9; 8 %	8.8; 41 %	8.4; 40 %	2.9; 14 %; 4.6; 22 %
Shanghai (NV10; NV35)	5.2; 21 %	4.9; 20 %	1.0; 4 %; 3.0; 12 %	10.3; 45 %	9.9; 43 %	3.4; 15 %; 7.9; 35 %
New Delhi (NV10; NV35)	3.7; 7 %	3.5; 6 %	0.4; 1 %; 0.5; 1 %	7.6; 16 %	7.1; 15 %	1.9; 4 %; 2.1; 4 %

5.2.2. Increased Cumulative Exposure to PM2.5

The increase in cumulative indoor exposure to PM2.5 of outdoor origin is presented on the left side of Figure 39 (California), Figure 40 (Europe) and Figure 41 (Asia). The green bar is the exposure in case of the NoNV scenario. The additional bars represent the increase in cumulative exposure for each of the three scenarios, in growing order: black for NVF, blue for NVS and red for NVP. The vertical axis units are mg h m^{-3} $year^{-1}$ (instead of µg h m^{-3} $year^{-1}$) to reduce the number of trailing zeros on the axis labels. On the right side of the same figures, each point gives the average annual indoor PM2.5 concentration during working hours, for each city and NV-use scenario, with the same coloring scheme: green for NoNV, black for NVF, blue for NVS and red for NVP. Table 33 presents the increase in yearly cumulative exposure to PM2.5 for each NV-use scenario relative to the NoNV scenario.

Expectedly, the full-time use of a high-efficiency cloth filter leads to the lowest cumulative exposure to PM2.5 in the NoNV scenarios. On the opposite end is the NVP scenario, which allows the use of NV whenever possible, allowing PM2.5 to frequently enter the indoor environment without any obstruction, increasing exposure to between 3.7 and 5.0 the NoNV exposure levels, with SC criteria, in California. The extended use of NV that occurs as a consequence of the availability of PCS furthers that exposure increase: 4.4 to 5.7 times the exposures found in the NoNV scenario. Both limiting the use of NV to moments of low outdoor PM2.5 levels (NVS) and using NV whenever possible with an ESF (NVF) lead to intermediate exposure levels. Nonetheless, in most Californian cities, NVF leads to lower increased cumulative exposure (up to 2.2 times the NoNV levels for SC, up to 2.4 for EC) than NVS (up to 3.2 for SC and up to 4.9 for EC). Exceptions are Burbank, where NVS exposure is lower than NVF exposure, and Fresno, where cumulative exposure levels are similar (both with SC criteria).

Using NV whenever possible leads (NVP) to an average indoor PM2.5 concentration above the regulated state and federal levels (12 µg/m^3) in Burbank (both with SC and EC criteria) and Fresno (EC only). Also in Burbank, NVS with EC criteria also results in an average indoor concentration above 12 µg/m^3. All other scenarios do not exceed this limit in California.

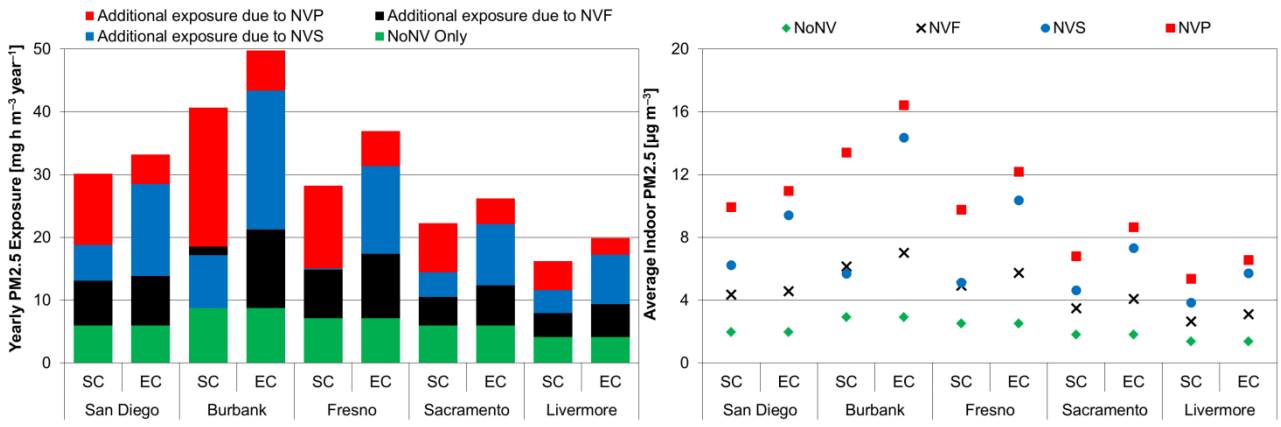

Figure 39 – Yearly cumulative exposure to PM2.5 and average indoor concentration for each NV-use scenario in California

In Europe, the maximized use of NV (NVP) increases occupant exposure by 1.9 to 4.2 times the NoNV levels with SC criteria and 2.2 to 5.4 with EC. These increases are lower than those found in California, although NV availability is also lower in this region. In most cities, the cumulative exposure levels that result from the NVF scenario are lower than with NVS: an increase of up to 2.1 for SC and up to 2.4 for EC, as opposed to up to 2.4 and up to 3.3, respectively. Exceptions are Skopje (both SC and EC criteria), Prague (SC only) and Strasbourg (SC only), where NVF and NVS exposure levels are nearly identical.

Average indoor PM2.5 concentrations exceed the WHO's guideline for PM2.5 exposure (10 µg/m^3) with NVP in several cities, especially with the increased availability of NV with PCS (EC criteria): Krakow (also with SC criteria), Lisbon, London, Paris, Skopje (also with SC) and Strasbourg. Additionally, in both Krakow and Skopje, the two exposure control approaches (NVS and NVF) fail to decrease the average indoor PM2.5 to below the WHO guideline, when PCS are available.

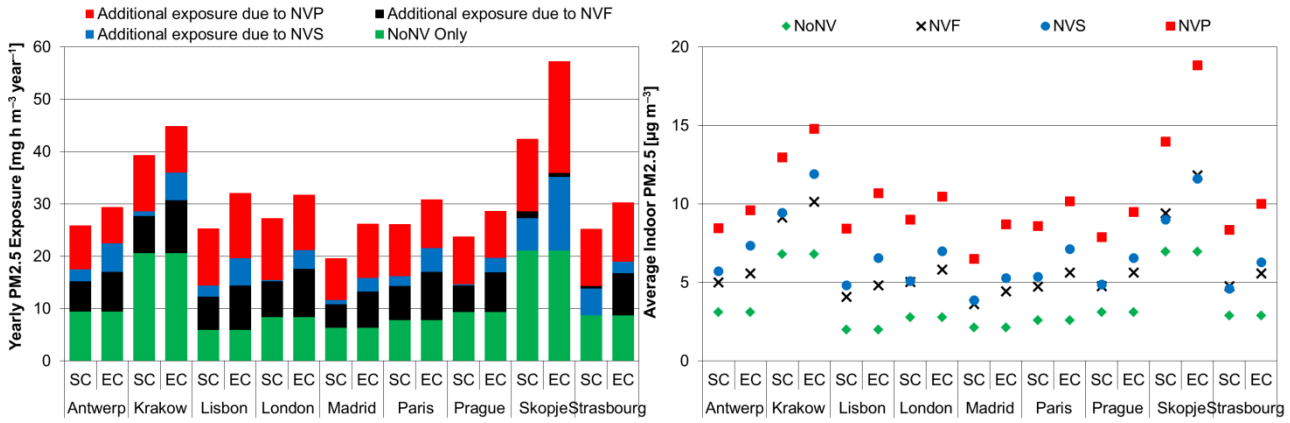

Figure 40 – Yearly cumulative exposure to PM2.5 and average indoor concentration for each NV-use scenario in Europe

In Asia, NVP increases occupant exposure by 2.3 to 3.0 times the NoNV exposure levels if PCS are not available and by 3.3 to 3.9 if they are. These increases are similar to those found in many cities in Europe, despite the lower NV availability. Limiting the availability of NV (NVS) leads to similar cumulative exposure levels with both thresholds (10 and 35 µg/m^3): up to 1.4 and up to 1.8 times the NoNV exposure, respectively, with SC criteria, and up to 2.1 and 2.6 times, with EC criteria. Limiting the penetration of outdoor PM2.5 with an ESF results in exposure levels similar to the two NVS scenarios in both Chinese cities (up to 1.9 times the NoNV exposure levels for SC, up to 2.2 for EC) and in New Delhi if PCS are available (1.9 times the NoNV levels). In the Indian city, if PCS are not available, NVF increases exposure to only 1.2 times the NoNV exposure, although this is a consequence of the very low availability and use of NV (1.2 times).

Shanghai is the only Asian city where the indoor average PM2.5 concentration is below the WHO's guideline of 10 µg/m^3, although only when the HVAC system (and its high-efficiency cloth filter) is in full-time operation. Also in this city, the average indoor concentration that result from the NVP scenarios are below the WHO's first interim target (35 µg/m^3). In both other cities, using NV whenever possible exceeds this threshold, although both the NVS and NVF exposure control approaches decrease the indoor PM2.5 concentration to below that level.

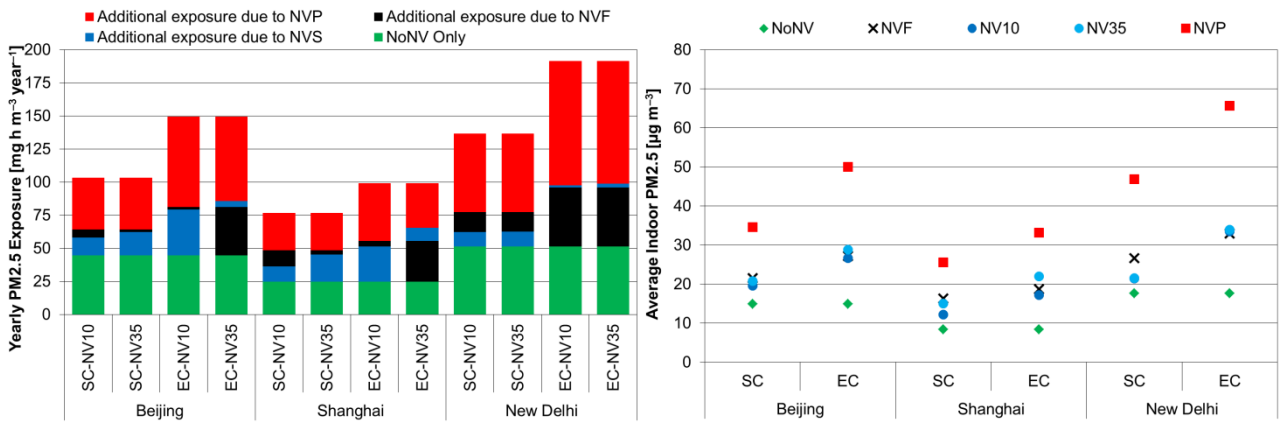

Figure 41 – Yearly cumulative exposure to PM2.5 and average indoor concentration for each NV-use scenario in Asia

Table 33 – Average increase in yearly cumulative exposure to PM2.5 (absolute [mg h m^{-3} $year^{-1}$] and relative increase) for each NV-use scenario relative to the NoNV scenario

City	SC			EC		
	NVP	NVF	NVS	NVP	NVF	NVS
San Diego	24; 5.0×	13; 2.2×	7; 3.2×	27; 5.5×	23; 2.3×	8; 4.8×
Burbank	32; 4.6×	8; 2.1×	10; 2.0×	41; 5.7×	35; 2.4×	12; 4.9×
Fresno	21; 3.9×	8; 2.1×	8; 2.1×	30; 5.2×	24; 2.4×	10; 4.4×
Sacramento	16; 3.7×	9; 1.8×	5; 2.4×	20; 4.4×	16; 2.1×	6; 3.7×
Livermore	12; 3.9×	7; 1.9×	4; 2.8×	16; 4.8×	13 2.3×	5; 4.2×
Antwerp	16; 2.7×	8; 1.6×	6; 1.8×	20; 3.1×	13; 1.8×	8; 2.4×
Krakow	19; 1.9×	8; 1.3×	7; 1.4×	24; 2.2×	15; 1.5×	10; 1.8×
Lisbon	19; 4.2×	8; 2.1×	6; 2.4×	26; 5.4×	14; 2.4×	8; 3.3×
London	19; 3.2×	7; 1.8×	7; 1.8×	23; 3.8×	13; 2.1×	9; 2.5×
Madrid	13; 3.1×	5; 1.7×	5; 1.8×	20; 4.1×	10; 2.1×	7; 2.5×
Paris	18; 3.3×	8; 1.8×	7; 2.1×	23; 3.9×	14; 2.2×	9; 2.8×
Prague	14; 2.5×	5; 1.5×	5; 1.6×	19; 3.1×	10; 1.8×	8; 2.1×
Skopje	21; 2.0×	6; 1.4×	7; 1.3×	36; 2.7×	14; 1.7×	15; 1.7×
Strasbourg	16; 2.9×	5; 1.6×	6; 1.6×	22; 3.5×	10; 1.9×	8; 2.2×
Beijing (NV10; NV35)	59; 2.3×	20; 1.4×	14; 1.3×; 18; 1.4×	105; 3.3×	37; 1.8×	35; 1.8×; 41; 1.9×
Shanghai (NV10; NV35)	51; 3.0×	24; 1.9×	11; 1.4×; 20; 1.8×	74; 3.9×	31; 2.2×	26; 2.1×; 41; 2.6×
New Delhi (NV10; NV35)	85; 2.7×	26; 1.5×	11; 1.2×; 11; 1.2×	140; 3.7×	45; 1.9×	46; 1.9×; 47; 1.9×

5.2.3. Ratio between Energy Savings and Increased Exposure

With the goal of quantifying the trade-off between energy savings and increased exposure, the ratio between the yearly energy savings (Δe) and the increase in cumulative exposure to PM2.5 of outdoor origin (ΔP) was calculated for each location and NV-use scenario. The most NV-favorable cities and scenarios will have the highest value of this indicator, since lower increases in particle levels for similar energy savings indicate that the combined weather and outdoor PM2.5 level conditions are more favorable to the use of NV. Further, comparing the results between the NVP and the NVS scenarios can show when natural ventilation is being used: a higher ratio in the NVS scenario indicates a higher use of natural ventilation when PM2.5 levels are low. The results are presented in Figure 42 for California, Figure 43 for Europe, Figure 44 for Asia and, finally, in Table 34 for all cities.

In the case of the NVP scenario with SC criteria, Fresno (0.33) and Burbank (0.31) show the lowest value among the Californian cities: Fresno has the lowest energy savings, while Burbank has the highest increase in exposure. On the other hand, this indicator is highest in Livermore (0.71), due to the lowest increase in exposure. Energy savings and increased exposure are lower in the NVS scenario, as expected. In all cities, the $\Delta e/\Delta P$ ratio increases, as natural ventilation is mostly used in moments with low outdoor PM2.5 concentrations. This ratio is highest in the NVF scenario. This is the result of taking advantage of the available energy saving potential (energy savings are similar to the NVP scenario), in addition to the electrostatic filter limiting occupant exposure to PM2.5 to levels similar to or below those of the NVS scenario. Despite some minor differences, the same pattern can be seen with EC criteria.

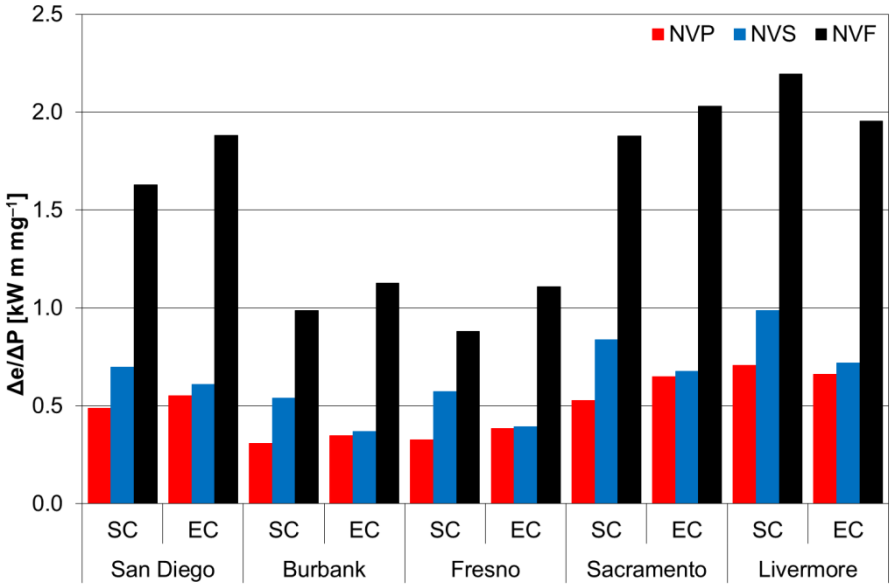

Figure 42 – Ratio between average energy savings and increase in PM2.5 exposure [kW m/mg] for each NV-use scenario in California

In Europe, the order of magnitude of the $\Delta e/\Delta P$ ratio is similar to California. Lisbon presents the highest indicator value, at 0.58, when NV is used whenever possible (NVP), with SC criteria. In all other cities, the $\Delta e/\Delta P$ ratio ranges from 0.30 to 0.41. Lisbon is also the city with the highest $\Delta e/\Delta P$ value in the NVS scenario (0.63). Skopje is the only city where this ratio decreases for this NV-use scenario, as most energy savings occur during moments of high pollution levels. Again, the $\Delta e/\Delta P$ ratio is highest when an electrostatic filter is used to limit the penetration of outdoor PM2.5, at a very low energy cost (NVF).

With EC criteria, the ratio decreases for most cities, except for Lisbon, Madrid and Skopje. These three cities have the highest increase in NV availability when PCS are available. Elsewhere, the low increase in NV potential results in an increase in exposure than is higher than the increase in energy savings.

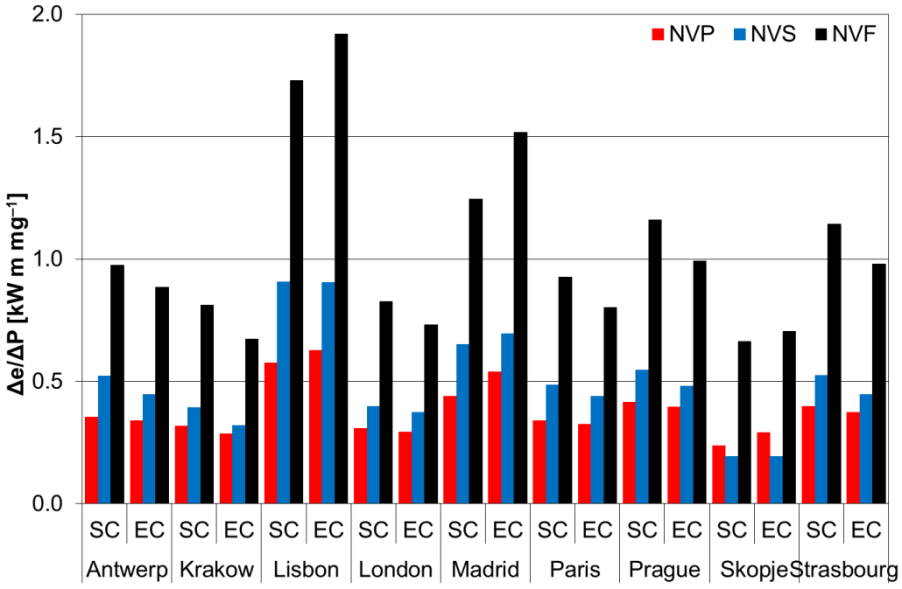

Figure 43 – Ratio between average energy savings and increase in PM2.5 exposure [kW m/mg] for each NV-use scenario in Europe

In the NVP scenario with SC criteria, Shanghai has the highest savings-to-increased exposure ratio (0.10) among the three Asian cities, while the ratio in Beijing is 0.06 and in New Delhi is 0.04. With EC criteria, Shanghai still has the highest ratio (0.14), while in Beijing and New Delhi, the ratio increases to 0.08 and 0.05, respectively. As can be seen, the ratios increase for all three Asian cities, showing that the combined use of NV and PCS leads to an increase in energy savings that is higher than the increase in indoor exposure. Nonetheless, these ratios are up to one order of magnitude lower than the ranges found for the European and Californian cities. This large difference is mostly due to the significantly higher increases in PM2.5 exposure that occur in these three cities. Further, in all three Asian cities, energy savings are lower than elsewhere, mostly due to the lower availability of NV. In California and Europe, air pollution regulations are stricter and have been in place for a longer period, effectively improving air quality. In China and India, those regulations are more recent and less stringent.

Although limiting the increased exposure, the NV10 scenario does not allow for significant energy savings, resulting in a $\Delta e/\Delta P$ ratio similar to NVP in Beijing and lower in Shanghai and New Delhi. By increasing the outdoor PM2.5 concentration threshold (NV35), indoor exposure also increases, but so do energy savings. In all three cities, energy savings have a higher relative increase, hence the higher $\Delta e/\Delta P$ ratios. However, in New Delhi, this ratio is still lower than that found for the NVP scenario. Finally, as with both other analyzed regions, the best savings-to-increased exposure ratios occur with the NVF scenario.

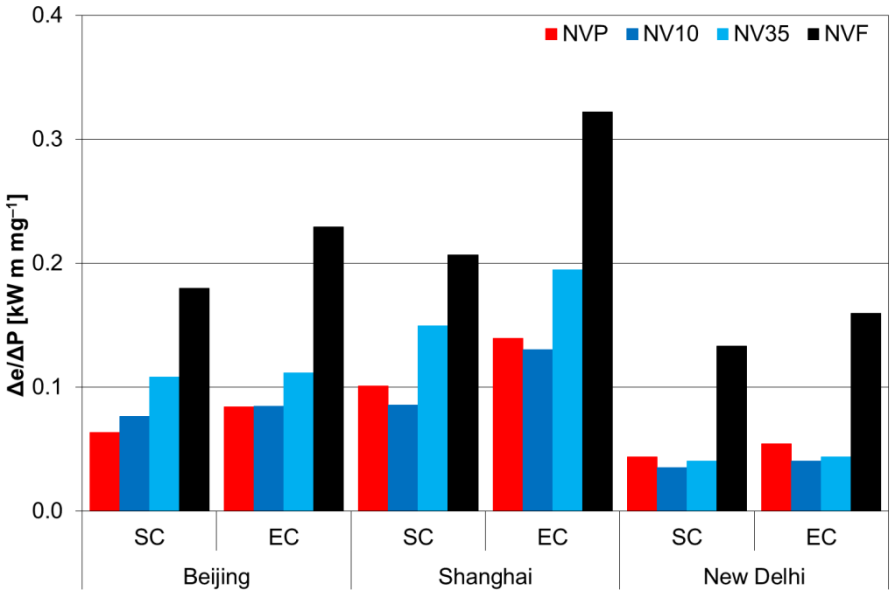

Figure 44 – Ratio between average energy savings and increase in PM2.5 exposure [kW m/mg] for each NV-use scenario in Asia

Table 34 – Ratio between average energy savings and increase in PM2.5 exposure [kW m/mg] for each NV-use scenario

City	SC			EC		
	NVP	NVF	NVS	NVP	NVF	NVS
San Diego	0.49	1.63	0.70	0.55	1.88	0.61
Burbank	0.31	0.99	0.54	0.35	1.13	0.37
Fresno	0.33	0.88	0.57	0.39	1.11	0.39
Sacramento	0.53	1.88	0.84	0.65	2.03	0.68
Livermore	0.71	2.20	0.99	0.66	1.95	0.72
Antwerp	0.35	0.97	0.52	0.34	0.89	0.45
Krakow	0.32	0.81	0.39	0.28	0.67	0.32
Lisbon	0.58	1.73	0.91	0.63	1.92	0.91
London	0.31	0.83	0.40	0.29	0.73	0.37
Madrid	0.44	1.24	0.65	0.54	1.52	0.69
Paris	0.34	0.93	0.48	0.33	0.80	0.44
Prague	0.41	1.16	0.55	0.39	0.99	0.48
Skopje	0.24	0.66	0.19	0.29	0.70	0.19
Strasbourg	0.40	1.14	0.52	0.37	0.98	0.45
Beijing (NV10; NV35)	0.06	0.18	0.08 0.11	0.08	0.23	0.08 0.11
Shanghai (NV10; NV35)	0.10	0.21	0.09 0.15	0.14	0.32	0.13 0.19
New Delhi (NV10; NV35)	0.04	0.13	0.04 0.04	0.05	0.16	0.04 0.04

6. CONCLUSIONS

Awareness on the negative health impact of airborne fine particle pollution is continuously increasing. Most airborne PM2.5 found in the urban environment can be traced back to man-made combustion from transport, industry, power generation and domestic fuel burning. Within the built environment, fine particles can be brought in from the outdoor environment, through infiltration or through natural or mechanical ventilation. In addition, PM2.5 can also be generated indoors, such as through the use of fuel for cooking and heating, or the occupant movement-induced re-suspension of particles that have previously settled onto surfaces. Natural ventilation typically does not provide any barrier to outdoor PM2.5, while in the case of mechanical ventilation, filters with a wide range of particle retention rates can be used. However, high filtration efficiency comes at the cost of a higher pressure load on the fan and, therefore, at the cost of a higher energy consumption.

This thesis assessed the impact of fine particle pollution on the potential for natural ventilative cooling of office buildings in California, Europe and Asia. The analysis used measured weather and particle concentration data for cities within the largest and most polluted metropolitan areas in each region. The analysis was performed in two stages with increasing complexity: a simple statistical analysis and a detailed simulation analysis. The first stage investigated correlations between PM2.5 concentration, weather variables (air temperature, wind speed and wind direction) and time of day and month. The second analysis stage predicted the impact of NV use on the HVAC energy consumption and occupant exposure to PM2.5 of an office building with a hybrid natural/mechanical HVAC system equipped with a highly efficient filter to lower the cumulative yearly occupant exposure to PM2.5 of outdoor origin.

The statistical analysis showed that, in the Californian cities of Burbank and San Diego, a significant majority (80 and 95 %, respectively) of working hours are within the temperature range for natural ventilation use (outdoor temperature between 10 and 26 °C). The NV potential is lower in Livermore (70 %), mainly due to colder winter temperatures. NV use in the remaining two cities of this region is limited by high summertime temperatures, resulting in potentials of 65 % (Sacramento) and 58 % (Fresno). Using PCS can extend the temperature range that allows the use of NV, increasing its potential. This mostly benefits locations where a significant fraction of the year is too warm for NV. In California, these locations are Fresno and Sacramento, where EC criteria allows the use of NV during an additional 12 and 10 % of the yearly working hours, respectively. Elsewhere in the state, the increase is below 8 %.

As expected, in the scenario where the use of NV is limited to moments with low PM2.5 concentrations (below 12 $\mu g/m^3$), all NV potentials are lower. Burbank has the highest reduction, dropping to 24 % of working hours. The potential in Fresno is reduced to 26 %. The next biggest reduction occurs in San Diego which, as a result, becomes similar to Livermore (58 %), the city with the lowest reduction in NV potential. Finally, Sacramento loses about a third of its potential use of NV.

A similar analysis methodology applied to European cities revealed that Lisbon has the highest NV potential, with a significant majority (80 %) of working hours within the NV temperature range (10 to 26 °C). In Skopje, the potential is less than half (40 %), while in all other cities, it ranges from half and two-thirds of the working hours. In Lisbon, Skopje and Madrid, where excessively warm summer temperatures are the main limitation to the use of NV, the use of PCS extends the potential for NV by 10 to 12 % of the annual working hours. In the remaining cities in Europe, the added NV potential from PCS use is nearly negligible.

In the scenario where high PM2.5 (in Europe, above 10 μg/m^3) restricts the use of NV, the percentages are significantly decreased, to below half of the original potential. In Antwerp and Lisbon, the decrease is approximately 50 %, while London and Skopje have the highest decreases in NV potential (82 and 95 %). In Krakow, Prague and Strasbourg, the decrease is about 70 %, and in Madrid and Paris, it is about 60 %.

The Asian megacities analyzed in this study present some of the lowest NV potentials: 23 to 53 % of the working hours. However, this region sees the highest benefit from the PCS-extended NV temperature range, which increases the availability of NV-favorable conditions by 12 to 14 %. Limiting the availability of NV to moments with PM2.5 levels below 10 μg/m^3 nearly eliminates the possibility for NV, while a less strict threshold of 35 μg/m^3 reduces the availability to between 3 and 26 % of the working hours.

Only a few of the analyzed cities showed a correlation between air temperature and PM2.5 levels. In San Diego and Burbank, the increase in temperature also increases the secondary formation of ammonium sulfate, which is then trapped by the frequently occurring low inversion layers, therefore increasing the average PM2.5 concentration. Inversely, in Krakow and Skopje, PM2.5 levels increase with the decrease in temperature, due to the higher use of mainly coal-based energy during colder time periods. In Shanghai, PM2.5 levels also decrease with the increase in temperature, although in this city, this is a consequence of the high precipitation levels during the warmer season.

Burbank is the only city where wind frequently transported PM2.5 from outside the city, namely from the nearby city of Los Angeles. In Livermore, Antwerp, Lisbon and Shanghai, the most frequent wind directions (with wind speeds above 3 m/s) transported in cleaner air. In the remaining cities, no consistent correlation exists between wind direction and PM2.5 levels. In the case of wind speed, a consistent pattern was found in all cities: PM2.5 levels decrease with the increase in wind speed. Since most particles are locally generated, the higher wind speeds remove the more polluted air, replacing it with cleaner air from neighboring locations.

PM2.5 levels are higher in Sacramento and Fresno during the winter months, since the locally generated particles are trapped by a combined effect of the surrounding mountain ranges and the low inversion layers that occur frequently during that season. Winter and colder mid-season months are also the most polluted in Krakow and Skopje, due to the aforementioned coal-based energy production, while the monsoon season decreases PM2.5 concentrations during the warmer months in Shanghai. In all cities, PM2.5 levels were highest in the morning and, in some cities, in the final hour of the working day, due to commuter traffic.

The detailed thermal simulations showed that the use of NV whenever it can provide a cooling effect decreased the HVAC energy consumption (NVP), in comparison to a scenario with full-working time HVAC operation (NoNV) by 26 to 83 % in California, 20 to 58 % in Europe and 7 to 21 % in Asia. The availability of PCS alone did not significantly decrease and, in some locations, even slightly increased the HVAC load. Nonetheless, these devices allowed an increase in NV use, which in turn increased its energy saving potential to 46 to 93 % in California, 44 to 77 % in Europe and 16 to 41 % in Asia. Expectedly, this increase is highest in cities with the highest increase in NV availability due to the extended NV temperature range, namely Fresno, Sacramento, Lisbon, Madrid, Skopje, Beijing, Shanghai and New Delhi.

In comparison with a standard full-time HVAC operation scenario, using NV significantly increases indoor occupant exposure to fine particles. This increase is 3.7 to 5.0 times in California, 1.9 to 4.2 times in Europe and 2.3 to 3.0 times in Asia. PCS extend the use of NV and, thus, further the increase in exposure: 4.4 to 5.7 times in California, 2.2 to 5.4 times in Europe and 3.3 to 3.9 times in Asia.

With the goal of quantifying the trade-off between energy savings and increased exposure, the ratio between the yearly energy savings and the increase in cumulative PM2.5 exposure was calculated for the different cities. The locations with the lowest increased indoor pollution levels for the same energy savings favor NV use. Among the analyzed cities, this ratio is highest in Livermore and lowest in New Delhi. On average, the energy savings-to-increased PM2.5 exposure ($\Delta e/\Delta P$) is highest in California, due to the typically high NV availability and lower PM2.5 levels, and lowest in Asia, by up to an order or magnitude, where local climate does not favor extensive NV use and where PM2.5 levels are exceptionally high. Europe is placed in a middle position, with $\Delta e/\Delta P$ ratios of the same order of magnitude though lower, on average, than in California, since the use of NV is more limited by local climate and PM2.5 concentrations are higher than those typically found in that U.S. state.

Two approaches were followed to limit the increase in exposure that occurs due to the higher use of NV: limiting its use to when outdoor PM2.5 levels are low (NVS, with different thresholds for each region: 12 $\mu g/m^3$ in California, 10 $\mu g/m^3$ in Europe and both 10 and 35 $\mu g/m^3$ in Asia) and using an electrostatic filter to reduce particle penetration (NVF).

Understandably, the reduction in NV use due to its limited availability to moments with low outdoor PM2.5 also reduces NV's energy saving potential: 17 to 63 % in California, 5 to 40 % in Europe and both 1 to 5 % (with a threshold of 10 $\mu g/m^3$) and 1 to 12 % (with 35 $\mu g/m^3$) in Asia. When PCS are available, the energy saving potential is also diminished: 38 to 86 % in California, 12 to 63 % in Europe and both 4 to 22 % and 4 to 35 % (thresholds of 10 and 35 $\mu g/m^3$, respectively) in Asia. Nevertheless, this exposure control approach achieves its goal of decreasing occupant exposure to PM2.5. In California, occupant exposure is between 2.0 and 3.2 times the exposure that results from the full-time use of HVAC, while in Europe, occupant exposure is between 1.4 and 2.8 times the NoNV levels. In Asia, both thresholds place a strict restraint on the use of NV, limiting occupant exposure to between 1.2 and 1.8 times the NoNV levels. The higher use of NV that results from the use of PCS also increases occupant exposure, even in this exposure control approach: 3.7 to 4.9 times the NoNV exposure in California, 1.7 to 3.3 times in Europe and 1.9 to 2.6 in Asia. With few exceptions, namely Skopje, Shanghai (in the case of the 10 $\mu g/m^3$ threshold) and New Delhi (for both the 10 and 35 $\mu g/m^3$ thresholds), the $\Delta e/\Delta P$ ratio is higher when NV is limited to moments of low outdoor PM2.5, since most energy savings occur during moments with low outdoor particle levels.

The use of electrostatic façade NV inflow filters seems to achieve the best of both worlds. These filters have a very low energy cost which, combined with the possibility of using NV whenever it can provide a cooling effect, result in energy savings that are nearly identical to those found in the NVP scenario. At the same time, these filters allow occupant exposure levels that are, in most cases, similar to or lower than those associated with the NVS approach. As a result, the energy savings-to-increased PM2.5 exposure ratio is highest for this scenario.

Overall, NV has an energy-saving potential of up to 83 %, with standard NV criteria, or 93 %, in the case of available PCS, which extend the NV-favorable temperature range. However, NV is not a solution that can easily be used in any location, since some climates nearly eliminate any possible NV use, even with an extended NV temperature range. Further, the unrestricted use of NV can increase indoor exposure to fine particles of outdoor origin by up to five-fold (or sixfold, if used in combination with PCS) in comparison with an office using an HVAC system in full-time operation with a high-efficiency fine particle filter.

Two approaches can be used to limit this increase in exposure to 2 to 3 times. Using NV only when outdoor PM2.5 concentrations are low is a solution that could be implemented with ease in existing commercial buildings. In this case, the energy-saving potential of NV is reduced to 63 % (86 % if used in combination with PCS), although this reduction is lower than the reduction in cumulative exposure. Using NV with openings equipped with an electrostatic filter can also decrease indoor PM2.5 levels and at a very low energy cost, thus, taking advantage of nearly all of NV's energy saving potential. However, any attempt to apply this approach in an existing building has not been found.

Still, limiting man-made combustion, namely by decreasing traffic or shifting to cleaner energy sources is the most efficient path for decreasing outdoor PM2.5. The use of cleaner energy sources indoors also decreases PM2.5 levels within the built environment, as does the use of effective extraction ventilation for indoor sources. The proposed innovative solutions limit the penetration of outdoor PM2.5 through the incoming airflow and can also be part of the solution to decrease exposure to PM2.5. Ultimately, one of the most important steps is to increase public awareness of PM2.5, encouraging people and national governments, on their behalf, to engage in these solutions as well as developing other solutions.

7. REFERENCES

[1] United Nations Department of Economic and Social Affairs, World Urbanization Prospects – The 2014 Revision – Highlights, United Nations, 2014, New York, New York, United States, ISBN 978-92-1-151517-6, https://esa.un.org/unpd/wup/publications/files/wup2014-highlights.pdf

[2] Alexander Baklanov, Luisa T. Molina, Michael Gauss, Megacities, air quality and climate, Atmospheric Environment, Volume 126, February 2016, Pages 235-249, ISSN 1352-2310, https://doi.org/10.1016/j.atmosenv.2015.11.059

[3] Chun Chen, Bin Zhao, Review of relationship between indoor and outdoor particles: I/O ratio, infiltration factor and penetration factor, Atmospheric Environment, Volume 45, Issue 2, January 2011, Pages 275-288, ISSN 1352-2310, https://doi.org/10.1016/j.atmosenv.2010.09.048

[4] Rima Habre, Brent Coull, Erin Moshier, James Godbold, Avi Grunin, Amit Nath, William Castro, Neil Schachter, Annette Rohr, Meyer Kattan, John Spengler, Petros Koutrakis, Sources of indoor air pollution in New York City residences of asthmatic children, Journal of Exposure Science and Environmental Epidemiology, Volume 24, Issue 3, May/June 2014, Pages 269-278, ISSN 1559-0631, https://doi.org/10.1038/jes.2013.74

[5] Dorota A. Chwieduk, Towards modern options of energy conservation in buildings, Renewable Energy, Volume 101, February 2017, Pages 1194-1202, ISSN 0960-1481, https://doi.org/10.1016/j.renene.2016.09.061

[6] Ricardo Forgiarini Rupp, Natalia Giraldo Vásquez, Roberto Lamberts, A review of human thermal comfort in the built environment, Energy and Buildings, Volume 105, 15 October 2015, Pages 178-205, ISSN 0378-7788, https://doi.org/10.1016/j.enbuild.2015.07.047

[7] Ivan Oropeza-Perez, Poul Alberg Østergaard, Potential of natural ventilation in temperate countries – A case study of Denmark, Applied Energy, Volume 114, February 2014, Pages 520-530, ISSN 0306-2619, https://doi.org/10.1016/j.apenergy.2013.10.008

[8] Ivan Oropeza-Perez, Poul Alberg Østergaard, Energy saving potential of utilizing natural ventilation under warm conditions – A case study of Mexico, Applied Energy, Volume 130, 1 October 2014, Pages 20-32, ISSN 0306-2619, https://doi.org/10.1016/j.apenergy.2014.05.035

[9] California Building Standards Commission, California Code of Regulations, Title 24 – Building Standards Code, Part 4 – California Mechanical Code, 2013

[10] G. Carrilho da Graça, N.C. Daish, P.F. Linden, A two-zone model for natural cross-ventilation, Building and Environment, Volume 89, July 2015, Pages 72-85, ISSN 0360-1323, https://doi.org/10.1016/j.buildenv.2015.02.014

[11] Mika Nomura, Kyosuke Hiyama, A review: Natural ventilation performance of office buildings in Japan, Renewable and Sustainable Energy Reviews, Volume 74, July 2017, Pages 746-754, ISSN 1364-0321, https://doi.org/10.1016/j.rser.2017.02.083

[12] Runming Yao, Baizhan Li, Koen Steemers, Alan Short, Assessing the natural ventilation cooling potential of office buildings in different climate zones in China, Renewable Energy, Volume 34, Issue 12, December 2009, Pages 2697-2705, ISSN 0960-1481, https://doi.org/10.1016/j.renene.2009.05.015

[13] G. Carrilho da Graça, P.F. Linden, P. Haves, Design and testing of a control strategy for a large, naturally ventilated office building, Building Services Engineering Research and Technology, Volume 25, Number 3, August 2004, Pages 223-239, ISSN 0143-6244, https://doi.org/10.1191/0143624404bt107oa

[14] Guilherme Carrilho da Graça, Paul Linden, Ten questions about natural ventilation of non-domestic buildings, Building and Environment, Volume 107, October 2016, Pages 263-273, ISSN 0360-1323, https://doi.org/10.1016/j.buildenv.2016.08.007

[15] Guilherme Carrilho da Graça, Nuno R. Martins, Cristina S. Horta, Thermal and airflow simulation of a naturally ventilated shopping mall, Energy and Buildings, Volume 50, July 2012, Pages 177-188, ISSN 0378-7788, https://doi.org/10.1016/j.enbuild.2012.03.037

[16] Mat Santamouris, Cooling the buildings – past, present and future, Energy and Buildings, Volume 128, 15 September 2016, Pages 617-638, ISSN 0378-7788, https://doi.org/10.1016/j.enbuild.2016.07.034

[17] Rubina Ramponi, Adriana Angelotti, Bert Blocken, Energy saving potential of night ventilation: Sensitivity to pressure coefficients for different European climates, Applied Energy, Volume 123, 15 June 2014, Pages 185-195, ISSN 0306-2619, https://doi.org/10.1016/j.apenergy.2014.02.041

[18] Ben Richard Hughes, John Kaiser Calautit, Saud Abdul Ghani, The development of commercial wind towers for natural ventilation: A review, Applied Energy, Volume 92, April 2012, Pages 606-627, ISSN 0306-2619, https://doi.org/10.1016/j.apenergy.2011.11.066

[19] O. Seppänen O, W.J. Fisk WJ, Association of ventilation system type with SBS symptoms in office workers, Indoor Air, Volume 12, Issue 2, June 2002, Pages 98-112, ISSN 1600-0668, https://doi.org/10.1034/j.1600-0668.2002.01111.x

[20] Spencer M. Dutton, David Banks, Samuel L. Brunswick, William J. Fisk, Health and economic implications of natural ventilation in California offices, Building and Environment, Volume 67, September 2013, Pages 34-45, ISSN 0360-1323, https://doi.org/10.1016/j.buildenv.2013.05.002

[21] Cheng Li, Tianzhen Hong, Da Yan, An insight into actual energy use and its drivers in high-performance buildings, Applied Energy, Volume 131, 15 October 2014, Pages 394-410, ISSN 0306-2619, https://doi.org/10.1016/j.apenergy.2014.06.032

[22] Zheming Tong, Yujiao Chen, Ali Malkawi, Zhu Liu, Richard B. Freeman, Energy saving potential of natural ventilation in China: The impact of ambient air pollution, Applied Energy, Volume 179, 1 October 2016, Pages 660-668, ISSN 0306-2619, https://doi.org/10.1016/j.apenergy.2016.07.019

[23] Lester B. Lave, Eugene P. Seskin, Air Pollution and Human Health, Science, Volume 169, Number 3947, 21 August 1970, Pages 723-733, ISSN 1095-9203, https://doi.org/10.1126/science.169.3947.723

[24] B.G. Ferris Jr., F.E. Speizer, J.D. Spengler , D. Dockery , Y.M.M. Bishop , M. Wolfson , C. Humble, Effects of Sulfur Oxides and Respirable Particles on Human Health. Methodology and demography of

populations in study, American Review of Respiratory Disease, Volume 120, Number 4, 1 October 1979, Pages 767-779, ISSN 0003-0805, https://www.atsjournals.org/doi/abs/10.1164/arrd.1979.120.4.767

[25] World Health Organization, Review of evidence on health aspects of air pollution – REVIHAAP project: Technical Report, WHO Regional Office for Europe, 2013, Copenhagen, Denmark, http://www.euro.who.int/__data/assets/pdf_file/0004/193108/REVIHAAP-Final-technical-report.pdf

[26] Tracy L. Thatcher, Alvin C.K. Lai, Rosa Moreno-Jackson, Richard G. Sextro, William W. Nazaroff, Effects of room furnishings and air speed on particle deposition rates indoors, Atmospheric Environment, Volume 36, Issue 11, April 2002, Pages 1811-1819, ISSN 1352-2310, https://doi.org/10.1016/S1352-2310(02)00157-7

[27] Jing Meng, Junfeng Liu, Shan Guo, Ye Huang, Shu Tao, The impact of domestic and foreign trade on energy-related PM emissions in Beijing, Applied Energy, Volume 184, 15 December 2016, Pages 853-862, ISSN 0306-2619, https://doi.org/10.1016/j.apenergy.2015.09.082

[28] William J. Farrell, Laure Deville Cavellin, Scott Weichenthal, Mark Goldberg, Marianne Hatzopoulou, Capturing the urban canyon effect on particle number concentrations across a large road network using spatial analysis tools, Building and Environment, Volume 92, October 2015, Pages 328-334, ISSN 0360-1323, https://doi.org/10.1016/j.buildenv.2015.05.004

[29] M.E. Popa, A.J. Segers, H.A.C. Denier van der Gon, M.C. Krol, A.J.H. Visschedijk, M. Schaap, T. Röckmann, Impact of a future H2 transportation on atmospheric pollution in Europe, Atmospheric Environment, Volume 113, July 2015, Pages 208-222, ISSN 1352-2310, https://doi.org/10.1016/j.atmosenv.2015.03.022

[30] Detlef Westphalen, Scott Koszalinski, Energy Consumption Characteristics of Commercial Building HVAC Systems – Volume II: Thermal Distribution, Auxiliary Equipment, and Ventilation, Office of Building Equipment, Office of Building Technology State and Community Programs, U.S. Department of Energy, October 1999, https://www1.eere.energy.gov/buildings/publications/pdfs/commercial_initiative/hvac_volume2_final_report.pdf

[31] Parham Azimi, Dan Zhao, Brent Stephens, Estimates of HVAC filtration efficiency for fine and ultrafine particles of outdoor origin, Atmospheric Environment, Volume 98, December 2014, Pages 337-346, ISSN 1352-2310, https://doi.org/10.1016/j.atmosenv.2014.09.007

[32] Luis Pérez-Lombard, José Ortiz, Christine Pout, A review on buildings energy consumption information, Energy and Buildings, Volume 40, Issue 3, 2008, Pages 394-398, ISSN 0378-7788, https://doi.org/10.1016/j.enbuild.2007.03.007

[33] L.D. Danny Harvey, Recent Advances in Sustainable Buildings: Review of the Energy and Cost Performance of the State-of-the-Art Best Practices from Around the World, Annual Review of Environment and Resources, Volume 38, 2013, Pages 281-309, ISSN 1543-5938, https://doi.org/10.1146/annurev-environ-070312-101940

[34] Sebastian Herkel, Ulla Knapp, Jens Pfafferott, Towards a model of user behaviour regarding the manual control of windows in office buildings, Building and Environment, Volume 43, Issue 4, April 2008, Pages 588-600, ISSN 0360-1323, https://doi.org/10.1016/j.buildenv.2006.06.031

[35] International Organization for Standardization, ISO 7730:2005 – Ergonomics of the thermal environment – Analytical determination and interpretation of thermal comfort using calculation of the PMV and PPD indices and local thermal comfort criteria, November 2005

[36] Hui Zhang, Edward Arens, Yongchao Zhai, A review of the corrective power of personal comfort systems in non-neutral ambient environments, Building and Environment, Volume 91, September 2015, Pages 15-41, ISSN 0360-1323, https://doi.org/10.1016/j.buildenv.2015.03.013

[37] Yongchao Zhai, Yufeng Zhang, Hui Zhang, Wilmer Pasut, Edward Arens, Qinglin Meng, Human comfort and perceived air quality in warm and humid environments with ceiling fans, Building and Environment, Volume 90, August 2015, Pages 178-185, ISSN 0360-1323, https://doi.org/10.1016/j.buildenv.2015.04.003

[38] Shinichi Watanabe, Toshimichi Shimomura, Hironori Miyazaki, Thermal evaluation of a chair with fans as an individually controlled system, Building and Environment, Volume 44, Issue 7, July 2009, Pages 1392-1398, ISSN 0360-1323, https://doi.org/10.1016/j.buildenv.2008.05.016

[39] H. Pallubinsky, L. Schellen, T.A. Rieswijk, C.M.G.A.M. Breukel, B.R.M. Kingma, W.D. van Marken Lichtenbelt, Local cooling in a warm environment, Energy and Buildings, Volume 113, 1 February 2016, Pages 15-22, ISSN 0378-7788, https://doi.org/10.1016/j.enbuild.2015.12.016

[40] Wilmer Pasut, Hui Zhang, Ed Arens, Yongchao Zhai, Energy-efficient comfort with a heated/cooled chair: Results from human subject tests, Building and Environment, Volume 84, January 2015, Pages 10-21, ISSN 0360-1323, https://doi.org/10.1016/j.buildenv.2014.10.026

[41] Nuno R. Martins, Guilherme Carrilho da Graça, A Climate Performance Indicator for Analysis of Low Energy Buildings, Proceedings of BS2013: 13th Conference of International Building Performance Simulation Association, Chambéry, France, August 26-28 2013, Pages 1348-1356, ISBN 9782746662940, www.ibpsa.org/proceedings/BS2013/p_1182.pdf

[42] Nuno R. Martins, Guilherme Carrilho da Graça, Validation of numerical simulation tools for wind-driven natural ventilation design, Building Simulation, Volume 9, Issue 1, February 2016, Pages 75-87, ISSN 1996-8744, https://doi.org/10.1007/s12273-015-0251-6

[43] Nuno R. Martins, Guilherme Carrilho da Graça, Impact of outdoor PM2.5 on natural ventilation usability in California's nondomestic buildings, Applied Energy, Volume 189, 1 March 2017, Pages 711-724, ISSN 0306-2619, https://doi.org/10.1016/j.apenergy.2016.12.103

[44] Nuno R. Martins, Guilherme Carrilho da Graça, Simulation of the effect of fine particle pollution on the potential for natural ventilation of non-domestic buildings in European cities, Building and Environment, Volume 115, April 2017, Pages 236-250, ISSN 0360-1323, https://doi.org/10.1016/j.buildenv.2017.01.030

[45] Nuno R. Martins, Guilherme Carrilho da Graça, Effects of airborne fine particle pollution on the usability of natural ventilation in office buildings in three megacities in Asia, Renewable Energy, Volume 117, March 2018, Pages 357-373, ISSN 0960-1481, https://doi.org/10.1016/j.renene.2017.10.089

[46] Nuno R. Martins, Guilherme Carrilho da Graça, Impact of PM2.5 in the built environment: a review, submitted to Renewable and Sustainable Energy Reviews, 2017

[47] Norbert Englert, Fine particles and human health—a review of epidemiological studies, Toxicology Letters, Volume 149, Issues 1-3, 1 April 2004, Pages 235-242, ISSN 0378-4274, https://doi.org/10.1016/j.toxlet.2003.12.035

[48] Jes Fenger, Air pollution in the last 50 years – From local to global, Atmospheric Environment, Volume 43, Issue 1, January 2009, Pages 13-22, ISSN 1352-2310, https://doi.org/10.1016/j.atmosenv.2008.09.061

[49] Evelyn O. Talbott, Vincent C. Arena, Judith R. Rager, Jane E. Clougherty, Drew R. Michanowicz, Ravi K. Sharma, Shaina L. Stacy, Fine particulate matter and the risk of autism spectrum disorder, Environmental Research, Volume 140, July 2015, Pages 414-420, ISSN 0013-9351, https://doi.org/10.1016/j.envres.2015.04.021

[50] Giuliano Polichetti, Stefania Cocco, Alessandra Spinali, Valentina Trimarco, Alfredo Nunziata, Effects of particulate matter (PM10, PM2.5 and PM1) on the cardiovascular system, Toxicology, Volume 261, Issues 1-2, 30 June 2009, Pages 1-8, ISSN 0300-483X, https://doi.org/10.1016/j.tox.2009.04.035

[51] Rohi Jan, Ritwika Roy, Suman Yadav, P. Gursumeeran Satsangi, Exposure assessment of children to particulate matter and gaseous species in school environments of Pune, India, Building and Environment, Volume 111, January 2017, Pages 207-217, ISSN 0360-1323, https://doi.org/10.1016/j.buildenv.2016.11.008

[52] Lida Gharibvand, David Shavlik, Mark Ghamsary, W. Lawrence Beeson, Samuel Soret, Raymond Knutsen, Synnove F. Knutsen, The Association between Ambient Fine Particulate Air Pollution and Lung Cancer Incidence: Results from the AHSMOG-2 Study, Environmental Health Perspectives, 12 August 2016, ISSN-L 0091-6765, https://doi.org/10.1289/EHP124

[53] Marie-Eve Héroux, H. Ross Anderson, Richard Atkinson, Bert Brunekreef, Aaron Cohen, Francesco Forastiere, Fintan Hurley, Klea Katsouyanni, Daniel Krewski, Michal Krzyzanowski, Nino Künzli, Inga Mills, Xavier Querol, Bart Ostro, Heather Walton, Quantifying the health impacts of ambient air pollutants: recommendations of a WHO/Europe project, International Journal of Public Health, Volume 60, Issue 5, July 2015, ISSN 1661-8556, Pages 619-627, https://doi.org/10.1007/s00038-015-0690-y

[54] Shaolong Feng, Dan Gao, Fen Liao, Furong Zhou, Xinming Wang, The health effects of ambient PM2.5 and potential mechanisms, Ecotoxicology and Environmental Safety, Volume 128, June 2016, Pages 67-74, ISSN 0147-6513, https://doi.org/10.1016/j.ecoenv.2016.01.030

[55] Rui Chen, Bin Hu, Ying Liu, Jianxun Xu, Guosheng Yang, Diandou Xu, Chunying Chen, Beyond PM2.5: The role of ultrafine particles on adverse health effects of air pollution, Biochimica et Biophysica Acta (BBA) - General Subjects, Volume 1860, Issue 12, December 2016, Pages 2844-2855, ISSN 0304-4165, https://doi.org/10.1016/j.bbagen.2016.03.019

[56] Stefano Zauli Sajani, Isabella Ricciardelli, Arianna Trentini, Dimitri Bacco, Claudio Maccone, Silvia Castellazzi, Paolo Lauriola, Vanes Poluzzi, Roy M. Harrison, Spatial and indoor/outdoor gradients in urban concentrations of ultrafine particles and PM2.5 mass and chemical components, Atmospheric Environment, Volume 103, February 2015, Pages 307-320, ISSN 1352-2310, https://doi.org/10.1016/j.atmosenv.2014.12.064

[57] Patricia Velasco, Katarzyna Turkiewicz, Theresa Najita, Jeff Lindberg, Characterization of Ambient PM10 and PM2.5 in California – Technical Report, Air Resources Board, California Environmental Protection Agency, June 2005, https://www.arb.ca.gov/pm/pmmeasures/pmch05/stateover05.pdf

[58] Chun-Sheng Liang, Feng-Kui Duan, Ke-Bin He, Yong-Liang Ma, Review on recent progress in observations, source identifications and countermeasures of PM2.5, Environment International, Volume 86, January 2016, Pages 150-170, ISSN 0160-4120, https://doi.org/10.1016/j.envint.2015.10.016

[59] Brett J. Tunno, Rebecca Dalton, Drew R. Michanowicz, Jessie L.C. Shmool, Ellen Kinnee, Sheila Tripathy, Leah Cambal, Jane E. Clougherty, Spatial patterning in PM2.5 constituents under an inversion-focused sampling design across an urban area of complex terrain, Journal of Exposure Science and Environmental Epidemiology, Volume 26, Issue 4, June 2016, Pages 385-396, ISSN 1559-0631, https://doi.org/10.1038/jes.2015.59

[60] Marianne Hatzopoulou, Scott Weichenthal, Hussam Dugum, Graeme Pickett, Luis Miranda-Moreno, Ryan Kulka, Ross Andersen, Mark Goldberg, The impact of traffic volume, composition, and road geometry on personal air pollution exposures among cyclists in Montreal, Canada, Journal of Exposure Science and Environmental Epidemiology, Volume 23, Issue 1, January 2013, Pages 46-51, ISSN 1559-0631, https://doi.org/10.1038/jes.2012.85

[61] Miriam E. Marlier, Ruth S. DeFries, Apostolos Voulgarakis, Patrick L. Kinney, James T. Randerson, Drew T. Shindell, Yang Chen, Greg Faluvegi, El Niño and health risks from landscape fire emissions in southeast Asia, Nature Climate Change, Volume 3, February 2013, Pages 131-136, ISSN 1758-678X, https://doi.org/10.1038/nclimate1658

[62] Federico Karagulian, Claudio A. Belis, Carlos Francisco C. Dora, Annette M. Prüss-Ustün, Sophie Bonjour, Heather Adair-Rohani, Markus Amann, Contributions to cities' ambient particulate matter (PM): A systematic review of local source contributions at global level, Atmospheric Environment, Volume 120, November 2015, Pages 475-483, ISSN 1352-2310, https://doi.org/10.1016/j.atmosenv.2015.08.087

[63] A. Polidori, J. Kwon, B.J. Turpin, C. Weisel, Source proximity and residential outdoor concentrations of PM2.5, OC, EC, and PAHs, Journal of Exposure Science and Environmental Epidemiology, Volume 20, Issue 5, July 2010, Pages 457-468, ISSN 1559-0631, https://doi.org/10.1038/jes.2009.39

[64] Lijian Han, Weiqi Zhou, Weifeng Li, Fine particulate (PM2.5) dynamics during rapid urbanization in Beijing, 1973–2013, Scientific Reports, Volume 6, Article Number 23604, 31 March 2016, ISSN 2045-2322, https://doi.org/10.1038/srep23604

[65] Ming-Tung Chuang, Yu-Chieh Chen, Chung-Te Lee, Chung-Hao Cheng, Yu-Jen Tsai, Shih-Yu Chang, Zhen-Sen Su, Apportionment of the sources of high fine particulate matter concentration events in a developing aerotropolis in Taoyuan, Taiwan, Environmental Pollution, Volume 214, July 2016, Pages 273-281, ISSN 0269-7491, https://doi.org/10.1016/j.envpol.2016.04.045

[66] C.F. Isley, P.F. Nelson, M.P. Taylor, F.S. Mani, M. Maata, A. Atanacio, E. Stelcer, D.D. Cohen, PM2.5 and aerosol black carbon in Suva, Fiji, Atmospheric Environment, Volume 150, February 2017, Pages 55-66, ISSN 1352-2310, https://doi.org/10.1016/j.atmosenv.2016.11.041

[67] Judith C. Chow, L.-W. Antony Chen, John G. Watson, Douglas H. Lowenthal, Karen A. Magliano, Kasia Turkiewicz, Donald E. Lehrman, PM2.5 chemical composition and spatiotemporal variability during the California Regional PM10/PM2.5 Air Quality Study (CRPAQS), Journal of Geophysical Research, Volume 111, Issue D10, May 2006, Pages 2156-2202, ISSN 2169-8996, https://doi.org/10.1029/2005JD006457

[68] Rong Lu, Richard P. Turco, Air pollutant transport in a coastal environment—II. Three-dimensional simulations over Los Angeles basin, Atmospheric Environment, Volume 29, Issue 13, July 1995, Pages 1499-1518, ISSN 1352-2310, https://doi.org/10.1016/1352-2310(95)00015-Q

[69] H. Choi, M.S. Speer, Effects of atmospheric circulation and boundary layer structure on the dispersion of suspended particulates in the Seoul metropolitan area, Meteorology and Atmospheric Physics, Volume 92, Issue 3, April 2006, Pages 239-254, ISSN 1436-5065, https://doi.org/10.1007/s00703-005-0147-6

[70] Sergio Rodríguez, Emilio Cuevas, Yenny González, Ramón Ramos, Pedro Miguel Romero, Noemí Pérez, Xavier Querol, Andrés Alastuey, Influence of sea breeze circulation and road traffic emissions on the relationship between particle number, black carbon, PM1, PM2.5 and PM2.5 –10 concentrations in a coastal city, Atmospheric Environment, Volume 42, Issue 26, August 2008, Pages 6523-6534, ISSN 1352-2310, https://doi.org/10.1016/j.atmosenv.2008.04.022

[71] Jieqiong Luo, Peijun Du, Alim Samat, Junshi Xia, Meiqin Che, Zhaohui Xue, Spatiotemporal Pattern of PM2.5 Concentrations in Mainland China and Analysis of Its Influencing Factors using Geographically Weighted Regression, Scientific Reports, Volume 7, Article Number 40607, 12 January 2017, ISSN 2045-2322, https://doi.org/10.1038/srep40607

[72] Wenjing Ji, Bin Zhao, Numerical study of the effects of trees on outdoor particle concentration distributions, Building Simulation, Volume 7, Issue 4, August 2014, Pages 417-427, ISSN 1996-8744, https://doi.org/10.1007/s12273-014-0180-9

[73] Zhaowen Qiu, Xiaoqin Xu, Jianhua Song, Yaping Luo, Ruini Zhao, Bihai Xiang Wencai Zhou, Xiaoxia Li, Yanzhao Hao, Pedestrian exposure to traffic PM on different types of urban roads: A case study of Xi'an, China, Sustainable Cities and Society, Volume 32, July 2017, Pages 475-485, ISSN 2210-6707, https://doi.org/10.1016/j.scs.2017.04.007

[74] V.S. Chithra, S.M. Shiva Nagendra, Impact of outdoor meteorology on indoor PM10, PM2.5 and PM1 concentrations in a naturally ventilated classroom, Urban Climate, Volume 10, Part 1, December 2014, Pages 77-91, ISSN 2212-0955, https://doi.org/10.1016/j.uclim.2014.10.001

[75] Zhen Cheng, Lina Luo, Shuxiao Wang, Yungang Wang, Sumit Sharma, Hikari Shimadera, Xiaoliang Wang, Michael Bressi, Regina Maura de Miranda, Jingkun Jiang, Wei Zhou, Oscar Fajardo, Naiqiang Yan, Jiming Hao, Status and characteristics of ambient PM2.5 pollution in global megacities, Environment International, Volumes 89-90, April-May 2016, Pages 212-221, ISSN 0160-4120, https://doi.org/10.1016/j.envint.2016.02.003

[76] Yan-Lin Zhang, Fang Cao, Fine particulate matter (PM2.5) in China at a city level, Scientific Reports, Volume 5, Article Number 14884, 15 October 2015, ISSN 2045-2322, https://doi.org/10.1038/srep23604

[77] Nichole Baldwin, Owais Gilani, Suresh Raja, Stuart Batterman, Rajiv Ganguly, Philip Hopke, Veronica Berrocal, Thomas Robins, Sarah Hoogterp, Factors affecting pollutant concentrations in the near-road environment, Atmospheric Environment, Volume 115, August 2015, Pages 223-235, ISSN 1352-2310, https://doi.org/10.1016/j.atmosenv.2015.05.024

[78] Otto O. Hänninen, Raimo O. Salonen, Kimmo Koistinen, Timo Lanki, Lars Barregard, Matti Jantunen, Population exposure to fine particles and estimated excess mortality in Finland from an East European

wildfire episode, Journal of Exposure Science and Environmental Epidemiology, Volume 19, Issue 4, May 2009, Pages 414-422, ISSN 1559-0631, https://doi.org/10.1038/jes.2008.31

[79] Qiang Zhang, Xujia Jiang, Dan Tong, Steven J. Davis, Hongyan Zhao, Guannan Geng, Tong Feng, Bo Zheng, Zifeng Lu, David G. Streets, Ruijing Ni, Michael Brauer, Aaron van Donkelaar, Randall V. Martin, Hong Huo, Zhu Liu, Da Pan, Haidong Kan, Yingying Yan, Jintai Lin, Kebin He, Dabo Guan, Transboundary health impacts of transported global air pollution and international trade, Nature, Volume 543, Issue 7647, 30 March 2017, Pages 705-709, ISSN 0028-0836, https://doi.org/10.1038/nature21712

[80] Bong Mann Kim, Jihoon Seo, Jin Young Kim, Ji Yi Lee, Yumi Kim, Transported vs. local contributions from secondary and biomass burning sources to PM2.5, Atmospheric Environment, Volume 144, November 2016, Pages 24-36, ISSN 1352-2310, https://doi.org/10.1016/j.atmosenv.2016.08.072

[81] Fengwen Wang, Zhigang Guo, Tian Lin, Limin Hu, Yingjun Chen, Yifang Zhu, Characterization of carbonaceous aerosols over the East China Sea: The impact of the East Asian continental outflow, Atmospheric Environment, Volume 110, June 2015, Pages 163-173, ISSN 1352-2310, https://doi.org/10.1016/j.atmosenv.2015.03.059

[82] Fumikazu Ikemori, Koji Honjyo, Makiko Yamagami, Toshio Nakamura, Influence of contemporary carbon originating from the 2003 Siberian forest fire on organic carbon in PM2.5 in Nagoya, Japan, Science of The Total Environment, Volumes 530-531, 15 October 2015, Pages 403-410, ISSN 0048-9697, https://doi.org/10.1016/j.scitotenv.2015.05.006

[83] Donald J. Wuebbles, Hang Lei, Jintai Lin, Intercontinental transport of aerosols and photochemical oxidants from Asia and its consequences, Environmental Pollution, Volume 150, Issue 1, November 2007, Pages 65-84, ISSN 0269-7491, https://doi.org/10.1016/j.envpol.2007.06.066

[84] Choong-Min Kang, Diane Gold, Petros Koutrakis, Downwind O3 and PM2.5 speciation during the wildfires in 2002 and 2010, Atmospheric Environment, Volume 95, October 2014, Pages 511-519, ISSN 1352-2310, https://doi.org/10.1016/j.atmosenv.2014.07.008

[85] Amos P.K. Tai, Loretta J. Mickley, Daniel J. Jacob, Correlations between fine particulate matter (PM2.5) and meteorological variables in the United States: Implications for the sensitivity of PM2.5 to climate change, Atmospheric Environment, Volume 44, Issue 32, October 2010, Pages 3976-3984, ISSN 1352-2310, https://doi.org/10.1016/j.atmosenv.2010.06.060

[86] S. Tiwari, A.K. Srivastava, D.S. Bisht, P. Parmita, Manoj K. Srivastava, S.D. Attri, Diurnal and seasonal variations of black carbon and PM2.5 over New Delhi, India: Influence of meteorology, Atmospheric Research, Volumes 125-126, May 2013, Pages 50-62, ISSN 0169-8095, https://doi.org/10.1016/j.atmosres.2013.01.011

[87] Richard Toro A., Raúl G.E. Morales S., Mauricio Canales, Claudio Gonzalez-Rojas, Manuel A. Leiva G., Inhaled and inspired particulates in Metropolitan Santiago Chile exceed air quality standards, Building and Environment, Volume 79, September 2014, Pages 115-123, ISSN 0360-1323, https://doi.org/10.1016/j.buildenv.2014.05.004

[88] Lidiia Iavorivska, Elizabeth W. Boyer, David R. DeWalle, Atmospheric deposition of organic carbon via precipitation, Atmospheric Environment, Volume 146, December 2016, Pages 153-163, ISSN 1352-2310, https://doi.org/10.1016/j.atmosenv.2016.06.006

[89] Nehzat Motallebi, Wintertime PM2.5 and PM10 Source Apportionment at Sacramento, California, Journal of the Air & Waste Management Association, Volume 49, Issue 9, September 1999, Pages 25-34, ISSN 2162-2906, https://doi.org/10.1080/10473289.1999.10463881

[90] Xiaoyan Wang, Kaicun Wang, Liangyuan Su, Contribution of Atmospheric Diffusion Conditions to the Recent Improvement in Air Quality in China, Scientific Reports, Volume 6, Article Number 36404, 2 November 2016, ISSN 2045-2322, https://doi.org/10.1038/srep36404

[91] Bangtian Zhou, Huizhong Shen, Ye Huang, Wei Li, Han Chen, Yanyan Zhang, Shu Su, Yuanchen Chen, Nan Lin, Shaojie Zhuo, Qirui Zhong, Junfeng Liu, Bengang Li, Shu Tao, Daily variations of size-segregated ambient particulate matter in Beijing, Environmental Pollution, Volume 197, February 2015, Pages 36-42, ISSN 0269-7491, https://doi.org/10.1016/j.envpol.2014.11.029

[92] Yuan Cheng, Ke-bin He, Zhen-yu Du, Mei Zheng, Feng-kui Duan, Yong-liang Ma, Humidity plays an important role in the PM2.5 pollution in Beijing, Environmental Pollution, Volume 197, February 2015, Pages 68-75, ISSN 0269-7491, https://doi.org/10.1016/j.envpol.2014.11.028

[93] Wenju Cai, Ke Li, Hong Liao, Huijun Wang, Lixin Wu, Weather conditions conducive to Beijing severe haze more frequent under climate change, Nature Climate Change, Volume 7, Issue 4, April 2017, Pages 257-262, ISSN 1758-678X, https://doi.org/10.1038/nclimate3249

[94] Haifeng Zhang, Zhaohai Wang, Wenzhong Zhang, Exploring spatiotemporal patterns of PM2.5 in China based on ground-level observations for 190 cities, Environmental Pollution, Volume 216, September 2016, Pages 559-567, ISSN 0269-7491, https://doi.org/10.1016/j.envpol.2016.06.009

[95] Congbo Song, Lin Wu, Yaochen Xie, Jianjun He, Xi Chen, Ting Wang, Yingchao Lin, Taosheng Jin, Anxu Wang, Yan Liu, Qili Dai, Baoshuang Liu, Ya-nan Wang, Hongjun Mao, Air pollution in China: Status and spatiotemporal variations, Environmental Pollution, Volume 227, August 2017, Pages 334-347, ISSN 0269-7491, https://doi.org/10.1016/j.envpol.2017.04.075

[96] Janice Ser Huay Lee, Zeehan Jaafar, Alan Khee Jin Tan, Luis R. Carrasco, J. Jackson Ewing, David P. Bickford, Edward L. Webb, Lian Pin Koh, Toward clearer skies: Challenges in regulating transboundary haze in Southeast Asia, Environmental Science & Policy, Volume 55, Part 1, January 2016, Pages 87-95, ISSN 1462-9011, https://doi.org/10.1016/j.envsci.2015.09.008

[97] L.A. Díaz-Robles, J.S. Fu, G.D. Reed, A.J. DeLucia, Seasonal distribution and modeling of diesel particulate matter in the Southeast US, Environment International, Volume 35, Issue 6, August 2009, Pages 956-964, ISSN 0160-4120, https://doi.org/10.1016/j.envint.2009.04.005

[98] Gregor Kiesewetter, Wolfgang Schoepp, Chris Heyes, Markus Amann, Modelling PM2.5 impact indicators in Europe: Health effects and legal compliance, Environmental Modelling & Software, Volume 74, December 2015, Pages 201-211, ISSN 1364-8152, https://doi.org/10.1016/j.envsoft.2015.02.022

[99] World Health Organization, Air Quality Guidelines – Global Update 2005: Particulate matter, ozone, nitrogen dioxide and sulfur dioxide, WHO Regional Office for Europe, 2006, Copenhagen, Denmark, ISBN 92-890-2192-6, http://www.euro.who.int/__data/assets/pdf_file/0005/78638/E90038.pdf

[100] Australian Government – Federal Register of Legislative Instruments, F2016C00215: National Environment Protection (Ambient Air Quality) Measure, 25 February 2016

[101] B.C. Ministry of Environment – Environmental Quality Branch, British Columbia Ambient Air Quality Objectives, 2009

[102] Environment and Climate Change Canada, Canadian Ambient Air Quality Standards, 25 May 2013

[103] Horacio Riojas-Rodríguez, Agnes Soares da Silva, José Luis Texcalac-Sangrador, Grea Litai Moreno-Banda, Air pollution management and control in Latin America and the Caribbean: implications for climate change, Revista Panamericana de Salud Pública, Volume 40, Issue 3, September 2016, Pages 150-159, ISSN 1680-5348, http://www.scielosp.org/pdf/rpsp/v40n3/1020-4989-RPSP-40-03-150.pdf

[104] U.S. Government Publishing Office, Code of Federal Regulations, Title 40: Protection of Environment, Chapter I: Environmental Protection Agency, Subchapter C: Air Programs, Part 50: National Primary and Secondary Ambient Air Quality Standards, § 50.18: National primary ambient air quality standards for PM2.5, 15 January 2013

[105] Barclays Official California Code of Regulations, Title 17: Public Health, Division 3: Air Resources, Chapter 1: Air Resources Board, Subchapter 1.5: Air Basins and Air Quality Standards, Article 2: Ambient Air Quality Standards, § 70200: Table of Standards, 17 May 2006

[106] Joanne Green, Sergio Sánchez, Air Quality in Latin America: An Overview, The Clean Air Institute, May 2013, Washington D.C., United States, http://www.cleanairinstitute.org/calidaddelaireamericalatina/cai-report-english.pdf

[107] Secretaria de Recursos Naturales y Ambiente, Acuerdo Ejecutivo 1566-2010: Reglamento para el Control de Emisiones Generadas por Fuentes Fijas, 2010 [in Spanish; Secretary of Natural Resources and the Environment, Executive Agreement 1566-2010: Regulation for the Control of Emissions Generated by Fixed Sources]

[108] Ministerio de Ambiente, Decreto No. 05: Libro VI Anexo 4: Norma de Calidad del Aire Ambiente o nivel de Inmisión, 4 April 2011 [in Spanish; Ministry of Environment, Decree No. 05: Book VI Annex 4: Ambient Air Quality Standard or Level of Intake]

[109] Ministerio del Ambiente, Decreto Supremo N° 074-2001-PCM: Reglamento de Estándares Nacionales de Calidad Ambiental del Aire, 22 June 2001 [in Spanish; Ministry of the Environment, Supreme Decree No. 074-2001-PCM: Regulation of National Environmental Quality Standards of the Air]

[110] Legislatura de la Ciudad Autónoma de Buenos Aires, Ley Nº 1356/04: Calidad Atmosférica, 10 June 2004 [in Spanish; Legislature of the Autonomous City of Buenos Aires, Law No. 1356/04: Air Quality]

[111] Këshilli i Ministrave, Vendim Nr. 115 – Për miratimin e raportit për gjendjen e mjedisit në Shqipëri, për vitin 2010, 15 February 2012 [in Albanian; Council of Ministers, Decision No. 115 – Adoption of the report on the environmental situation in Albania for 2010]

[112] Ministry of Environment & Forests, Bangladesh National Ambient Air Quality Standards, 2005

[113] 東京都環境局, 微小粒子状物質（ＰＭ2.5）検討会報告書の概要, 29 July 2011 [in Japanese; Tokyo Metropolitan Environment Bureau, Outline of Report on Micro Particulate Substance (PM2.5) Review Board]

[114] Ministry of Environment, Ambient Air Quality Standards (No. 1140/2006), 2006

[115] Said Munir, Safwat Gabr, Turki M. Habeebullah, Mamoun A. Janajrah, Spatiotemporal analysis of fine particulate matter (PM2.5) in Saudi Arabia using remote sensing data, The Egyptian Journal of Remote Sensing and Space Science, Volume 19, Issue 2, December 2016, Pages 195-205, ISSN 1110-9823, https://doi.org/10.1016/j.ejrs.2016.06.001

[116] 行政院環境保護署, 清淨空氣行動計畫 (104 年至 109 年), August 2015 [in Chinese; Environmental Protection Department of the Executive Yuan, Clean Air Action Plan (2015 to 2020)]

[117] Ministry of Environment and Water & Ministry of Health, Regulation No. 9: Limit Values for Sulphur Dioxide, Nitrogen Dioxide, Fine Particulate Matter and Lead in Ambient Air, 3 May 1999

[118] Ministerio del Medio Ambiente, Decreto 12: Establece Norma Primaria de Calidad Ambiental para Material Particulado Fino Respirable MP 2,5, 1 January 2012 [in Spanish; Ministry of Environment, Decree 12: Establishes Primary Environmental Quality Standard for Respirable Fine Particulate Material PM2.5]

[119] Parliament of the Republic of South Africa, Government Gazette, No. 39 of 2004: National Environment Management: Air Quality Act, 2004

[120] European Parliament and of the Council, Directive 2008/50/EC on ambient air quality and cleaner air for Europe, 21 May 2008

[121] Vlada Crne Gore, Uredbu o utvrđivanju vrsta zagađujućih materija, graničnih vrijednosti i drugih standarda kvaliteta vazduha, 29 March 2012 [in Montenegrin; The Government of Montenegro, Regulation of determining type of pollutants, limit values and other air quality standards]

[122] Miljødirektoratet, M-129-2014: Grenseverdier og nasjonale mål, 2014 [in Norwegian; Environment Directorate, M-129-2014: Limits and national goals]

[123] Visare Hoxha, Development of an Air Quality Monitoring Network for Kosovo, Ministry of Environment and Spatial Planning – Department of Environment, December 2010

[124] Минюстом России, Постановление № 26: Предельно допустимые концентрации (ПДК) загрязняющих веществ в атмосферном воздухе населенных мест, 19 April 2010 [in Russian; Russian Ministry of Justice, Decree No. 26: Maximum permissible concentration (MPC) of pollutants in the ambient air of populated areas]

[125] Ministerio de Ambiente, Vivienda y Desarrollo Territorial, Resolución Número (610), 24 March 2010 [in Spanish; Ministry of Environment, Housing and Territorial Development, Resolution Number 610]

[126] Монгол улсын Стандарт, MNS 4585:2007: Агаарын чанар. Техникийн ерөнхий шаардлага, 12 December 2007 [in Mongolian; Mongolian National Standard, MNS 4585:2007: Air quality. General Technical Requirements]

[127] Department of Environment and Natural Resources, DENR Administrative Order No. 2013-13: Establishing the Provisional National Ambient Air Quality Guideline Values for Particulate Matter 2.5 (PM2.5), 7 March 2013

[128] 환경부, 환경정책기본법시행, 1 January 2015 [in Korean; Ministry of Environment, Enactment of Basic Law on Environmental Policy]

[129] Royal Government Gazette, Notification of the National Environment Board, No. 36: B.E.2553, 28 January 2010

[130] 环**境保**护**部**, **中**华人民共和国国家标准 GB 3095-2012: 环境空气质量标准, 29 February 2012 [in Chinese; Ministry of Environmental Protection, National standards of People's Republic of China GB 3095-2012: Ambient air quality standards]

[131] Environmental Protection Department, Air Pollution Control Ordinance (Cap. 311), 10 April 2014

[132] Ministry of Natural Resources & Environment – Department of Environment, New Malaysia Ambient Air Quality Standard, 2015

[133] The Minister of Environment and Lands, Ministerial Order No. 003/16.01 Preventing Activities that Pollute the Atmosphere, 15 July 2010

[134] Central Pollution Control Board, No. B-29016/20/90/PCI-I.: National Ambient Air Quality Standards, 18 November 2009

[135] Bert Brunekreef, Nino Künzli, Juha Pekkanen, Isabella Annesi-Maesano, Bertil Forsberg, Torben Sigsgaard, Menno Keuken, Francesco Forastiere, Maeve Barry, Xavier Querol, Roy M. Harrison, Clean air in Europe: beyond the horizon?, European Respiratory Journal, Volume 45, Issue 1, 2015, Pages 7-10, ISSN 0903-1936, https://doi.org/10.1183/09031936.00186114

[136] Chun Chen, Bin Zhao, Wanting Zhou, Xinyi Jiang, Zhongchao Tan, A methodology for predicting particle penetration factor through cracks of windows and doors for actual engineering application, Building and Environment, Volume 47, January 2012, Pages 339-348, ISSN 0360-1323, https://doi.org/10.1016/j.buildenv.2011.07.004

[137] Guofeng Shen, Miao Xue, Yuanchen Chen, Chunli Yang, Wei Li, Huizhong Shen, Ye Huang, Yanyan Zhang, Han Chen, Ying Zhu, Haisuo Wu, Aijun Ding, Shu Tao, Comparison of carbonaceous particulate matter emission factors among different solid fuels burned in residential stoves, Atmospheric Environment, Volume 89, June 2014, Pages 337-345, ISSN 1352-2310, https://doi.org/10.1016/j.atmosenv.2014.01.033

[138] Ming Shan, Pengsu Wang, Jiarong Li, Guangxi Yue, Xudong Yang, Energy and environment in Chinese rural buildings: Situations, challenges, and intervention strategies, Building and Environment, Volume 91, September 2015, Pages 271-282, ISSN 0360-1323, https://doi.org/10.1016/j.buildenv.2015.03.016

[139] Tianxin Li, Suzhen Cao, Delong Fan, Yaqun Zhang, Beibei Wang, Xiuge Zhao, Brian P. Leaderer, Guofeng Shen, Yawei Zhang, Xiaoli Duan, Household concentrations and personal exposure of PM2.5 among urban residents using different cooking fuels, Science of The Total Environment, Volumes 548-549, 1 April 2016, Pages 6-12, ISSN 0048-9697, https://doi.org/10.1016/j.scitotenv.2016.01.038

[140] Amanda L. Northcross, S. Katharine Hammond, Eduardo Canuz, Kirk R. Smith, Dioxin inhalation doses from wood combustion in indoor cookfires, Atmospheric Environment, Volume 49, March 2012, Pages 415-418, ISSN 1352-2310, https://doi.org/10.1016/j.atmosenv.2011.11.054

[141] Nuno Canha, Susana Marta Almeida, Maria do Carmo Freitas, Hubert Th. Wolterbeek, João Cardoso, Casimiro Pio, Alexandre Caseiro, Impact of wood burning on indoor PM2.5 in a primary school in rural Portugal, Atmospheric Environment, Volume 94, September 2014, Pages 663-670, ISSN 1352-2310, https://doi.org/10.1016/j.atmosenv.2014.05.080

[142] Yue Xu, Yan Wang, Yingjun Chen, Chongguo Tian, Yanli Feng, Jun Li, Gan Zhang, Characterization of fine and carbonaceous particles emissions from pelletized biomass-coal blends combustion: Implications on residential crop residue utilization in China, Atmospheric Environment, Volume 141, September 2016, Pages 312-319, ISSN 1352-2310, https://doi.org/10.1016/j.atmosenv.2016.06.073

[143] Haryono S. Huboyo, Susumu Tohno, Puji Lestari, Akira Mizohata, Motonori Okumura, Characteristics of indoor air pollution in rural mountainous and rural coastal communities in Indonesia, Atmospheric Environment, Volume 82, January 2014, Pages 343-350, ISSN 1352-2310, https://doi.org/10.1016/j.atmosenv.2013.10.044

[144] Amod K. Pokhrel, Michael N. Bates, Jiwan Acharya, Palle Valentiner-Branth, Ram K. Chandyo, Prakash S. Shrestha, Anil K. Raut, Kirk R. Smith, PM2.5 in household kitchens of Bhaktapur, Nepal, using four different cooking fuels, Atmospheric Environment, Volume 113, July 2015, Pages 159-168, ISSN 1352-2310, https://doi.org/10.1016/j.atmosenv.2015.04.060

[145] Wei Huang, Jill Baumgartner, Yuanxun Zhang, Yuqin Wang, James J. Schauer, Source apportionment of air pollution exposures of rural Chinese women cooking with biomass fuels, Atmospheric Environment, Volume 104, March 2015, Pages 79-87, ISSN 1352-2310, https://doi.org/10.1016/j.atmosenv.2014.12.066

[146] Deborah Bennett, Xiangmei (May) Wu, Amber Trout, Michael Apte, David Faulkner, Randy Maddalena, Doug Sullivan, Indoor environmental quality and heating, ventilating and air conditioning survey of small and medium size commercial buildings – Field Study, California Energy Commission & California Air Resources Board, October 2011, CEC-500-2011-043, http://www.energy.ca.gov/2011publications/CEC-500-2011-043/CEC-500-2011-043.pdf

[147] Radha Goyal, Prashant Kumar, Indoor–outdoor concentrations of particulate matter in nine microenvironments of a mix-use commercial building in megacity Delhi, Air Quality, Atmosphere and Health, Volume 6, Issue 4, December 2013, Pages 747-757, ISSN 1873-9326, https://doi.org/10.1007/s11869-013-0212-0

[148] Mohamed F. Yassin, Bothaina E.Y. AlThaqeb, Eman A.E. Al-Mutiri, Assessment of indoor PM2.5 in different residential environments, Atmospheric Environment, Volume 56, September 2012, Pages 65-68, ISSN 1352-2310, https://doi.org/10.1016/j.atmosenv.2012.03.051

[149] S.W. See, R. Balasubramanian, Characterization of fine particle emissions from incense burning, Building and Environment, Volume 46, Issue 5, May 2011, Pages 1074-1080, ISSN 0360-1323, https://doi.org/10.1016/j.buildenv.2010.11.006

[150] Su-Ching Kuo, Ying I. Tsai, Khajornsak Sopajaree, Emission identification and health risk potential of allergy-causing fragrant substances in PM2.5 from incense burning, Building and Environment, Volume 87, May 2015, Pages 23-33, ISSN 0360-1323, https://doi.org/10.1016/j.buildenv.2015.01.012

[151] Eva Höllbacher, Thomas Ters, Cornelia Rieder-Gradinger, Ewald Srebotnik, Emissions of indoor air pollutants from six user scenarios in a model room, Atmospheric Environment, Volume 150, February 2017, Pages 389-394, ISSN 1352-2310, https://doi.org/10.1016/j.atmosenv.2016.11.033

[152] Tran Ngoc Quang, Congrong He, Lidia Morawska, Luke D. Knibbs, Influence of ventilation and filtration on indoor particle concentrations in urban office buildings, Atmospheric Environment, Volume 79, November 2013, Pages 41-52, ISSN 1352-2310, https://doi.org/10.1016/j.atmosenv.2013.06.009

[153] Paraskevi Vivian Dorizas, Margarita-Niki Assimakopoulos, Constantinos Helmis, Mattheos Santamouris, An integrated evaluation study of the ventilation rate, the exposure and the indoor air quality in naturally ventilated classrooms in the Mediterranean region during spring, Science of The Total Environment, Volume 502, 1 January 2015, Pages 557-570, ISSN 0048-9697, https://doi.org/10.1016/j.scitotenv.2014.09.060

[154] L. Stabile, F.C. Fuoco, G. Buonanno, Characteristics of particles and black carbon emitted by combustion of incenses, candles and anti-mosquito products, Building and Environment, Volume 56, October 2012, Pages 184-191, ISSN 0360-1323, https://doi.org/10.1016/j.buildenv.2012.03.005

[155] Xinhua Wang, Xinhui Bi, Duohong Chen, Guoying Sheng, Jiamo Fu, Hospital indoor respirable particles and carbonaceous composition, Building and Environment, Volume 41, Issue 8, August 2006, Pages 992-1000, ISSN 0360-1323, https://doi.org/10.1016/j.buildenv.2005.04.024

[156] Iman Goldasteh, Yilin Tian, Goodarz Ahmadi, Andrea R. Ferro, Human induced flow field and resultant particle resuspension and transport during gait cycle, Building and Environment, Volume 77, July 2014, Pages 101-109, ISSN 0360-1323, https://doi.org/10.1016/j.buildenv.2014.03.016

[157] Norbert Serfozo, Sofia Eirini Chatoutsidou, Mihalis Lazaridis, The effect of particle resuspension during walking activity to PM10 mass and number concentrations in an indoor microenvironment, Building and Environment, Volume 82, December 2014, Pages 180-189, ISSN 0360-1323, https://doi.org/10.1016/j.buildenv.2014.08.017

[158] Maher Elbayoumi, Nor Azam Ramli, Noor Faizah Fitri Md Yusof, Spatial and temporal variations in particulate matter concentrations in twelve schools environment in urban and overpopulated camps landscape, Building and Environment, Volume 90, August 2015, Pages 157-167, ISSN 0360-1323, https://doi.org/10.1016/j.buildenv.2015.03.036

[159] Fang Wang, Dan Meng, Xiuwei Li, Junjie Tan, Indoor-outdoor relationships of PM2.5 in four residential dwellings in winter in the Yangtze River Delta, China, Environmental Pollution, Volume 215, August 2016, Pages 280-289, ISSN 0269-7491, https://doi.org/10.1016/j.envpol.2016.05.023

[160] F. Amato, I. Rivas, M. Viana, T. Moreno, L. Bouso, C. Reche, M. Àlvarez-Pedrerol, A. Alastuey, J. Sunyer, X. Querol, Sources of indoor and outdoor PM2.5 concentrations in primary schools, Science of The Total Environment, Volume 490, 15 August 2014, Pages 757-765, ISSN 0048-9697, https://doi.org/10.1016/j.scitotenv.2014.05.051

[161] Nikmatun Yusro Yang Razali, Mohd Talib Latif, Doreena Dominick, Noorlin Mohamad, Fazrul Razman Sulaiman, Thunwadee Srithawirat, Concentration of particulate matter, CO and CO2 in selected schools in Malaysia, Building and Environment, Volume 87, May 2015, Pages 108-116, ISSN 0360-1323, https://doi.org/10.1016/j.buildenv.2015.01.015

[162] Lidia Morawska, Congrong He, Jane Hitchins, Dale Gilbert, Sandhya Parappukkaran, The relationship between indoor and outdoor airborne particles in the residential environment, Atmospheric Environment, Volume 35, Issue 20, July 2001, Pages 3463-3473, ISSN 1352-2310, https://doi.org/10.1016/S1352-2310(01)00097-8

[163] C.M. Ní Riain, D. Mark, M. Davies, R.M. Harrison, M.A. Byrne, Averaging periods for indoor–outdoor ratios of pollution in naturally ventilated non-domestic buildings near a busy road, Atmospheric Environment, Volume 37, Issue 29, September 2003, Pages 4121-4132, ISSN 1352-2310, https://doi.org/10.1016/S1352-2310(03)00509-0

[164] Yafeng Wang, Chao Chen, Ping Wang, Yali Wan, Ziguang Chen, Li Zhao, Experimental Investigation on Indoor/Outdoor PM2.5 Concentrations of an Office Building Located in Guangzhou, Procedia Engineering, Volume 121, 2015, Pages 333-340, ISSN 1877-7058, https://doi.org/10.1016/j.proeng.2015.08.1076

[165] G. Sangiorgi, L. Ferrero, B.S. Ferrini, C. Lo Porto, M.G. Perrone, R. Zangrando, A. Gambaro, Z. Lazzati, E. Bolzacchini, Indoor airborne particle sources and semi-volatile partitioning effect of outdoor fine PM in offices, Atmospheric Environment, Volume 65, February 2013, Pages 205-214, ISSN 1352-2310, https://doi.org/10.1016/j.atmosenv.2012.10.050

[166] Zhihua Zhou, Yurong Liu, Jianjuan Yuan, Jian Zuo, Guanyi Chen, Linyu Xu, Raufdeen Rameezdeen, Indoor PM2.5 concentrations in residential buildings during a severely polluted winter: A case study in Tianjin, China, Renewable and Sustainable Energy Reviews, Volume 64, October 2016, Pages 372-381, ISSN 1364-0321, https://doi.org/10.1016/j.rser.2016.06.018

[167] Hyeon-Ju Oh, In-Sick Nam, Hyunjun Yun, Jinman Kim, Jinho Yang, Jong-Ryeul Sohn, Characterization of indoor air quality and efficiency of air purifier in childcare centers, Korea, Building and Environment, Volume 82, December 2014, Pages 203-214, ISSN 0360-1323, https://doi.org/10.1016/j.buildenv.2014.08.019

[168] Marian Fe Theresa C. Lomboy, Leni L. Quirit, Victorio B. Molina, Godofreda V. Dalmacion, Joel D. Schwartz, Helen H. Suh, Emmanuel S. Baja, Characterization of particulate matter 2.5 in an urban tertiary care hospital in the Philippines, Building and Environment, Volume 92, October 2015, Pages 432-439, ISSN 0360-1323, https://doi.org/10.1016/j.buildenv.2015.05.018

[169] Chung-Min Liao, Su-Jui Huang, Hsin Yu, Size-dependent particulate matter indoor/outdoor relationships for a wind-induced naturally ventilated airspace, Building and Environment, Volume 39, Issue 4, April 2004, Pages 411-420, ISSN 0360-1323, https://doi.org/10.1016/j.buildenv.2003.09.015

[170] D. Massey, J. Masih, A. Kulshrestha, M. Habil, A. Taneja, Indoor/outdoor relationship of fine particles less than 2.5 μm (PM2.5) in residential homes locations in central Indian region, Building and Environment, Volume 44, Issue 10, October 2009, Pages 2037-2045, ISSN 0360-1323, https://doi.org/10.1016/j.buildenv.2009.02.010

[171] Li Zhao, Chao Chen, Ping Wang, Ziguang Chen, Shijie Cao, Qingqin Wang, Guangya Xie, Yali Wan, Yafeng Wang, Bin Lu, Influence of atmospheric fine particulate matter (PM2.5) pollution on indoor environment during winter in Beijing, Building and Environment, Volume 87, May 2015, Pages 283-291, ISSN 0360-1323, https://doi.org/10.1016/j.buildenv.2015.02.008

[172] D. Saraga, S. Pateraki, A. Papadopoulos, Ch. Vasilakos, Th. Maggos, Studying the indoor air quality in three non-residential environments of different use: A museum, a printery industry and an office, Building and Environment, Volume 46, Issue 11, November 2011, Pages 2333-2341, ISSN 0360-1323, https://doi.org/10.1016/j.buildenv.2011.05.013

[173] I. Rivas, M. Viana, T. Moreno, M. Pandolfi, F. Amato, C. Reche, L. Bouso, M. Àlvarez-Pedrerol, A. Alastuey, J. Sunyer, X. Querol, Child exposure to indoor and outdoor air pollutants in schools in Barcelona, Spain, Environment International, Volume 69, August 2014, Pages 200-212, ISSN 0160-4120, https://doi.org/10.1016/j.envint.2014.04.009

[174] Reto Meier, Marloes Eeftens, Harish C. Phuleria, Alex Ineichen, Elisabetta Corradi, Mark Davey, Martin Fierz, Regina E. Ducret-Stich, Inmaculada Aguilera, Christian Schindler, Thierry Rochat, Nicole Probst-Hensch, Ming-Yi Tsai, Nino Künzli, Differences in indoor versus outdoor concentrations of ultrafine particles, PM2.5, PMabsorbance and NO2 in Swiss homes, Journal of Exposure Science and Environmental Epidemiology, Volume 25, Issue 5, September/October 2015, Pages 499-505, ISSN 1559-0631, https://doi.org/10.1038/jes.2015.3

[175] Avril Challoner, Laurence Gill, Indoor/outdoor air pollution relationships in ten commercial buildings: PM2.5 and NO2, Building and Environment, Volume 80, October 2014, Pages 159-173, ISSN 0360-1323, https://doi.org/10.1016/j.buildenv.2014.05.032

[176] Jinhua Hu, Nianping Li, Variation of PM2.5 Concentrations in Shopping Malls in Autumn, Changsha, Procedia Engineering, Volume 121, 2015, Pages 692-698, ISSN 1877-7058, https://doi.org/10.1016/j.proeng.2015.09.006

[177] Jianlin Ren, Junjie Liu, Xiaodong Cao, Yuefei Hou, Influencing factors and energy-saving control strategies for indoor fine particles in commercial office buildings in six Chinese cities, Energy and Buildings, Volume 149, 15 August 2017, Pages 171-179, ISSN 0378-7788, https://doi.org/10.1016/j.enbuild.2017.05.061

[178] Chien-Cheng Jung, Pei-Chih Wu, Chao-Heng Tseng, Huey-Jen Su, Indoor air quality varies with ventilation types and working areas in hospitals, Building and Environment, Volume 85, February 2015, Pages 190-195, ISSN 0360-1323, https://doi.org/10.1016/j.buildenv.2014.11.026

[179] Shanshan Shi, Bin Zhao, Occupants' interactions with windows in 8 residential apartments in Beijing and Nanjing, China, Building Simulation, Volume 9, Issue 2, April 2016, Pages 221-231, ISSN 1996-8744, https://doi.org/10.1007/s12273-015-0266-z

[180] Markey Johnson, Morgan MacNeill, Alice Grgicak-Mannion, Elizabeth Nethery, Xiaohong Xu, Robert Dales, Pat Rasmussen, Amanda Wheeler, Development of temporally refined land-use regression models predicting daily household-level air pollution in a panel study of lung function among asthmatic children, Journal of Exposure Science and Environmental Epidemiology, Volume 23, Issue 3, May/June 2013, Pages 259-267, ISSN 1559-0631, https://doi.org/10.1038/jes.2013.1

[181] Adams Rackes, Michael S. Waring, Modeling impacts of dynamic ventilation strategies on indoor air quality of offices in six US cities, Building and Environment, Volume 60, February 2013, Pages 243-253, ISSN 0360-1323, https://doi.org/10.1016/j.buildenv.2012.10.013

[182] Elliott T. Gall, Ailu Chen, Victor Wei-Chung Chang, William W Nazaroff, Exposure to particulate matter and ozone of outdoor origin in Singapore, Building and Environment, Volume 93, Part 1, November 2015, Pages 3-13, ISSN 0360-1323, https://doi.org/10.1016/j.buildenv.2015.03.027

[183] C. Dimitroulopoulou, M.R. Ashmore, M.T.R. Hill, M.A. Byrne, R. Kinnersley, INDAIR: A probabilistic model of indoor air pollution in UK homes, Atmospheric Environment, Volume 40, Issue 33, October 2006, Pages 6362-6379, ISSN 1352-2310, https://doi.org/10.1016/j.atmosenv.2006.05.047

[184] J.A. McGrath, M.A. Byrne, M.R. Ashmore, A.C. Terry, C. Dimitroulopoulou, A simulation study of the changes in PM2.5 concentrations due to interzonal airflow variations caused by internal door opening patterns, Atmospheric Environment, Volume 87, April 2014, Pages 183-188, ISSN 1352-2310, https://doi.org/10.1016/j.atmosenv.2014.01.050

[185] Xiangdong Li, Yihuan Yan, Yidan Shang, Jiyuan Tu, An Eulerian–Eulerian model for particulate matter transport in indoor spaces, Building and Environment, Volume 86, April 2015, Pages 191-202, ISSN 0360-1323, https://doi.org/10.1016/j.buildenv.2015.01.010

[186] Hong-Ming Kao, Tsang-Jung Chang, Yi-Fang Hsieh, Chia-Ho Wang, Cheng-I. Hsieh, Comparison of airflow and particulate matter transport in multi-room buildings for different natural ventilation patterns, Energy and Buildings, Volume 41, Issue 9, September 2009, Pages 966-974, ISSN 0378-7788, https://doi.org/10.1016/j.enbuild.2009.04.005

[187] Tiantian Zhang, Yufei Tan, Xuedan Zhang, Zhigao Li, A glazed transpired solar wall system for improving indoor environment of rural buildings in northeast China, Building and Environment, Volume 98, March 2016, Pages 158-179, ISSN 0360-1323, https://doi.org/10.1016/j.buildenv.2016.01.011

[188] Alvin C.K. Lai, F.Z. Chen, Modeling of cooking-emitted particle dispersion and deposition in a residential flat: A real room application, Building and Environment, Volume 42, Issue 9, September 2007, Pages 3253-3260, ISSN 0360-1323, https://doi.org/10.1016/j.buildenv.2006.08.015

[189] Andrius Jurelionis, Laura Gagytė, Tadas Prasauskas, Darius Čiužas, Edvinas Krugly, Lina Šeduikytė, Dainius Martuzevičius, The impact of the air distribution method in ventilated rooms on the aerosol particle dispersion and removal: The experimental approach, Energy and Buildings, Volume 86, January 2015, Pages 305-313, ISSN 0378-7788, https://doi.org/10.1016/j.enbuild.2014.10.014

[190] Yu Liu, Huixing Li, Guohui Feng, Simulation of inhalable aerosol particle distribution generated from cooking by Eulerian approach with RNG k–epsilon turbulence model and pollution exposure in a residential kitchen space, Building Simulation, Volume 10, Issue 1, February 2017, Pages 135-144, ISSN 1996-8744, https://doi.org/10.1007/s12273-016-0313-4

[191] Tom Ben-David, Michael S. Waring, Impact of natural versus mechanical ventilation on simulated indoor air quality and energy consumption in offices in fourteen U.S. cities, Building and Environment, Volume 104, 1 August 2016, Pages 320-336, ISSN 0360-1323, https://doi.org/10.1016/j.buildenv.2016.05.007

[192] Yudi Liu, Qing Cao, Wei Liu, Chao-Hsin Lin, Daniel Wei, Steven Baughcum, Zhengwei Long, Xiong Shen, Qingyan Chen, Numerical modeling of particle deposition in the environmental control systems of commercial airliners on ground, Building Simulation, Volume 10, Issue 2, April 2017, Pages 265-275, ISSN 1996-8744, https://doi.org/10.1007/s12273-016-0323-2

[193] Tracy L. Thatcher, David W. Layton, Deposition, resuspension, and penetration of particles within a residence, Atmospheric Environment, Volume 29, Issue 13, July 1995, Pages 1487-1497, ISSN 1352-2310, https://doi.org/10.1016/1352-2310(95)00016-R

[194] Jonathan M. Gaffin, Carter R. Petty, Marissa Hauptman, Choong-Min Kang, Jack M. Wolfson, Yara Abu Awad, Qian Di, Peggy S. Lai, William J. Sheehan, Sachin Baxi, Brent A. Coull, Joel D. Schwartz, Diane R. Gold, Petros Koutrakis, Wanda Phipatanakul, Modeling indoor particulate exposures in inner-city school classrooms, Journal of Exposure Science and Environmental Epidemiology, 7 September 2016, Pages 1-7, ISSN 1559-064X, https://doi.org/10.1038/jes.2016.52

[195] Natasha Hodas, Qingyu Meng, Melissa M. Lunden, David Q. Rich, Halûk Özkaynak, Lisa K. Baxter, Qi Zhang, Barbara J. Turpin, Variability in the fraction of ambient fine particulate matter found indoors and observed heterogeneity in health effect estimates, Journal of Exposure Science and Environmental Epidemiology, Volume 22, Issue 5, September/October 2012, Pages 448-454, ISSN 1559-0631, https://doi.org/10.1038/jes.2012.34

[196] Ziguang Chen, Chao Chen, Shen Wei, Yuqin Wu, Yafeng Wang, Yali Wan, Impact of the external window crack structure on indoor PM2.5 mass concentration, Building and Environment, Volume 108, 1 November 2016, Pages 240-251, ISSN 0360-1323, https://doi.org/10.1016/j.buildenv.2016.08.031

[197] Yuchen Shi, Xiaofeng Li, Haoru Li, A new method to assess infiltration rates in large shopping centers, Building and Environment, Volume 119, July 2017, Pages 140-152, ISSN 0360-1323, https://doi.org/10.1016/j.buildenv.2017.04.011

[198] Wenjing Ji, Bin Zhao, Contribution of outdoor-originating particles, indoor-emitted particles and indoor secondary organic aerosol (SOA) to residential indoor PM2.5 concentration: A model-based estimation, Building and Environment, Volume 90, August 2015, Pages 196-205, ISSN 0360-1323, https://doi.org/10.1016/j.buildenv.2015.04.006

[199] Byung Hee Lee, Su Whan Yee, Dong Hwa Kang, Myoung Souk Yeo, Kwang Woo Kim, Multi-zone simulation of outdoor particle penetration and transport in a multi-story building, Building Simulation, Volume 10, Issue 4, August 2017, Pages 525-534, ISSN 1996-8744, https://doi.org/10.1007/s12273-016-0340-1

[200] Alvin C.K. Lai, Modeling of airborne particle exposure and effectiveness of engineering control strategies, Building and Environment, Volume 39, Issue 6, June 2004, Pages 599-610, ISSN 0360-1323, https://doi.org/10.1016/j.buildenv.2003.12.005

[201] Payel Das, Clive Shrubsole, Benjamin Jones, Ian Hamilton, Zaid Chalabi, Michael Davies, Anna Mavrogianni, Jonathon Taylor, Using probabilistic sampling-based sensitivity analyses for indoor air quality modelling, Building and Environment, Volume 78, August 2014, Pages 171-182, ISSN 0360-1323, https://doi.org/10.1016/j.buildenv.2014.04.017

[202] Payel Das, Zaid Chalabi, Benjamin Jones, James Milner, Clive Shrubsole, Michael Davies, Ian Hamilton, Ian Ridley, Paul Wilkinson, Multi-objective methods for determining optimal ventilation rates in dwellings, Building and Environment, Volume 66, August 2013, Pages 72-81, ISSN 0360-1323, https://doi.org/10.1016/j.buildenv.2013.03.021

[203] Tom Marsik, Ron Johnson, Use of Simulink to evaluate the air-quality and energy performance of HRV-equipped residences in Fairbanks, Alaska, Energy and Buildings, Volume 40, Issue 8, 2008, Pages 1605-1613, ISSN 0378-7788, https://doi.org/10.1016/j.enbuild.2008.02.007

[204] Tom Marsik, Ron Johnson, HVAC air-quality model and its use to test a PM2.5 control strategy, Building and Environment, Volume 43, Issue 11, November 2008, Pages 1850-1857, ISSN 0360-1323, https://doi.org/10.1016/j.buildenv.2007.11.001

[205] J. Taylor, C. Shrubsole, M. Davies, P. Biddulph, P. Das, I. Hamilton, S. Vardoulakis, A. Mavrogianni, B. Jones, E. Oikonomou, The modifying effect of the building envelope on population exposure to PM2.5 from outdoor sources, Indoor Air, Volume 24, Issue 6, December 2014, Pages 639-651, ISSN 1600-0668, https://doi.org/10.1111/ina.12116

[206] Toby C. Lewis, Thomas G. Robins, Graciela B. Mentz, Xiaohui Zhang, Bhramar Mukherjee, Xihong Lin, Gerald J. Keeler, J. Timothy Dvonch, Fuyuen Y. Yip, Marie S. O'Neill, Edith A. Parker, Barbara A. Israel, Paul T. Max, Angela Reyes, Air pollution and respiratory symptoms among children with asthma: Vulnerability by corticosteroid use and residence area, Science of The Total Environment, Volume 448, 15 March 2013, Pages 48-55, ISSN 0048-9697, https://doi.org/10.1016/j.scitotenv.2012.11.070

[207] Jing Hua, Yong Yin, Li Peng, Li Du, Fuhai Geng, Liping Zhu, Acute effects of black carbon and PM2.5 on children asthma admissions: A time-series study in a Chinese city, Science of The Total Environment, Volume 481, 15 May 2014, Pages 433-438, ISSN 0048-9697, https://doi.org/10.1016/j.scitotenv.2014.02.070

[208] Tatsuya Mimura, Takamichi Ichinose, Satoru Yamagami, Hiroshi Fujishima, Yuko Kamei, Mari Goto, Sachiko Takada, Masao Matsubara, Airborne particulate matter (PM2.5) and the prevalence of allergic conjunctivitis in Japan, Science of The Total Environment, Volume 487, 15 July 2014, Pages 493-499, ISSN 0048-9697, https://doi.org/10.1016/j.scitotenv.2014.04.057

[209] Barnaba Giuseppina Ponticiello, Assunta Capozzella, Valeria Di Giorgio, Teodorico Casale, Roberto Giubilati, Gianfranco Tomei, Francesco Tomei, Maria Valeria Rosati, Angela Sancini, Overweight and urban pollution: Preliminary results, Science of The Total Environment, Volumes 518-519, 15 June 2015, Pages 61-64, ISSN 0048-9697, https://doi.org/10.1016/j.scitotenv.2015.02.084

[210] Jun Liu, Yiqun Han, Xiao Tang, Jiang Zhu, Tong Zhu, Estimating adult mortality attributable to PM2.5 exposure in China with assimilated PM2.5 concentrations based on a ground monitoring network, Science of The Total Environment, Volume 568, 15 October 2016, Pages 1253-1262, ISSN 0048-9697, https://doi.org/10.1016/j.scitotenv.2016.05.165

[211] Congbo Song, Jianjun He, Lin Wu, Taosheng Jin, Xi Chen, Ruipeng Li, Peipei Ren, Li Zhang, Hongjun Mao, Health burden attributable to ambient PM2.5 in China, Environmental Pollution, Volume 223, April 2017, Pages 575-586, ISSN 0269-7491, https://doi.org/10.1016/j.envpol.2017.01.060

[212] Siming You, Yen Wah Tong, Koon Gee Neoh, Yanjun Dai, Chi-Hwa Wang, On the association between outdoor PM2.5 concentration and the seasonality of tuberculosis for Beijing and Hong Kong, Environmental Pollution, Volume 218, November 2016, Pages 1170-1179, ISSN 0269-7491, https://doi.org/10.1016/j.envpol.2016.08.071

[213] Zhuoxin Peng, Cong Liu, Biao Xu, Haidong Kan, Weibing Wang, Long-term exposure to ambient air pollution and mortality in a Chinese tuberculosis cohort, Science of The Total Environment, Volume 580, 15 February 2017, Pages 1483-1488, ISSN 0048-9697, https://doi.org/10.1016/j.scitotenv.2016.12.128

[214] Die Fang, Qin'geng Wang, Huiming Li, Yiyong Yu, Yan Lu, Xin Qian, Mortality effects assessment of ambient PM2.5 pollution in the 74 leading cities of China, Science of The Total Environment, Volume 569, 1 November 2016, Pages 1545-1552, ISSN 0048-9697, https://doi.org/10.1016/j.scitotenv.2016.06.248

[215] Yang Xia, Dabo Guan, Xujia Jiang, Liqun Peng, Heike Schroeder, Qiang Zhang, Assessment of socioeconomic costs to China's air pollution, Atmospheric Environment, Volume 139, August 2016, Pages 147-156, ISSN 1352-2310, https://doi.org/10.1016/j.atmosenv.2016.05.036

[216] Meng Gao, Sarath K. Guttikunda, Gregory R. Carmichael, Yuesi Wang, Zirui Liu, Charles O. Stanier, Pablo E. Saide, Man Yu, Health impacts and economic losses assessment of the 2013 severe haze event in Beijing area, Science of The Total Environment, Volume 511, 1 April 2015, Pages 553-561, ISSN 0048-9697, https://doi.org/10.1016/j.scitotenv.2015.01.005

[217] Hao Yin, Massimo Pizzol, Linyu Xu, External costs of PM2.5 pollution in Beijing, China: Uncertainty analysis of multiple health impacts and costs, Environmental Pollution, Volume 226, July 2017, Pages 356-369, ISSN 0269-7491, https://doi.org/10.1016/j.envpol.2017.02.029

[218] Jiandong Wang, Shuxiao Wang, A. Scott Voorhees, Bin Zhao, Carey Jang, Jingkun Jiang, Joshua S. Fu, Dian Ding, Yun Zhu, Jiming Hao, Assessment of short-term PM2.5-related mortality due to different emission sources in the Yangtze River Delta, China, Atmospheric Environment, Volume 123, Part B, December 2015, Pages 440-448, ISSN 1352-2310, https://doi.org/10.1016/j.atmosenv.2015.05.060

[219] N.A.H. Janssen, P. Fischer, M. Marra, C. Ameling, F.R. Cassee, Short-term effects of PM2.5, PM10 and PM2.5-10 on daily mortality in the Netherlands, Science of The Total Environment, Volumes 463-464, 1 October 2013, Pages 20-26, ISSN 0048-9697, https://doi.org/10.1016/j.scitotenv.2013.05.062

[220] Cristina Ortiz, Cristina Linares, Rocio Carmona, Julio Díaz, Evaluation of short-term mortality attributable to particulate matter pollution in Spain, Environmental Pollution, Volume 224, May 2017, Pages 541-551, ISSN 0269-7491, https://doi.org/10.1016/j.envpol.2017.02.037

[221] D R Culqui, C Linares, C Ortiz, R Carmona, J Díaz, Association between environmental factors and emergency hospital admissions due to Alzheimer's disease in Madrid, Science of The Total Environment, Volume 592, 15 August 2017, Pages 451-457, ISSN 0048-9697, https://doi.org/10.1016/j.scitotenv.2017.03.089

[222] Dimosthenis A. Sarigiannis, Spyros P. Karakitsios, Marianthi V. Kermenidou, Health impact and monetary cost of exposure to particulate matter emitted from biomass burning in large cities, Science of The Total Environment, Volumes 524-525, 15 August 2015, Pages 319-330, ISSN 0048-9697, https://doi.org/10.1016/j.scitotenv.2015.02.108

[223] Siobhan Crichton, Benjamin Barratt, Anastassia Spiridou, Uy Hoang, Shao Fen Liang, Yevgeniya Kovalchuk, Sean D. Beevers, Frank J. Kelly, Brendan Delaney, Charles DA Wolfe, Associations between exhaust and non-exhaust particulate matter and stroke incidence by stroke subtype in South London, Science of The Total Environment, Volume 568, 15 October 2016, Pages 278-284, ISSN 0048-9697, https://doi.org/10.1016/j.scitotenv.2016.06.009

[224] Roy M. Harrison, Dimitrios Bousiotis, A.M. Mohorjy, A.K. Alkhalaf, M. Shamy, M. Alghamdi, M. Khoder, M. Costa, Health risk associated with airborne particulate matter and its components in Jeddah, Saudi Arabia, Science of The Total Environment, Volumes 590-591, 15 July 2017, Pages 531-539, ISSN 0048-9697, https://doi.org/10.1016/j.scitotenv.2017.02.216

[225] Manuel A. Leiva G, Daniela A. Santibañez, Sergio Ibarra E, Patricia Matus C, Rodrigo Seguel, A five-year study of particulate matter (PM2.5) and cerebrovascular diseases, Environmental Pollution, Volume 181, October 2013, Pages 1-6, ISSN 0269-7491, https://doi.org/10.1016/j.envpol.2013.05.057

[226] Weeberb J Requia, Matthew D Adams, Petros Koutrakis, Association of PM2.5 with diabetes, asthma, and high blood pressure incidence in Canada: A spatiotemporal analysis of the impacts of the energy generation and fuel sales, Science of The Total Environment, Volumes 584-585, 15 April 2017, Pages 1077-1083, ISSN 0048-9697, https://doi.org/10.1016/j.scitotenv.2017.01.166

[227] Xiaoli Zhao, Sufang Zhang, Chunyang Fan, Environmental externality and inequality in China: Current Status and future choices, Environmental Pollution, Volume 190, July 2014, Pages 176-179, ISSN 0269-7491, https://doi.org/10.1016/j.envpol.2014.02.027

[228] Nor Azura Sulong, Mohd Talib Latif, Md Firoz Khan, Norhaniza Amil, Matthew J. Ashfold, Muhammad Ikram Abdul Wahab, Kok Meng Chan, Mazrura Sahani, Source apportionment and health risk assessment among specific age groups during haze and no-haze episodes in Kuala Lumpur, Malaysia, Science of The Total Environment, Volumes 601-602, 1 December 2017, Pages 556-570, ISSN 0048-9697, https://doi.org/10.1016/j.scitotenv.2017.05.153

[229] Takashi Yorifuji, Saori Kashima, Hiroyuki Doi, Associations of acute exposure to fine and coarse particulate matter and mortality among older people in Tokyo, Japan, Science of The Total Environment, Volume 542, Part A, 15 January 2016, Pages 354-359, ISSN 0048-9697, https://doi.org/10.1016/j.scitotenv.2015.10.113

[230] Soledad Burgos, Pablo Ruiz, Rosalina Koifman, Changes to indoor air quality as a result of relocating families from slums to public housing, Atmospheric Environment, Volume 70, May 2013, Pages 179-185, ISSN 1352-2310, https://doi.org/10.1016/j.atmosenv.2012.12.044

[231] Raphael E. Arku, Kathie L. Dionisio, Allison F. Hughes, Jose Vallarino, John D. Spengler, Marcia C. Castro, Samuel Agyei-Mensah, Majid Ezzati, Personal particulate matter exposures and locations of students in four neighborhoods in Accra, Ghana, Journal of Exposure Science and Environmental Epidemiology, Volume 25, Issue 6, November-December 2015, Pages 557-566, ISSN 1559-0631, https://doi.org/10.1038/jes.2014.56

[232] Bang-Quan He, Advances in emission characteristics of diesel engines using different biodiesel fuels, Renewable and Sustainable Energy Reviews, Volume 60, July 2016, Pages 570-586, ISSN 1364-0321, https://doi.org/10.1016/j.rser.2016.01.093

[233] Muhammad Imran Khan, Tabassum Yasmin, Abdul Shakoor, Technical overview of compressed natural gas (CNG) as a transportation fuel, Renewable and Sustainable Energy Reviews, Volume 51, November 2015, Pages 785-797, ISSN 1364-0321, https://doi.org/10.1016/j.rser.2015.06.053

[234] Xiaokun Han, Qingjun Guo, Congqiang Liu, Harald Strauss, Junxing Yang, Jian Hu, Rongfei Wei, Liyan Tian, Jing Kong, Marc Peters, Effect of the pollution control measures on PM2.5 during the 2015 China

Victory Day Parade: Implication from water-soluble ions and sulfur isotope, Environmental Pollution, Volume 218, November 2016, Pages 230-241, ISSN 0269-7491, https://doi.org/10.1016/j.envpol.2016.06.038

[235] Lixin Chen, Chenming Liu, Rui Zou, Mao Yang, Zhiqiang Zhang, Experimental examination of effectiveness of vegetation as bio-filter of particulate matters in the urban environment, Environmental Pollution, Volume 208, Part A, January 2016, Pages 198-208, ISSN 0269-7491, https://doi.org/10.1016/j.envpol.2015.09.006

[236] Zheming Tong, Thomas H. Whitlow, Patrick F. MacRae, Andrew J. Landers, Yoshiki Harada, Quantifying the effect of vegetation on near-road air quality using brief campaigns, Environmental Pollution, Volume 201, June 2015, Pages 141-149, ISSN 0269-7491, https://doi.org/10.1016/j.envpol.2015.02.026

[237] Xinming Jin, Lijun Yang, Xiaoze Du, Yongping Yang, Transport characteristics of PM2.5 inside urban street canyons: The effects of trees and vehicles, Building Simulation, Volume 10, Issue 3, June 2017, Pages 337-350, ISSN 1996-8744, https://doi.org/10.1007/s12273-016-0324-1

[238] Yuan Chen, Nina Schleicher, Mathieu Fricker, Kuang Cen, Xiu-li Liu, Uwe Kaminski, Yang Yu, Xue-fang Wu, Stefan Norra, Long-term variation of black carbon and PM2.5 in Beijing, China with respect to meteorological conditions and governmental measures, Environmental Pollution, Volume 212, May 2016, Pages 269-278, ISSN 0269-7491, https://doi.org/10.1016/j.envpol.2016.01.008

[239] R.M. Qadir, G. Abbaszade, J. Schnelle-Kreis, J.C. Chow, R. Zimmermann, Concentrations and source contributions of particulate organic matter before and after implementation of a low emission zone in Munich, Germany, Environmental Pollution, Volume 175, April 2013, Pages 158-167, ISSN 0269-7491, https://doi.org/10.1016/j.envpol.2013.01.002

[240] Sina Hasheminassab, Nancy Daher, Bart D. Ostro, Constantinos Sioutas, Long-term source apportionment of ambient fine particulate matter (PM2.5) in the Los Angeles Basin: A focus on emissions reduction from vehicular sources, Environmental Pollution, Volume 193, October 2014, Pages 54-64, ISSN 0269-7491, https://doi.org/10.1016/j.envpol.2014.06.012

[241] Maggie L. Grabow, Scott N. Spak, Tracey Holloway, Brian Stone Jr., Adam C. Mednick, Jonathan A. Patz, Air quality and exercise-related health benefits from reduced car travel in the midwestern United States, Environmental Health Perspectives, Volume 120, Issue 1, January 2012, Pages 68-76, ISSN 0091-6765, https://doi.org/10.1289/ehp.1103440

[242] Shi Shu, Christina Batteate, Brian Cole, John Froines, Yifang Zhu, Air quality impacts of a CicLAvia event in Downtown Los Angeles, CA, Environmental Pollution, Volume 208, Part A, January 2016, Pages 170-176, ISSN 0269-7491, https://doi.org/10.1016/j.envpol.2015.09.010

[243] Thomas H. Whitlow, Andrew Hall, K. Max Zhang, Juan Anguita, Impact of local traffic exclusion on near-road air quality: Findings from the New York City “Summer Streets” campaign, Environmental Pollution, Volume 159, Issues 8-9, August-September 2011, Pages 2016-2027, ISSN 0269-7491, https://doi.org/10.1016/j.envpol.2011.02.033

[244] Ma Shuangchen, Chai Jin, Chen Gongda, Yu Weijing, Zhu Sijie, Research on desulfurization wastewater evaporation: Present and future perspectives, Renewable and Sustainable Energy Reviews, Volume 58, May 2016, Pages 1143-1151, ISSN 1364-0321, https://doi.org/10.1016/j.rser.2015.12.252

[245] Ricardo L. Carvalho, Ole M. Jensen, Luís A.C. Tarelho, Mapping the performance of wood-burning stoves by installations worldwide, Energy and Buildings, Volume 127, 1 September 2016, Pages 658-679, ISSN 0378-7788, https://doi.org/10.1016/j.enbuild.2016.06.010

[246] Aminul Islam, Eng-Seng Chan, Yun Hin Taufiq-Yap, Md. Alam Hossain Mondal, M. Moniruzzaman, Moniruzzaman Mridha, Energy security in Bangladesh perspective—An assessment and implication, Renewable and Sustainable Energy Reviews, Volume 32, April 2014, Pages 154-171, ISSN 1364-0321, https://doi.org/10.1016/j.rser.2014.01.021

[247] Mehdi Amouei Torkmahalleh, Ulmeken Kaibaldiyeva, Aida Kadyrbayeva, A new computer model for the simulation of particulate matter formation from heated cooking oils using Aspen Plus, Building Simulation, Volume 10, Issue 4, August 2017, Pages 535-550, ISSN 1996-8744, https://doi.org/10.1007/s12273-016-0341-0

[248] M. Amouei Torkmahalleh, Y. Zhao, P.K. Hopke, A. Rossner, A.R. Ferro, Additive impacts on particle emissions from heating low emitting cooking oils, Atmospheric Environment, Volume 74, August 2013, Pages 194-198, ISSN 1352-2310, https://doi.org/10.1016/j.atmosenv.2013.03.038

[249] Xiao-Dan Yan, Qi-Ming Wang, Cai Tie, Hong-Tao Jin, Yan-Xing Han, Jin-Lan Zhang, Xiao-Ming Yu, Qi Hou, Piao-Piao Zhang, Ai-Ping Wang, Pei-Cheng Zhang, Zhonggao Gao, Jian-Dong Jiang, Polydatin protects the respiratory system from PM2.5 exposure, Scientific Reports, Volume 7, Article Number 40030, 9 January 2017, ISSN 2045-2322, https://doi.org/10.1038/srep40030

[250] Nan Zhang, Bin Han, Fei He, Jia Xu, Ruojie Zhao, Yujuan Zhang, Zhipeng Bai, Chemical characteristic of PM2.5 emission and inhalational carcinogenic risk of domestic Chinese cooking, Environmental Pollution, Volume 227, August 2017, Pages 24-30, ISSN 0269-7491, https://doi.org/10.1016/j.envpol.2017.04.033

[251] James Johnston, John Counsell, P. A. Strachan, Trends in Office Internal Gains and the Impact on Space Heating and Cooling, CIBSE Technical Symposium, DeMontfort University, Leicester, UK, 6th and 7th September 2011, https://strathprints.strath.ac.uk/id/eprint/39288

[252] Bjarke Mølgaard, Antti Joonas Koivisto, Tareq Hussein, Kaarle Hämeri, A New Clean Air Delivery Rate Test Applied to Five Portable Indoor Air Cleaners, Aerosol Science and Technology, Volume 48, Issue 4, 3 April 2014, Pages 409-417, ISSN 0278-6826, https://doi.org/10.1080/02786826.2014.883063

[253] Huan Ma, Henggen Shen, Tiantian Shui, Qing Li, Liuke Zhou, Experimental Study on Ultrafine Particle Removal Performance of Portable Air Cleaners with Different Filters in an Office Room, International Journal of Environmental Research and Public Health, Volume 13, Number 1, 5 January 2016, Article Number 102, ISSN 1660-4601, https://doi.org/10.3390/ijerph13010102

[254] Sangita Vyas, Nikhil Srivastav, Dean Spears, An Experiment with Air Purifiers in Delhi during Winter 2015-2016, PLoS ONE, Volume 11, Issue 12, 15 December 2016, Article Number e0167999, ISSN 1932-6203, https://doi.org/10.1371/journal.pone.0167999

[255] Maneerat Ongwandee, Artiya Kruewan, Evaluation of Portable Household and In-Car Air Cleaners for Air Cleaning Potential and Ozone-Initiated Pollutants, Indoor and Built Environment, Volume 22, Issue 4, 1 August 2013, Pages 659-668, ISSN 1420-326X, https://doi.org/10.1177/1420326X12460254

[256] Michal P. Spilak, Gabriela D. Karottki, Barbara Kolarik, Marie Frederiksen, Steffen Loft, Lars Gunnarsen, Evaluation of building characteristics in 27 dwellings in Denmark and the effect of using particle filtration units on PM2.5 concentrations, Building and Environment, Volume 73, March 2014, Pages 55-63, ISSN 0360-1323, https://doi.org/10.1016/j.buildenv.2013.11.020

[257] Julie F. Hart, Tony J. Ward, Terry M. Spear, Richard J. Rossi, Nicholas N. Holland, Brodie G. Loushin, Evaluating the Effectiveness of a Commercial Portable Air Purifier in Homes with Wood Burning Stoves: A Preliminary Study, Journal of Environmental and Public Health, Volume 2011, 2011, Article Number 324809, ISSN 1687-9813, https://doi.org/10.1155/2011/324809

[258] Siamak Rahimi Ardkapan, Alireza Afshari, Niels C. Bergsøe, Peter V. Nielsen, Evaluation of air cleaning technologies existing in the Danish market: Experiments in a duct and in a test room, Indoor and Built Environment, Volume 23, Issue 8, 1 December 2014, Pages 1177-1186, ISSN 1420-326X, https://doi.org/10.1177/1420326X13501097

[259] Kwang-Chul Noh, Se-Jin Yook, Evaluation of clean air delivery rates and operating cost effectiveness for room air cleaner and ventilation system in a small lecture room, Energy and Buildings, Volume 119, 1 May 2016, Pages 111-118, ISSN 0378-7788, https://doi.org/10.1016/j.enbuild.2016.03.027

[260] Prabjit Barn, Timothy Larson, Melanie Noullett, Susan Kennedy, Ray Copes, Michael Brauer, Infiltration of forest fire and residential wood smoke: an evaluation of air cleaner effectiveness, Journal of Exposure Science and Environmental Epidemiology, Volume 18, Issue 5, 5 December 2015, Pages 503-511, ISSN 1559-0631, https://doi.org/10.1038/sj.jes.7500640

[261] J. A. Siegel, Primary and secondary consequences of indoor air cleaners, Indoor Air, Volume 88, Issue 1, February 2016, Pages 88-96, ISSN 1600-0668, https://doi.org/doi:10.1111/ina.12194

[262] P.J. Irga, N.J. Paull, P. Abdo, F.R. Torpy, An assessment of the atmospheric particle removal efficiency of an in-room botanical biofilter system, Building and Environment, Volume 115, April 2017, Pages 281-290, ISSN 0360-1323, https://doi.org/10.1016/j.buildenv.2017.01.035

[263] Tengfei (Tim) Zhang, Shugang Wang, Gangsen Sun, Linxiao Xu, Daizo Takaoka, Flow impact of an air conditioner to portable air cleaning, Building and Environment, Volume 45, Issue 9, 2010, Pages 2047-2056, ISSN 0360-1323, https://doi.org/10.1016/j.buildenv.2009.11.006

[264] Lin Chen, Xinming Jin, Lijun Yang, Xiaoze Du, Yongping Yang, Particle transport characteristics in indoor environment with an air cleaner: The effect of nonuniform particle distributions, Building Simulation, Volume 10, Issue 1, February 2017, Pages 123-133, ISSN 1996-8744, https://doi.org/10.1007/s12273-016-0310-7

[265] Xinming Jin, Lijun Yang, Xiaoze Du, Yongping Yang, Particle transport characteristics in indoor environment with an air cleaner, Indoor and Built Environment, Volume 25, Issue 6, 1 October 2016, Pages 987-996, ISSN 1420-326X, https://doi.org/10.1177/1420326X15592253

[266] Z.T. Ai, C.M. Mak, From street canyon microclimate to indoor environmental quality in naturally ventilated urban buildings: Issues and possibilities for improvement, Building and Environment, Volume 94, Part 2, December 2015, Pages 489-503, ISSN 0360-1323, https://doi.org/10.1016/j.buildenv.2015.10.008

[267] Federico Noris, Gary Adamkiewicz, William W. Delp, Toshifumi Hotchi, Marion Russell, Brett C. Singer, Michael Spears, Kimberly Vermeer, William J. Fisk, Indoor environmental quality benefits of apartment energy retrofits, Building and Environment, Volume 68, October 2013, Pages 170-178, ISSN 0360-1323, https://doi.org/10.1016/j.buildenv.2013.07.003

[268] M.S. Zuraimi, Zhongchao Tan, Impact of residential building regulations on reducing indoor exposures to outdoor PM2.5 in Toronto, Building and Environment, Volume 89, July 2015, Pages 336-344, ISSN 0360-1323, https://doi.org/10.1016/j.buildenv.2015.03.010

[269] Qingliang Cao, Ailu Chen, Jin Zhou, Victor Wei-Chung Chang, Performance evaluation of filter applications in fan-coil units during the 2015 Southeast Asian haze episode, Building and Environment, Volume 107, October 2016, Pages 191-197, ISSN 0360-1323, https://doi.org/10.1016/j.buildenv.2016.08.004

[270] Arman Shehabi, Srirupa Ganguly, Lara A. Gundel, Arpad Horvath, Thomas W. Kirchstetter, Melissa M. Lunden, William Tschudi, Ashok J. Gadgil, William W. Nazaroff, Can combining economizers with improved filtration save energy and protect equipment in data centers?, Building and Environment, Volume 45, Issue 3, March 2010, Pages 718-726, ISSN 0360-1323, https://doi.org/10.1016/j.buildenv.2009.08.009

[271] James F. Montgomery, Sheldon I. Green, Steven N. Rogak, Karen Bartlett, Predicting the energy use and operation cost of HVAC air filters, Energy and Buildings, Volume 47, April 2012, Pages 643-650, ISSN 0378-7788, https://doi.org/10.1016/j.enbuild.2012.01.001

[272] Marwa Zaatari, Atila Novoselac, Jeffrey Siegel, The relationship between filter pressure drop, indoor air quality, and energy consumption in rooftop HVAC units, Building and Environment, Volume 73, March 2014, Pages 151-161, ISSN 0360-1323, https://doi.org/10.1016/j.buildenv.2013.12.010

[273] Hao Lu, Lin Lu, Numerical investigation on particle deposition enhancement in duct air flow by ribbed wall, Building and Environment, Volume 85, February 2015, Pages 61-72, ISSN 0360-1323, https://doi.org/10.1016/j.buildenv.2014.11.031

[274] Hao Lu, Lin Lu, A numerical study of particle deposition in ribbed duct flow with different rib shapes, Building and Environment, Volume 94, Part 1, December 2015, Pages 43-53, ISSN 0360-1323, https://doi.org/10.1016/j.buildenv.2015.07.030

[275] Bert Blocken, Rob Vervoort, Twan van Hooff, Reduction of outdoor particulate matter concentrations by local removal in semi-enclosed parking garages: A preliminary case study for Eindhoven city center, Journal of Wind Engineering and Industrial Aerodynamics, Volume 159, December 2016, Pages 80-98, ISSN 0167-6105, https://doi.org/10.1016/j.jweia.2016.10.008

[276] Mohamad T. Araji, Stephen D. Ray, Luke Leung, Pilot-study on airborne PM2.5 filtration with particle accelerated collision technology in office environments, Sustainable Cities and Society, Volume 28, January 2017, Pages 101-107, ISSN 2210-6707, https://doi.org/10.1016/j.scs.2016.08.023

[277] Chong Liu, Po-Chun Hsu, Hyun-Wook Lee, Meng Ye, Guangyuan Zheng, Nian Liu, Weiyang Li, Yi Cui, Transparent air filter for high-efficiency PM2.5 capture, Nature Communications, Volume 6, Article Number 6205, 2015, ISSN 2041-1723, https://doi.org/10.1038/ncomms7205

[278] Xinglei Zhao, Shan Wang, Xia Yin, Jianyong Yu, Bin Ding, Slip-Effect Functional Air Filter for Efficient Purification of PM2.5, Scientific Reports, Volume 6, Article Number 35472, 17 October 2016, ISSN 2045-2322, https://doi.org/10.1038/srep35472

[279] J. Podliński, A. Niewulis, V. Shapoval, J. Mizeraczyk, Electrohydrodynamic Secondary Flow and Particle Collection Efficiency in a One-sided Spike-plate Type Electrostatic Precipitator, IEEE Transactions on Dielectrics and Electrical Insulation, Volume 18, Number 5, October 2011, Pages 1401-1407, ISSN 1070-9878, https://doi.org/10.1109/TDEI.2011.6032808

[280] J. Podliński, A. Berendt, J. Mizeraczyk, Electrohydrodynamic Secondary Flow and Particle Collection Efficiency in Spike-plate Multi-electrode Electrostatic Precipitator, IEEE Transactions on Dielectrics and Electrical Insulation, Volume 20, Number 5, October 2013, Pages 1481-1488, ISSN 1070-9878, https://doi.org/10.1109/TDEI.2013.6633674

[281] Janusz Podliński, Jarosław Dekowski, Jerzy Mizeraczyk, Drazena Brocilo, Jen-Shih Chang, Electrohydrodynamic gas flow in a positive polarity wire-plate electrostatic precipitator and the related dust particle collection efficiency, Journal of Electrostatics, Volume 64, Issues 3-4, March 2006, Pages 259-262, ISSN 0304-3886, https://doi.org/10.1016/j.elstat.2005.06.006

[282] S. Tokarek, A. Bernis, An Exemple of Particle Concentration Reduction in Parisian Subway Stations by Electrostatic Precipitation, Environmental Technology, Volume 27, Issue 11, November 2006, Pages 1279-1288, ISSN 0959-3330, https://doi.org/10.1080/09593332708618746

[283] Sidi-Mohamed Remaoun, Farid Miloua, Nacera Hammadi, Noureddine Zouzou, Lucian Dascalescu, Optimization of a Cost-Effective "Wire-Plate"-Type ESP for Installation in a Medical Waste Incinerator, IEEE Transactions on Industry Applications, Volume 50, Number 2, March/April 2014, Pages 1391-1396, ISSN 0093-9994, https://doi.org/10.1109/TIA.2013.2272607

[284] Niloofar Farnoosh, G. S. Peter Castle, Kazimierz Adamiak, A 3D simulation of a single section electrostatic precipitator for dust particles removal, 2011 24th Canadian Conference on Electrical and Computer Engineering (CCECE), Niagara Falls, ON, Canada, 8-11 May 2011, Pages 749-752, ISSN 0840-7789, https://doi.org/10.1109/CCECE.2011.6030555

[285] Jianping Zhang, Dacheng Xu, Jianxing Ren, Helen Wu, Weiguo Pan, Modeling and simulation of PM2.5 collection efficiency in a wire-plate ESP subjected to magnetic field and diffusion charging, Environmental Progress & Sustainable Energy, Volume 34, Issue 3, May/June 2015, Pages 697-702, ISSN 1944-7450, https://doi.org/10.1002/ep.12052

[286] P.F. Linden, The fluid mechanics of natural ventilation, Annual Review of Fluid Mechanics, Volume 31, Issue 1, 1 January 1999, Pages 201-238, ISSN 0066-4189, https://doi.org/10.1146/annurev.fluid.31.1.201

[287] H. Montazeri, B. Blocken, CFD simulation of wind-induced pressure coefficients on buildings with and without balconies: Validation and sensitivity analysis, Building and Environment, Volume 60, February 2013, Pages 137-149, ISSN 0360-1323, https://doi.org/10.1016/j.buildenv.2012.11.012

[288] Chaobin Zhou, Zhiqiang Wang, Qingyan Chen, Yi Jiang, Jingjing Pei, Design optimization and field demonstration of natural ventilation for high-rise residential buildings, Energy and Buildings, Volume 82, October 2014, Pages 457-465, ISSN 0378-7788, https://doi.org/10.1016/j.enbuild.2014.06.036

[289] L. James Lo, David Banks, Atila Novoselac, Combined wind tunnel and CFD analysis for indoor airflow prediction of wind-driven cross ventilation, Building and Environment, Volume 60, February 2013, Pages 12-23, ISSN 0360-1323, https://doi.org/10.1016/j.buildenv.2012.10.022

[290] Annamaria Belleri, Roberto Lollini, Spencer M. Dutton, Natural ventilation design: An analysis of predicted and measured performance, Building and Environment, Volume 81, November 2014, Pages 123-138, ISSN 0360-1323, https://doi.org/10.1016/j.buildenv.2014.06.009

[291] Matthieu Labat, Monika Woloszyn, Géraldine Garnier, Jean Jacques Roux, Assessment of the air change rate of airtight buildings under natural conditions using the tracer gas technique. Comparison with numerical modelling, Building and Environment, Volume 60, February 2013, Pages 37-44, ISSN 0360-1323, https://doi.org/10.1016/j.buildenv.2012.10.010

[292] Per Heiselberg, Kjeld Svidt, Peter V. Nielsen, Characteristics of airflow from open windows, Building and Environment, Volume 36, Issue 7, August 2001, Pages 859-869, ISSN 0360-1323, https://doi.org/10.1016/S0360-1323(01)00012-9

[293] Per Heiselberg, Erik Bjørn, Peter V. Nielsen, Impact of Open Windows on Room Air Flow and Thermal Comfort, International Journal of Ventilation, Volume 1, Issue 2, 1 October 2002, Pages 91-100, ISSN 1473-3315, https://doi.org/10.1080/14733315.2002.11683625

[294] Leighton Cochran, Russ Derickson, A physical modeler's view of Computational Wind Engineering, Journal of Wind Engineering and Industrial Aerodynamics, Volume 99, Issue 4, April 2011, Pages 139-153, ISSN 0167-6105, https://doi.org/10.1016/j.jweia.2011.01.015

[295] James Axley, Multizone Airflow Modeling in Buildings: History and Theory, HVAC&R Research, Volume 13, Issue 6, 1 November 2007, Pages 907-928, ISSN 1078-9669, https://doi.org/10.1080/10789669.2007.10391462

[296] Drury B. Crawley, Linda K. Lawrie, Frederick C. Winkelmann, W.F. Buhl, Y. Joe Huang, Curtis O. Pedersen, Richard K. Strand, Richard J. Liesen, Daniel E. Fisher, Michael J. Witte, Jason Glazer, EnergyPlus: creating a new-generation building energy simulation program, Energy and Buildings, Volume 33, Issue 4, April 2001, Pages 319-331, ISSN 0378-7788, https://doi.org/10.1016/S0378-7788(00)00114-6

[297] Girma Bitsuamlak, Application of computational wind engineering: A practical perspective, Third National Conference in Wind Engineering, Pages 1-19

[298] Bert Blocken, 50 years of Computational Wind Engineering: Past, present and future, Journal of Wind Engineering and Industrial Aerodynamics, Volume 129, June 2014, Pages 69-102, ISSN 0167-6105, https://doi.org/10.1016/j.jweia.2014.03.008

[299] Qingyan Chen, Ventilation performance prediction for buildings: A method overview and recent applications, Building and Environment, Volume 44, Issue 4, April 2009, Pages 848-858, ISSN 0360-1323, https://doi.org/10.1016/j.buildenv.2008.05.025

[300] Yi Jiang, Donald Alexander, Huw Jenkins, Rob Arthur, Qingyan Chen, Natural ventilation in buildings: measurement in a wind tunnel and numerical simulation with large-eddy simulation, Journal of Wind Engineering and Industrial Aerodynamics, Volume 91, Issue 3, February 2003, Pages 331-353, ISSN 0167-6105, https://doi.org/10.1016/S0167-6105(02)00380-X

[301] James O.P. Cheung, Chun-Ho Liu, CFD simulations of natural ventilation behaviour in high-rise buildings in regular and staggered arrangements at various spacings, Energy and Buildings, Volume 43, Issue 5, May 2011, Pages 1149-1158, ISSN 0378-7788, https://doi.org/10.1016/j.enbuild.2010.11.024

[302] Q. Chen, Comparison of different k-ε models for indoor air flow computations, Numerical Heat Transfer, Part B: Fundamentals, Volume 28, Issue 3, 1 October 1995, Pages 353-369, ISSN 1040-7790, https://doi.org/10.1080/10407799508928838

[303] M. Glória Gomes, A. Moret Rodrigues, Pedro Mendes, Experimental and numerical study of wind pressures on irregular-plan shapes, Journal of Wind Engineering and Industrial Aerodynamics, Volume 93, Issue 10, October 2005, Pages 741-756, ISSN 0167-6105, https://doi.org/10.1016/j.jweia.2005.08.008

[304] Renate Teppner, Bernd Langensteiner, Walter Meile, Günter Brenn, Sybill Kerschbaumer, Air change rates driven by the flow around and through a building storey with fully open or tilted windows: An experimental and numerical study, Energy and Buildings, Volume 80, September 2014, Pages 570-583, ISSN 0378-7788, https://doi.org/10.1016/j.enbuild.2014.07.020

[305] Nikos Nikolopoulos, Aristeidis Nikolopoulos, Tine S. Larsen, Konstantinos-Stefanos P. Nikas, Experimental and numerical investigation of the tracer gas methodology in the case of a naturally cross-ventilated building, Building and Environment, Volume 56, October 2012, Pages 379-388, ISSN 0360-1323, https://doi.org/10.1016/j.buildenv.2012.04.006

[306] Yoshihide Tominaga, Akashi Mochida, Shuzo Murakami, Satoshi Sawaki, Comparison of various revised k-ε models and LES applied to flow around a high-rise building model with 1:1:2 shape placed within the surface boundary layer, Journal of Wind Engineering and Industrial Aerodynamics, Volume 96, Issue 4, April 2008, Pages 389-411, ISSN 0167-6105, https://doi.org/10.1016/j.jweia.2008.01.004

[307] G. Evola, V. Popov, Computational analysis of wind driven natural ventilation in buildings, Energy and Buildings, Volume 38, Issue 5, May 2006, Pages 491-501, ISSN 0378-7788, https://doi.org/10.1016/j.enbuild.2005.08.008

[308] Yi Jiang, Qingyan Chen, Effect of fluctuating wind direction on cross natural ventilation in buildings from large eddy simulation, Building and Environment, Volume 37, Issue 4, April 2002, Pages 379-386, ISSN 0360-1323, https://doi.org/10.1016/S0360-1323(01)00036-1

[309] K.-S. Nikas, N. Nikolopoulos, A. Nikolopoulos, Numerical study of a naturally cross-ventilated building, Energy and Buildings, Volume 42, Issue 4, April 2010, Pages 422-434, ISSN 0378-7788, https://doi.org/10.1016/j.enbuild.2009.10.010

[310] Omar S. Asfour, Mohamed B. Gadi, A comparison between CFD and Network models for predicting wind-driven ventilation in buildings, Building and Environment, Volume 42, Issue 12, December 2007, Pages 4079-4085, ISSN 0360-1323, https://doi.org/10.1016/j.buildenv.2006.11.021

[311] Xiong Shen, Guoqiang Zhang, Bjarne Bjerg, Comparison of different methods for estimating ventilation rates through wind driven ventilated buildings, Energy and Buildings, Volume 54, November 2012, Pages 297-306, ISSN 0378-7788, https://doi.org/10.1016/j.enbuild.2012.07.017

[312] Hazim B. Awbi, Ventilation of Buildings, June 2003, Taylor & Francis, ISBN 978-0-415-27055-7, https://doi.org/10.4324/9780203634479

[313] John Kaiser Calautit, Ben Richard Hughes, Wind tunnel and CFD study of the natural ventilation performance of a commercial multi-directional wind tower, Building and Environment, Volume 80, October 2014, Pages 71-83, ISSN 0360-1323, https://doi.org/10.1016/j.buildenv.2014.05.022

[314] Tomohiro Kobayashi, Mats Sandberg, Hisashi Kotani, Leif Claesson, Experimental investigation and CFD analysis of cross-ventilated flow through single room detached house model, Building and Environment, Volume 45, Issue 12, December 2010, Pages 2723-2734, ISSN 0360-1323, https://doi.org/10.1016/j.buildenv.2010.06.001

[315] Xiaoping Liu, Jianlei Niu, Kenny C. S. Kwok, Evaluation of RANS turbulence models for simulating wind-induced mean pressures and dispersions around a complex-shaped high-rise building, Building Simulation, Volume 6, Issue 2, June 2013, Pages 151-164, ISSN 1996-8744, https://doi.org/10.1007/s12273-012-0097-0

[316] Joachim Seifert, Yuguo Li, James Axley, Markus Rösler, Calculation of wind-driven cross ventilation in buildings with large openings, Journal of Wind Engineering and Industrial Aerodynamics, Volume 94, Issue 12, December 2006, Pages 925-947, ISSN 0167-6105, https://doi.org/10.1016/j.jweia.2006.04.002

[317] T. van Hooff, B. Blocken, L. Aanen, B. Bronsema, A venture-shaped roof for wind-induced natural ventilation of buildings: Wind tunnel and CFD evaluation of different design configurations, Building and Environment, Volume 46, Issue 9, September 2011, Pages 1797-1807, ISSN 0360-1323, https://doi.org/10.1016/j.buildenv.2011.02.009

[318] Aishe Zhang, Ming Gu, Wind tunnel tests and numerical simulations of wind pressures on buildings in staggered arrangement, Journal of Wind Engineering and Industrial Aerodynamics, Volume 96, Issues 10-11, October-November 2008, Pages 2067-2079, ISSN 0167-6105, https://doi.org/10.1016/j.jweia.2008.02.013

[319] CPP Wind Engineering & Air Quality Experts – CPP Wind Engineering & Air Quality Consulting for Building Design, https://www.cppwind.com

[320] P.J. Richards, S.E. Norris, Appropriate boundary conditions for computational wind engineering models revisited, Journal of Wind Engineering and Industrial Aerodynamics, Volume 99, Issue 4, April 2011, Pages 257-266, ISSN 0167-6105, https://doi.org/10.1016/j.jweia.2010.12.008

[321] William H. Snyder, Guideline for Fluid Modeling of Atmospheric Diffusion, Environmental Sciences Research Laboratory, April 1981, EPA-600/8-81-009, http://nepis.epa.gov/Exe/ZyPURL.cgi?Dockey=2000MVTD.TXT

[322] J.E. Cermak, Laboratory Simulation of the Atmospheric Boundary Layer, Journal of Fluids Engineering, Volume 9, Issue 9, 1 September 1971, Pages 1754-1746, ISSN 0001-1452, https://doi.org/10.2514/3.49977

[323] J.E. Cermak, Applications of Fluid Mechanics to Wind Engineering — A Freeman Scholar Lecture, AIAA Journal, Volume 97, Issue 1, 1 March 1973, Pages 9-38, ISSN 0098-2202, https://doi.org/10.1115/1.3447225

[324] J.E. Cermak, Aerodynamics of Buildings, Annual Review of Fluid Mechanics, Volume 8, Issue 1, 1 January 1976, Pages 75-106, ISSN 0066-4189, https://doi.org/10.1146/annurev.fl.08.010176.000451

[325] CHAM Ltd, PHOENICS 2011 (64bit Intel 17/06/2012), 2012, London

[326] Yoshihide Tominaga, Akashi Mochida, Ryuichiro Yoshie, Hiroto Kataoka, Tsuyoshi Nozu, Masaru Yoshikawa, Taichi Shirasawa, AIJ guidelines for practical applications of CFD to pedestrian wind environment around buildings, Journal of Wind Engineering and Industrial Aerodynamics, Volume 96, Issues 10-11, October-November 2008, Pages 1749-1761, ISSN 0167-6105, https://doi.org/10.1016/j.jweia.2008.02.058

[327] Jorg Franke, Antti Hellsten, K. Heinke Schlunzen, Bertrand Carissimo, The COST 732 Best Practice Guideline for CFD simulation of flows in the urban environment: a summary, International Journal of Environment and Pollution, Volume 44, No. 1-4, 2011, Pages 419-427, ISSN 0957-4352, https://doi.org/10.1504/IJEP.2011.038443

[328] John D. Anderson Jr., Computational Fluid Dynamics – The Basics with Applications, McGraw-Hill, Inc., 1995, ISBN 978-0070016859

[329] T. van Hooff, B. Blocken, CFD evaluation of natural ventilation of indoor environments by the concentration decay method: CO2 gas dispersion from a semi-enclosed stadium, Building and Environment, Volume 61, March 2013, Pages 1-17, ISSN 0360-1323, https://doi.org/10.1016/j.buildenv.2012.11.021

[330] S. Wilcox, W. Marion, Users Manual for TMY3 Data Sets, National Renewable Energy Laboratory, May 2008, NREL/TP-581-43156, https://doi.org/10.2172/928611

[331] P. Karava, T. Stathopoulos, A.K. Athienitis, Airflow assessment in cross-ventilated buildings with operable façade elements, Building and Environment, Volume 46, Issue 1, January 2011, Pages 266-279, ISSN 0360-1323, https://doi.org/10.1016/j.buildenv.2010.07.022

[332] Shinsuke Kato, Shuzo Murakami, Akashi Mochida, Shin-ichi Akabayashi, Yoshihide Tominaga, Velocity-pressure field of cross ventilation with open windows analyzed by wind tunnel and numerical simulation, Journal of Wind Engineering and Industrial Aerodynamics, Volume 44, Issues 1-3, October 1992, Pages 2575-2586, ISSN 0167-6105, https://doi.org/10.1016/0167-6105(92)90049-G

[333] Guilherme C. C. Carrilho da Graça, Simplified models for heat transfer in rooms, PhD Dissertation, Department of Mechanical and Aerospace Engineering, University of California, San Diego, 2003, ISBN 9780496603251, http://www.academia.edu/download/35025162/GCG_Phd_Thesis_2003.pdf

[334] United States Department of Energy, Getting Started with EnergyPlus – Basic Concepts Manual – Essential Information You Need about Running EnergyPlus, EnergyPlus™ Documentation, 2015, https://energyplus.net/sites/default/files/pdfs_v8.3.0/GettingStarted.pdf

[335] United States Department of Energy, Engineering Reference – The Reference to EnergyPlus Calculations, EnergyPlus™ Documentation, 2015, https://energyplus.net/sites/default/files/pdfs_v8.3.0/EngineeringReference.pdf

[336] Michael Deru, Kristin Field, Daniel Studer, Kyle Benne, Brent Griffith, Paul Torcellini, Bing Liu, Mark Halverson, Dave Winiarski, Michael Rosenberg, Mehry Yazdanian, Joe Huang, Drury Crawley, U.S. Department of Energy Commercial Reference Building Models of the National Building Stock, National Renewable Energy Laboratory, February 2011, NREL/TP-5500-46861, https://doi.org/10.2172/1009264

[337] P. Haves, P.F. Linden, G. Carrilho da Graça, Use of simulation in the design of a large, naturally ventilated office building, Building Services Engineering Research and Technology, Volume 25, No. 3, August 2004, Pages 211-221, ISSN 0143-6244, https://doi.org/10.1191/0143624404bt102oa

[338] Jacques Descloitres, NASA Visible Earth: California and Nevada, MODIS Rapid Response Team, NASA/GSFC, 3 May 2004, https://visibleearth.nasa.gov/view.php?id=59834

[339] NASA/JPL-Caltech, PIA03445: Dusty Skies over Southern California, NASA/GSFC/LaRC/JPL, MISR Team, 20 February 2002, https://photojournal.jpl.nasa.gov/catalog/PIA03445

[340] United States Census Bureau, United States 2010 Census – Total Population, through American FactFinder, https://factfinder.census.gov/faces/nav/jsf/pages/searchresults.xhtml (accessed 5 November 2015)

[341] Markus Kottek, Jürgen Grieser, Christoph Beck, Bruno Rudolf, Franz Rubel, World Map of the Köppen-Geiger climate classification updated, Meteorologische Zeitschrift, Volume 15, Number 3, June 2006, Pages 259-263, ISSN 0941-2948, https://doi.org/10.1127/0941-2948/2006/0130

[342] Franz Rubel, Katharina Brugger, Klaus Haslinger, Ingeborg Auer, The climate of the European Alps: Shift of very high resolution Köppen-Geiger climate zones 1800-2100, Meteorologische Zeitschrift, Volume 26, Number 2, 24 January 2017, Pages 115-125, ISSN 0941-2948, https://doi.org/10.1127/metz/2016/0816

[343] ESA/VITO, Space in Images: Springtime in Europe, 4 June 2014, https://www.esa.int/spaceinimages/Images/2014/06/Springtime_in_Europe

[344] Marloes Eeftens, Ming-Yi Tsai, Christophe Ampe, Bernhard Anwander, Rob Beelen, Tom Bellander, Giulia Cesaroni, Marta Cirach, Josef Cyrys, Kees de Hoogh, Audrey De Nazelle, Frank de Vocht, Christophe Declercq, Audrius Dėdelė, Kirsten Eriksen, Claudia Galassi, Regina Gražulevičienė, Georgios Grivas, Joachim Heinrich, Barbara Hoffmann, Minas Iakovides, Alex Ineichen, Klea Katsouyanni, Michal Korek, Ursula Krämer, Thomas Kuhlbusch, Timo Lanki, Christian Madsen, Kees Meliefste, Anna Mölter, Gioia Mosler, Mark Nieuwenhuijsen, Marieke Oldenwening, Arto Pennanen, Nicole Probst-Hensch, Ulrich Quass, Ole Raaschou-Nielsen, Andrea Ranzi, Euripides Stephanou, Dorothee Sugiri, Orsolya Udvardy, Éva Vaskövi, Gudrun Weinmayr, Bert Brunekreef, Gerard Hoek, Spatial variation of PM2.5, PM10, PM2.5 absorbance and PMcoarse concentrations between and within 20 European study areas and the relationship with NO2 – Results of the ESCAPE project, Atmospheric Environment, Volume 62, December 2012, Pages 303-317, ISSN 1352-2310, https://doi.org/10.1016/j.atmosenv.2012.08.038

[345] Boston University/NASA GSFC, New Land Cover Classification Maps – Asia Print, Terra – Modis, 14 August 2002, https://visibleearth.nasa.gov/view.php?id=61004

[346] Siddartha Singh, S.K. Peshin, Environment and Sustainable Development, Chapter 6: Air Pollution Scenario over Delhi City, Springer India, 2014, Pages 77-85, ISBN 978-81-322-1166-2, https://doi.org/10.1007/978-81-322-1166-2_6

[347] Shi-Qi Yang, Andreas Matzarakis, Implementation of human thermal comfort information in Köppen-Geiger climate classification – the example of China, International Journal of Biometeorology, Volume 60, Issue 11, November 2016, Pages 1801-1805, ISSN 0020-7128, https://doi.org/10.1007/s00484-016-1155-6

[348] Aron P. Dobos, Standard Time Series Data File Format, National Renewable Energy Laboratory, August 2013, http://rredc.nrel.gov/solar/old_data/nsrdb/2005-2012/wfcsv.pdf

[349] M. Sengupta, A. Habte, P. Gotseff, A. Weekley, A. Lopez, C. Molling, A. Heidinger, A Physics-Based GOES Satellite Product for Use in NREL's National Solar Radiation Database, National Renewable Energy Laboratory, July 2014, NREL/CP-5D00-62237, https://www.nrel.gov/docs/fy14osti/62237.pdf

[350] Carsten Hoyer-Klick, Mireille Lefèvre, Marion Schroedter-Homscheidt, Lucien Wald, USER'S GUIDE to the MACC-RAD Services on solar energy radiation resources, Copernicus Atmospheric Monitoring Service, European Centre for Medium-Range Weather Forecasts, March 2015, https://atmosphere.copernicus.eu/sites/default/files/repository/MACCIII_RAD_DEL_D57.5_final_0.pdf

[351] National Centers for Environmental Information, Integrated Surface Data, NCEI DSI 3505 – gov.noaa.ncdc:C00532, National Environmental Satellite, Data, and Information Service, National Oceanic and Atmospheric Administration, U.S. Department of Commerce

[352] White Box Technologies, www.whiteboxtechnologies.com, 2016 WBT. Used by permission.

[353] California Air Resources Board, 2012 Air Quality Data DVD, August 2012, PTSD-2012-035-DVD

[354] European Environment Agency, AirBase – The European air quality database, Version 7, March 2014

[355] U.S. Department of State, StateAir – U.S. Department of State Air Quality Monitoring Program – Mission China

[356] U.S. Department of State, Mission India – U.S. Mission India NowCast Air Quality

[357] Heikki Junninen, Harri Niska, Kari Tuppurainen, Juhani Ruuskanen, Mikko Kolehmainen, Methods for imputation of missing values in air quality data sets, Atmospheric Environment, Volume 38, Issue 18, June 2004, Pages 2895-2907, ISSN 1352-2310, https://doi.org/10.1016/j.atmosenv.2004.02.026

[358] Jie Zhao, Bertrand Lasternas, Khee Poh Lam, Ray Yun, Vivian Loftness, Occupant behavior and schedule modeling for building energy simulation through office appliance power consumption data mining, Energy and Buildings, Volume 82, October 2014, Pages 341-355, ISSN 0378-7788, https://doi.org/10.1016/j.enbuild.2014.07.033

[359] M. Malato Lerer, G. Carrilho da Graça, P.F. Linden, Building energy demand response simulation for an office tower in New York, Proceedings of BS2013: 13th Conference of International Building Performance Simulation Association, Chambéry, France, August 26-28 2013, Pages 2511-2518, ISBN 9782746662940, http://www.ibpsa.org/proceedings/BS2013/p_1350.pdf

[360] Occupational Safety & Health Administration, Code of Federal Regulations, Title 29 – Labor, Part 1910 – Occupational Safety and Health Standards, Subpart J – General Environmental Controls, Standard Number 1910.141 – Sanitation

[361] Department of Justice, Americans with Disabilities Act of 1990, 2010 ADA Standards for Accessible Design, September 2010

[362] California Building Standards Commission, California Code of Regulations, Title 24 – Building Standards Code, Part 2 – California Building Code, 2013

[363] Occupational Safety & Health Administration, Code of Federal Regulations, Title 29 – Labor, Part 1910 – Occupational Safety and Health Standards, Subpart D – Walking-Working Surfaces, Standard Number 1910.24 – Fixed industrial stairs

[364] California Building Standards Commission, California Code of Regulations, Title 24 – Building Standards Code, Part 6 – California Energy Code, 2013

[365] Paul Raftery, Edwin Lee, Tom Webster, Tyler Hoyt, Fred Bauman, Effects of furniture and contents on peak cooling load, Energy and Buildings, Volume 85, December 2014, Pages 445-457, ISSN 0378-7788, https://doi.org/10.1016/j.enbuild.2014.09.081

[366] Krishnan Gowri, David W. Winiarski, Ronald E. Jarnagin, Infiltration modeling guidelines for commercial building energy analysis, Office of Scientific and Technical Information, United States, 2009, https://doi.org/10.2172/968203

[367] ASHRAE, 2013 ASHRAE Handbook – Fundamentals, American Society of Heating, Refrigerating, and Air Conditioning Engineers, Inc., Atlanta, GA, United States, 2013, ISBN 978-1-93-650446-6, ISSN 1523-7230

[368] Matthew Leach, Chad Lobato, Adam Hirsch, Shanti Pless, Paul Torcellini, Technical Support Document: Strategies for 50% Energy Savings in Large Office Buildings, National Renewable Energy Laboratory, September 2010, NREL/CP-550-49213, https://www.nrel.gov/docs/fy10osti/49213.pdf

[369] Ivar S. Ertesvåg, Uncertainties in heat-pump coefficient of performance (COP) and exergy efficiency based on standardized testing, Energy and Buildings, Volume 43, Issue 8, August 2011, Pages 1937-1946, ISSN 0378-7788, https://doi.org/10.1016/j.enbuild.2011.03.039

[370] Pinar Mert Cuce, Saffa Riffat, A comprehensive review of heat recovery systems for building applications, Renewable and Sustainable Energy Reviews, Volume 47, July 2015, Pages 665-682, ISSN 1364-0321, https://doi.org/10.1016/j.rser.2015.03.087

[371] Peg A. Pigeon-Bergmann, Mohsen Abrishami, Mark Ciminelli, Sylvia Bender, Valerie Hall, B.B. Blevins, California Commercial End-Use Survey – Report, California Energy Commission & Itron, Inc., March 2006, CEC-400-2006-005, http://www.energy.ca.gov/2006publications/CEC-400-2006-005/CEC-400-2006-005.PDF

[372] P. R. Warren, The analysis of single-sided ventilation measurements, Air Infiltration Review, Volume 7, Number 2, February 1986, Pages 3-5

[373] J. Fergus Nicol, Characterising occupant behaviour in buildings: towards a stochastic model of occupant use of windows, lights, blinds, heaters and fans, Proceedings of Seventh International IBPSA Conference: Building Simulation, 13-15 August 2001, Rio de Janeiro, Brazil, Pages 1073-1078, ISBN 9788590193944, http://www.ibpsa.org/proceedings/BS2001/BS01_1073_1078.pdf

[374] European Committee for Standardization, Particulate air filters for general ventilation. Determination of the filtration performance, EN 779:2012, April 2012

[375] W. J. Fisk, D. Faulkner, J. Palonen, O. Seppanen, Performance and costs of particle air filtration technologies, Indoor Air, Volume 12, Issue 4, December 2002, Pages 223-234, ISSN 1600-0668, https://doi.org/10.1034/j.1600-0668.2002.01136.x

[376] M. S. Waring, J. A. Siegel, Particle loading rates for HVAC filters, heat exchangers, and ducts, Indoor Air, Volume 18, Issue 3, June 2008, Pages 209-224, ISSN 1600-0668, https://doi.org/10.1111/j.1600-0668.2008.00518.x

[377] International Energy Agency, Energy Policies of IEA Countries – Poland 2011 Review, OECD/IEA, 2011, Paris, France, ISBN 978-92-64-09818-3, https://www.iea.org/publications/freepublications/publication/Poland2011_web.pdf

[378] World Development Indicators | World Data Bank, http://databank.worldbank.org/data/reports.aspx?source=2&series=EG.FEC.RNEW.ZS,EG.ELC.RNEW.ZS&country=MKD, accessed 01-09-2016, IBRD/IDA, The World Bank

[379] Zhen Cheng, Jingkun Jiang, Oscar Fajardo, Shuxiao Wang, Jiming Hao, Characteristics and health impacts of particulate matter pollution in China (2001-2011), Atmospheric Environment, Volume 65, February 2013, Pages 186-194, ISSN 1352-2310, https://doi.org/10.1016/j.atmosenv.2012.10.022